Implementing wind forecasting at a utility

Landberg, Lars; Hansen, M.A.; Vesterager, K.; Bergstrøm, W.

Publication date:
1997

Document Version
Publisher's PDF, also known as Version of record

RISØ DMI NESA

Risø-R-929(EN)

Implementing Wind Forecasting at a Utility

Lars Landberg
Risø National Laboratory

Mogens A. Hansen
Danish Meteorological Institute

Kurt Vesterager
ELKRAFT

Willy Bergstrøm
NESA

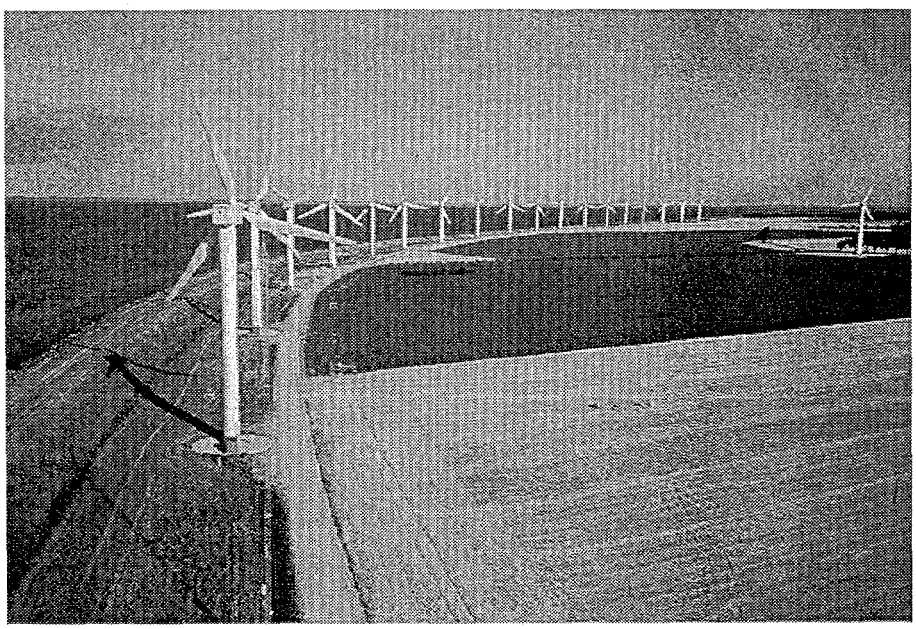

Risø National Laboratory, Roskilde, Denmark
March 1997

Implementing Wind Forecasting at a Utility

Risø-R-929(EN)

Lars Landberg
Risø National Laboratory

Mogens A. Hansen
Danish Meteorological Institute

Kurt Vesterager
ELKRAFT

Willy Bergstrøm
NESA

Risø National Laboratory, Roskilde, Denmark
March 1997

Abstract This report describes a project – funded by the Danish Ministry of Energy and the Environment – that has as its aim to implement prediction of the power produced by wind farms in the daily planning at the Danish utility ELKRAFT. The predictions are generated from forecasts from HIRLAM (HIgh Resolution Limited Area Model) of the Danish Meteorological Institute. These predictions are then made valid at individual sites (wind farms) by applying either a matrix generated by the sub-models of WASP (Wind Atlas Application and Analysis Program) or by use of a Kalman filter. In the project 17 wind farms have been selected for study. The farms are located on the Zealand (13) and Bornholm (4) islands and all belonging to the Danish utility ELKRAFT.

Photo: The Kappel wind farm. Courtesy of Flemming Hagensen, Test Station for Windmills, Risø National Laboratory, Denmark

ISBN 87–550–2229–4
ISSN 0106–2840

Information Service Department · Risø · 1997

Contents

1 Dansk sammendrag *5*

2 Introduction *6*
2.1 Brief outline of the report *6*

3 The Persistence Model *8*

4 The DMI Operational HIRLAM Forecasting System *10*

5 The DMI Model *11*
5.1 Statistical interpretation in meteorology *11*
5.2 The Kalman filter *11*
5.3 The data *13*
5.4 Applying the Kalman filter *14*
5.5 Overview *14*
5.6 Results *16*
5.7 Expanding to entire population *19*

6 The Risø Model *21*
6.1 Overview *21*
6.2 HIRLAM *21*
6.3 Surface transformation *23*
6.4 WA^{S}P *23*
6.5 Model Output Statistics (MOS) *24*
6.6 PARK *28*
6.7 Input to the model *28*
6.8 Output from the model *31*
6.9 Results *32*
6.10 Discussion *36*

7 Intensive test period *41*

8 Operational use of models *48*
8.1 Background *48*
8.2 Main tasks in the control centre *48*
8.3 Production planning, power exchange and load dispatching *48*
8.4 Load dispatching in a power supply system including wind power *49*
8.5 Implementation *49*
8.6 Further aspects *49*

9 Conclusions *50*

Acknowledgements *51*

References *52*

A The DMI model *53*
A.1 Data coverage *53*
A.2 The total rated power *53*
A.3 Figures showing wind-power relations *53*
A.4 Figures showing error and skill score vs. prognosis lengths *58*
A.5 Figures showing error vs. wind farm id *64*
A.6 Scatter plots for the best, the poorest and the total *66*
A.7 Kalman coefficients *74*

B The Risø Model *87*
Avedøre Holme *88*
Avedøre 1000 *89*
Flakkebjerg *90*
Kappel *91*
Kollerød *92*
Kyndby *93*
MAV82 *94*
Nybølle Hede *95*
Nøjsomhedsodde *96*
Prejehøj *97*
Rosendale *98*
Skovlænge *99*
Sose *100*
Sprove *101*
Tystofte *102*
Vindeby *103*
Østermarie *104*
B.1 The ASCII forecast file *105*
B.2 Full results *110*

C Results *119*

1 Dansk sammendrag

Denne rapport beskriver et projekt der havde som sit formål at implementere hos et elselskab to modeller til at forudsige el-produktionen fra vindmølleparker op til 36 timer frem i tiden. Projektets parter er Danmarks Meteorologiske Institut (DMI), elselskabet ELKRAFT og Forskningscenter Risø. De to modeller er udviklet af henholdsvis Risø og DMI. Begge modeller baserer sig på forudsigelser af vinden udført af DMI's prognosemodel HIRLAM. Risø's model bruger fysiske modeller (Risø's WASP og PARK) til at gøre forudsigelserne lokale og DMI bruger en statistisk metode baseret på Kalman filteret.

De to modeller har kørt operationelt hos DMI i et år (fra februar 1995 til januar 1996) og 36 timers forudsigelser er blevet genereret to gange i døgnet. Dette er foregået således at ELKRAFT har haft mulighed for at anvende disse forudsigelser i deres daglige planlægning.

Til at verificere de to modeller er der blevet anvendt et års observationer fra 17 vindmølleparker fordelt med 14 på Sjælland og 3 på Bornholm.

Resultaterne af projektet er at det er blevet vist at

1. Det er muligt at lave modeller der giver forudsigelser af en sådan kvalitet at de med både brændselsforbrug og økonomi for øje med udbytte kan anvendes
2. At det er muligt at køre disse modeller operationelt, dvs på en daglig basis gennem et år at have givet forudsigelser 36 timer frem to gange i døgnet.
3. At et elselskab kan bruge disse forudsigelser i deres daglige planlægning med resultater der er væsentligt bedre end hvis modellerne ikke havde været anvendt.

Det har ikke været muligt for ELKRAFT at udnytte forudsigelserne i hele perioden, men de var dog anvendt i et intensivt 14-dages test forløb.

Rapporten, der er forfattet på engelsk af alle projektdeltagerne, består af følgende afsnit: en indledning (kapitel 2) hvor problemstillingen ridses op, en beskrivelse og analyse af den såkaldte persistensmodel (kapitel 3), derefter er DMI's model kompleks beskrevet (kapitel 5), så er Risø's model beskrevet (kapitel 6), den 14-dages intensive test periode er beskrevet i kapitel 7, den mulige operationelle anvendelse er derefter ridset op (kapitel 8). Til sidst i reportens ordinære del er konklusionerne givet (kapitel 9). I hvert af modelafsnittene er de vigtigste resultater fra verifikationen af de respektive modeller givet og i appendiks C er en grundig gennemgang af verifikationsresultaterne for de to modeller og persistensmodellen givet. For at have en fuldstændig dokumentation af de to modeller er der i appendiks B og A givet en komplet listning af de anvendte modelparametre.

2 Introduction

To fully benefit from large amounts of wind energy in a grid, it is necessary to know the part of the electricity production generated by the wind. The time frame is up to two days in advance. This will enable the utility to control the conventionally fueled plants in such a way that fossil fuels will in fact be saved. With the abilities of present day numerical weather prediction models, it is now possible to accomplish the aforementioned task; this has been shown in a CEC-funded JOULE-project (Landberg et al, 1993).

This report will describe two models based on predictions from HIRLAM (High Resolution Limited Area Model) run by the Danish Meteorological Institute (DMI), (Machenhauer, 1988). The HIRLAM/Kalman model developed by DMI which is based on a Kalman filtering of the output from HIRLAM. The Kalman filter corrects for biases by using an adaptive algorithm. The HIRLAM/WA^{S}P model developed by Risø National Laboratory, which is based on the WA^{S}P (Wind Atlas Analysis and Application Program) model of Risø National Laboratory (Mortensen et al, 1994). The WA^{S}P model takes local phenomena into account. Local phenomena are e.g. the sheltering of wind breaks, the effect of different roughnesses and the changes in these and the speed-up/down by the orography.

The reason why *two* different models have been chosen is that the task of predicting the wind and hence the wind-farm-produced power can fundamentally be approached in two different ways:

- physical models
- statistical models

A sub-task of this project is therefore to assess the differences between these two different approaches.

The models have been at the disposal of the Danish utility ELKRAFT and they predict the production of 17 wind farms with a total capacity of 35.7 MW, see Figure 1 and Table 1. These 17 farms are then linked to the rest of the installed wind power (totalling approximately 100 MW) by a factor varying from hour to hour.

The project has three partners: ELKRAFT, The Danish Meteorological Institute, and Risø National Laboratory (coordinator). It is funded by the Danish Ministry of Energy under the EFP-programme.

2.1 Brief outline of the report

The report will describe the two models, the DMI/Kalman model in Chapter 5 and the Risø/WA^{S}P model in Chapter 6. To compare these two models a third, very simple, but also very powerful, model, the persistence model, has been used and is described in Chapter 3. In Chapter 7 an intensive test period is described where the two models were compared to the forecasts of the dispatchers at ELKRAFT. The operational perspectives of the models are discussed in Chapter 8. Finally in Chapter 9 the models are compared and conclusions drawn.

A number of appendices also appear. Appendix A describes the DMI model further and Appendix B the Risø model. In Appendix C a comprehensive listing of the results is given.

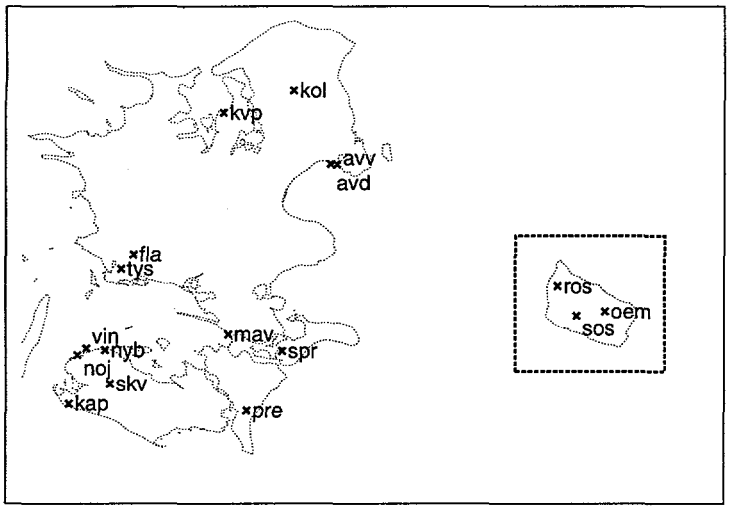

Figure 1. The 17 selected wind farms in the ELKRAFT/SK Power area. Each farm is indicated by its 3-letter code listed in Table 1. The farms have a total capacity of 35.7 MW.

*Table 1. The selected wind farms and their configuration. * means that the station will not be included in the calculation of the mean because of its low availability.*

Name	ID	#	Turbine [kW]	Total [kW]	Avail. [%]
Avedøre	avd*	12	300	3600	58
Avedøre 1000	avv*	1	1000	1000	58
Flakkebjerg	fla	1	225	225	72
Kappel	kap	24	400	9600	63
Kollerød	kol*	1	500	500	36
Kyndby	kvp	21	180	3780	76
MAV82	mav*	1	750	750	43
Nøjsomhedsodde	noj	23	225	5175	74
Nybølle Hede	nyb	2	500	1000	71
Prejehøj	pre*	1	500	500	68
Rosendale	ros	3	225	675	75
Skovlænge	skv	2	150	300	76
Sose	sos*	2	225	450	24
Sprove	spr	2	150	300	63
Tystofte	tys	3	450	1350	71
Vindeby	vin*	11	450	4950	47
Østermarie	oem	7	225	1575	66
Total	17	117		35730	

3 The Persistence Model

In order to establish a reference model, the *persistence model* has been chosen. The persistence model is the worst enemy of any forecast model in meteorology (and in many other fields, too). It has the advantage of being simple (very simple), and that it quite often gives good results. The model is as follows:

$$P(t+\ell) = P(t) \tag{1}$$

where $P(t)$ is the production at time t and ℓ is the look-ahead time. This model could popularly be called the 'what-you-see-is-what-you-get' (WYSIWYG) model!

This equation can easily be stated in words: the quantity one wants to forecast is the same ℓ hours ahead as it is now. The reason why this is a good approximation to flow in the atmosphere, is that the atmosphere can be considered quasi-stationary, ie changing very slowly. A characteristic time scale in the atmosphere is f^{-1}, where f is the Coriolis parameter. Using 10^{-4} s^{-1} for f gives that this scale is approximately 3 hours.

In this study the persistence model will be used as a frame of reference, because if the developed models are not better than persistence, they can not be considered as modelling the actual process, and certainly not be recommended for forecasting. Another reason is that most predictions for scheduling purposes presently are using this model.

In the statistical evaluation following, the mean error of the persistence model will typically be very small; this can easily be explained, since it follows from the definition of the error that:

$$e_{\text{persist}} = \frac{1}{N-\ell}\left(\sum_{i=1}^{\ell} x_i - \sum_{i=N-\ell+1}^{N} x_i\right)$$

where ℓ is the look-ahead time and x_i the ith value of the timeseries. As can be seen from this expression, the mean error depends only on the 'head' and 'tail' of the time series, so is the series of a certain extent, ie N large, $\ell \ll N$, and the head of the series is of the same magnitude as the tail (ie no trend), the mean error will be very small. The rms error, on the other hand, can get quite big: when ℓ is so large that the series can be considered un(auto)correlated the persistence model's standard deviation of the error, becomes equal to the standard deviation of the timeseries times $\sqrt{2}$.

As an example of the abilities of the persistence model, the persistence forecast for Kyndby wind farm is shown in Figure 2. This figure also introduces some of the error measures used in this study. The error measures are defined as follows:
mean error, ME:

$$\text{ME} = \frac{1}{N}\sum_{1}^{N} P_{\text{obs}} - P_{\text{prog}} \tag{2}$$

where N is the number of data points, P_{obs} the observed production, and P_{prog} the forecast production.
mean absolute error, MAE:

$$\text{MAE} = \frac{1}{N}\sum_{1}^{N} \mid P_{\text{obs}} - P_{\text{prog}} \mid \tag{3}$$

standard deviation of the error, σ:

$$\sigma = \sqrt{\frac{1}{N-1}\sum_{1}^{N}(P_{\text{obs}} - P_{\text{prog}} - \text{ME})^2} \tag{4}$$

note that this measure gives more weight to large errors than the MAE measure does.

In some cases the above measures are normalised with the total installed capacity of the wind farm to create measures which can be compared from one wind farm to another.

A final measure is the *skill score*, SS, defined as:

$$\mathrm{SS} = \frac{\mathrm{MAE}_{\mathrm{persist}} - \mathrm{MAE}_{\mathrm{model}}}{\mathrm{MAE}_{\mathrm{persist}}} = 1 - \frac{\mathrm{MAE}_{\mathrm{model}}}{\mathrm{MAE}_{\mathrm{persist}}} \tag{5}$$

which measures the scatter of the model error compared to the scatter of the persistence model. A skill score close to 1 indicates very small scatter of the model error, scores close to 0 indicate that the model does not perform better than the persistence model and scores below 0 indicate that the persistence model outperforms the model, ie the model can not be used.

As can be seen from this figure the scatter of the persistence model is quite small for the first 6 hours, it then rises gradually out to at least 36 hours but probably much further. As a base-line test of the abilities of the models developed in the following are compared to the abilities of the persistence model.

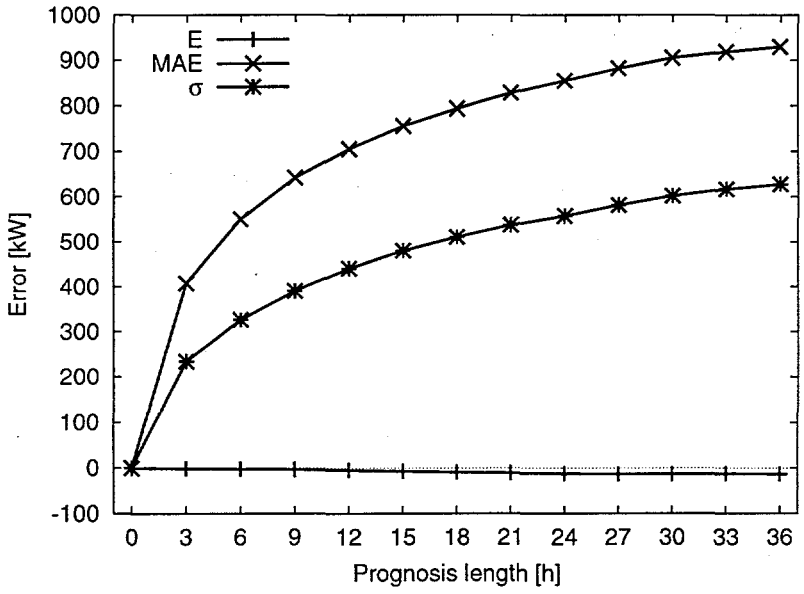

Figure 2. The mean error, E, *mean absolute error,* MAE, *and standard deviation,* σ, *(all in kW) versus forecast length in hours for the persistence model predicting the power produced from the Kyndby wind farm for the entire period. See figure for legend.*

4 The DMI Operational HIRLAM Forecasting System

A regional atmospheric forecasting system is operational at the Danish Meteorological Institute (DMI). The system is based on HIRLAM (High Resolution Limited Area Model). This forecasting system has been developed since 1985 by the national meteorological institutes of Sweden, Norway, Ireland, Iceland, Holland, Finland and Denmark. In addition, France and Spain have participated in the collaboration since 1992 . The HIRLAM level 1 system was established in 1988 (Machenhauer 1988). The operational system applied in this project is mainly based on HIRLAM level 2 (Gustafsson 1993).

The forecasting system is run on different areas. The coarse resolution model (GRV) run with a horizontal resolution of 0.42 degrees is forced with lateral boundary values from the ECMWF (European Centre for Medium range Weather Forecasts) global model. GRV provides input to the fine scale model (DKV) having a resolution of 0.21 degrees and used in this project. Both models are run with the same vertical resolution (31 pressure- hybrid coordinates) and carry out independent 6-hourly intermittent data-assimilation cycles.

The DKV model makes 36 hour forecasts from 00 and 12 UTC and it is those forecasts that has been used as input to the DMI and Risø models applied in this project.

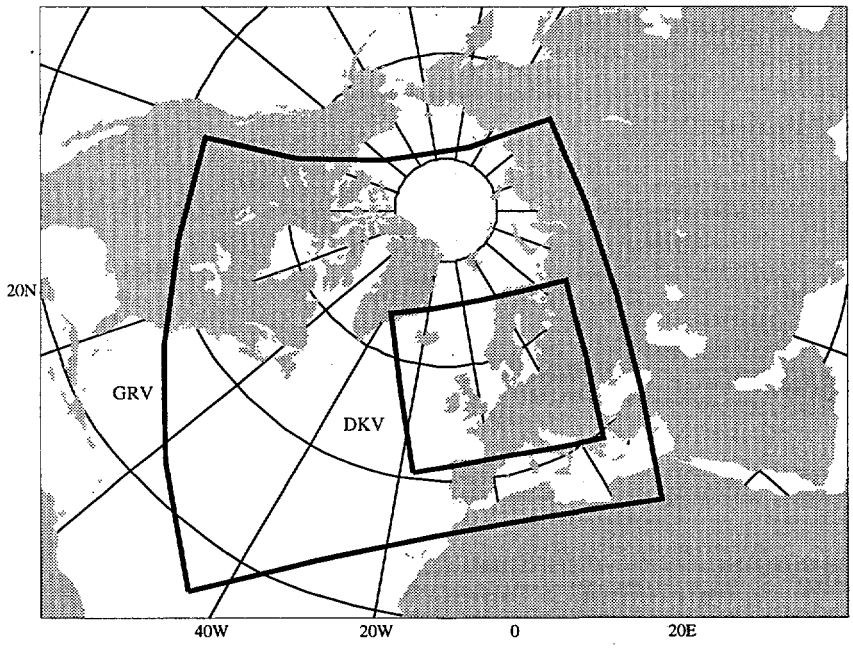

Figure 3. The geographical areas covered by the GRV and the DKV models.

5 The DMI Model

In this section the physical model of the Danish Meteorological Institute is described.

5.1 Statistical interpretation in meteorology

Objective forecasting of specific weather elements is often done by some kind of statistical interpretation of weather model data. Model Output Statistics (MOS) is the common name for the methods used.

In traditional MOS, the forecasts are made using a fixed set of equations describing the statistical dependency of the weather elements upon weather model forecast parameters. The equations are established on the basis of long series of corresponding observation and model data. Other data types can be used together with weather model data as input to the system (e.g., observations available at the time the forecast is produced).

Another type of statistically based forecasting, the so-called Perfect Prog scheme, exploits statistical relations between the parameters to be predicted and other observable quantities which the weather model is assumed to predict without bias.

The main advantage of the MOS methods as compared to Perfect Prog methods or raw model output is that systematic errors in the weather model forecasts are to some extent taken care of. The great disadvantage is that the statistical relations lose validity as a result of the frequent changes in operational weather models.

As a consequence, in these years the traditional methods are giving way to self-adaptive techniques in which the equations relating model data and observations are updated along the way. The Kalman filter, used in the present investigation and described below, is one such technique.

5.2 The Kalman filter

The Kalman filter was originally devised around 1960 by R.E. Kalman and R.S. Bucy for engineering applications (Kalman, 1960; Kalman and Bucy, 1961). A key reference in the Kalman literature is Harrison and Stevens (1976). Meinhold and Singpurwalla have given an instructive explanation of the Kalman filter in (1983). We will limit ourselves to the discussion of the simple linear filter used in the present study.

Let $Y = (y_1, y_2, ..., y_m)$ designate the m observable quantities which we want to predict, and let $F = (f_1, f_2, ..., f_n)$ be the n known quantities from which we would like to make the forecast. Y could be the wind force at some measuring site, in which case the f's would typically include weather model forecast wind force at some level at a nearby gridpoint. Y and F are the *vector of predictands* and the *vector of predictors*, respectively. The underlying statistical model of the Kalman filter can be expressed in two equations describing the dependency of Y on F and the change of this dependency with time:

Everywhere in the following, t is a time variable taking on discrete, equidistant values t = 0,1,2,... The first equation, the *observation equation*, states that Y and F are at any time t approximately linearly related,

$$Y(t) = F(t)\theta(t) + v(t). \tag{6}$$

Here, $\theta(t)$ is an $n \times m$ matrix describing the statistical dependency of Y on F at time t. $\theta(t)$ is an unknown matrix which can be thought of as the matrix of "true" regression constants connecting F and Y at time t. The vector $v(t)$, of dimension

m, is the error, which we assume is normally distributed with zero mean and a known variance $V(t)$:

$$v(t) \approx N(0, V(t)), \tag{7}$$

$$V(t) = E(v(t)v^T(t)). \tag{8}$$

The second equation, the *system equation*, describes the change of θ with time:

$$\theta(t) = G(t)\theta(t-1) + w(t) \tag{9}$$

The $n \times n$ matrix $G(t)$ is a *known* matrix expressing the trend of θ at time t; $w(t)$, *the system error*, is an n-dimensional error vector assumed normally distributed with zero mean and known variance $W(t)$:

$$w(t) \approx N(0, W(t)) \tag{10}$$

$$W(t) = E(w(t)w^T(t)) \tag{11}$$

Note that the statistic relation between the vector of predictors and the vector of predictands (described by θ) evolves in time as a result of both deterministic and stochastic processes (described by G and w, respectively). It is this last, stochastic part that makes the Kalman filter a self-adaptive system.

For the Kalman model to be a good description of any given piece of reality, the time scale of changes of θ must of course be very much longer than the time step and the time scales of the errors.

At time t (or a little after), when we wish to issue a forecast of Y valid at time $t+1$, the situation is as follows:

We know the value of the vector of predictors at time $t+1$, $F(t+1)$. We also know the corresponding values of F and Y at all times 0,1,2, ..., t up to now. Our aim, then, is from this data to get an estimate of the value of $\theta(t+1)$ to apply in Eq. 6.

This estimate can be arrived at in a recursive way, provided we know (or postulate) the values of G, V, and W at all times and can put up some (educated) guesses of the values at time zero of θ and one other parameter, S:

Suppose that, *before* observing $Y(t)$, we possessed an estimate $\hat{\theta}(t-1)$ of the value of θ at time $t-1$, and suppose this was the best estimate possible with the data then available. By (9), the best guess for $\theta(t)$ at that time was $G(t)\hat{\theta}(t-1)$, and the forecast for $Y(t)$ would have been

$$\hat{Y}(t) = F(t)G(t)\hat{\theta}(t-1) \tag{12}$$

According to (9), θ is at all times s normally distributed with a mean of $G(s)\theta(s-1)$ and variance $W(s)$. Assume that, in addition to $\hat{\theta}(t-1)$, we also had the variance $\Sigma(t-1)$ so that the best possible guess of the distribution of $\theta(t-1)$ at that time was

$$\theta(t-1) \sim N(\hat{\theta}(t-1), \Sigma(t-1)) \tag{13}$$

This is the *posterior* distribution of $\theta(t-1)$ in the Bayesian sense.

The recursive step comes into play when, after time t, we know the verifying $Y(t)$:

By means of probability theory (see, e.g., Meinhold and Singpurwalla (1983) for the proof) it can be shown that the posterior distribution of $\theta(t)$, i.e., the best possible guess of the distribution given $Y(t)$, $F(t)$, and (13), is expressed by

$$\theta(t) \sim N(\hat{\theta}(t), \Sigma(t)) \tag{14}$$

where

$$\hat{\theta}(t) = G(t)\hat{\theta}(t-1) + R(t)F^T(t)(V(t) + F(t)R(t)F^T(t))^{-1}e(t) \quad (15)$$

$$\Sigma(t) = R(t) - R(t)F^T(t)(V(t) + F(t)R(t)F^T(t))^{-1}F(t)R(t) \quad (16)$$

with

$$R(t) = G(t)\Sigma(t-1)G^T(t) + W(t) \quad (17)$$

$$e(t) = Y(t) - \hat{Y}(t) = Y(t) - F(t)G(t)\hat{\theta}(t-1) \quad (18)$$

All the terms in equation 14 can be evaluated at this point, and we are one step further in the process. We see that if we start out with some reasonable guess of $\hat{\theta}(0)$, $\Sigma(0)$, the procedure will give us the best possible $\hat{\theta}(s)$, $\Sigma(s)$ after observing $Y(s)$ for every subsequent time s.

Finally, the forecast we will issue for time $t+1$ is

$$\hat{Y}(t+1) = F(t+1)G(t+1)\hat{\theta}(t) \quad (19)$$

Experience shows that, provided the Kalman model is basically a sound description of the process in question, poor first guesses of $\hat{\theta}$ and Σ soon loose their influence -or, in other words, after a number of time steps $\hat{\theta}$ and Σ are virtually independent of the first guess.

More important is the choice of V and W. These functions determine the "memory" or "stiffness" of the system: Small values of V and/or large values of W give a sensitive filter reacting quickly to new data (including noise); with the opposite one gets a conservative, slowly adjusting system.

In many meteorological applications, as in the one described below, V and W are chosen as constants, independent of time, and G is set equal to the unit matrix, i.e., no systematic trend in θ is assumed.

5.3 The data

Model data

The data used to model the physical behavior of the wind at the chosen locations is taken from HIRLAM (HIgh Resolution Limited Area Model) of the Danish Meteorological Institute (DMI). We have used the wind data from the lowest level in the model (30 m a.g.l.). The data is modelled on a grid with a horizontal resolution of 23 km. So, in order to use it for the wind mill parks in the project, we had to apply a simple vector interpolation scheme. Hour of analysis is 00 and 12 UTC; time projections are +00 to +36 hours with 3 hours intervals (the "+00 hour forecast" is the analysis).

Observation data

The data from the wind farms was taken from ELKRAFT's FLEXMON systems data distribution. They were the readings directly from each mill in the park, consisting of power (kW) and wind speed (m/s) measurements. The data was collected every hour, day and night. In our project we only needed the data from every 3 hours, and only the gross value for the whole wind farm; therefore we averaged the data over the mills in the wind farms giving us a value for a norm mill.

The time stamps are given in Local Danish Time (without Daylight Saving), and they are not certain to be stated on the hour, but most often several minutes later because of the time the Flexmon system needs to scan all the wind farms.

5.4 Applying the Kalman filter

To apply the Kalman filter we have to find the best choices of predictors and predictands. The most elegant choice would have been the forecasted wind speed as predictor and the electrical power as the predictand. But this approach is not feasible because of the non-linearity of the wind-power relation which makes the prognosis too sensitive to the wind errors. Instead we used a simpler approach in which we Kalman filtered the wind speed (i.e. had wind speed as the predictand) and used the Kalman filtered value as entry in an empirical wind-to-power relation. The wind-to-power relation used was found from the data presented prior to the project start but was updated regularly. One such relation is seen on figure 4, showing the best fit of the observed data of Kappel

In appendix A we show the relations as well as the observations for all 17 wind farms (figures 47 to 49).

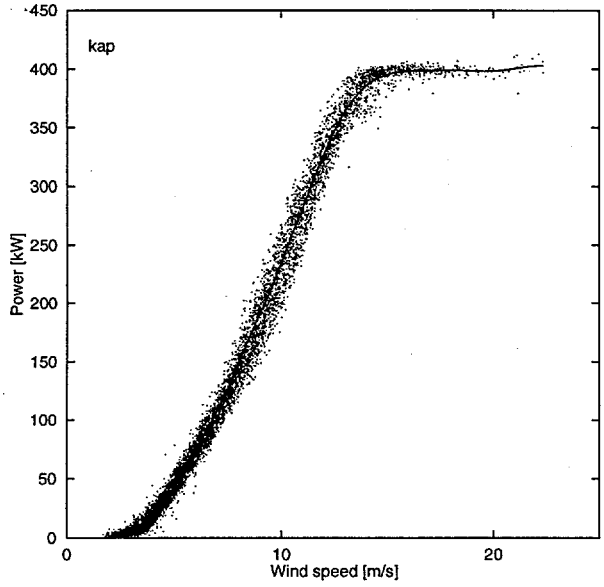

Figure 4. The best fit of the observed wind-to-power relation for the Kappel wind farm. The data for Kappel consists of measurements of the power and wind speed for 24 mills. These have all been averaged to give a norm mill. The dots are the observed data averaged over all mills in the farm, and the solid line is the best fit to the curve.

5.5 Overview

The data flow from the raw HIRLAM data to the final wind power forecasts is shown below in figure 5. In figure 6 the Kalman filter updating is shown.

The two processes, prediction and Kalman filter updating, is shown as two separate data flows. The reason for this is that the two processes actually runs independently of each other. Of course the prediction process needs the Kalman filters in order to work, but the two processes do not nessecarily need to be running synchronously or even be in the same system. The prediction process just wants some Kalman filters to be there, and do not care whether these have been updated today or a year ago; of course the prediction process always try to use the newest filters. On the other side, the Kalman filter process just reads its data and update if possible, and do not care whether the filters are being used or not.

This separation of the two systems was essential to our project as the data flow of the observations was very unsteady - they came in big chunks about every 6-8 weeks.

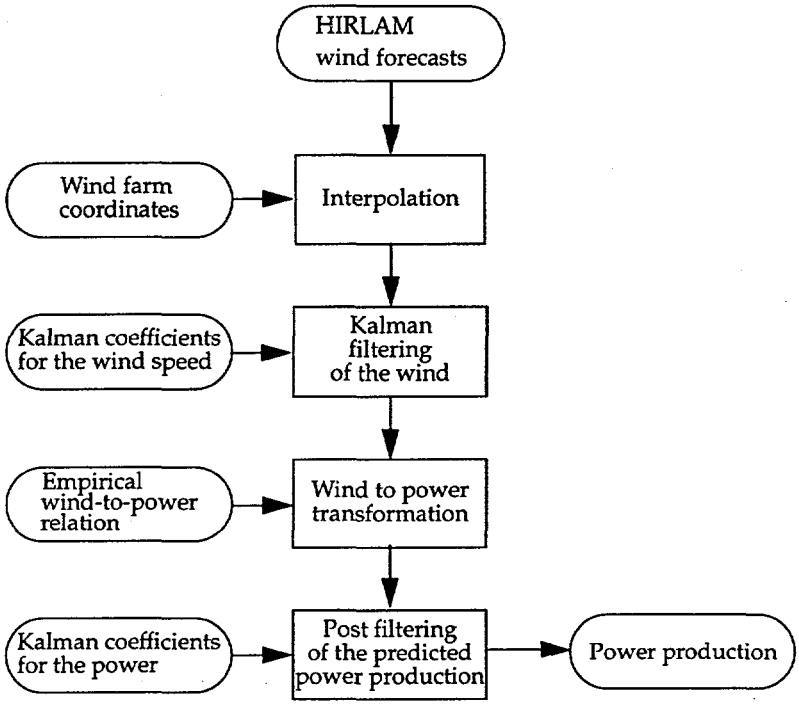

Figure 5. The data flow when predicting the power production.

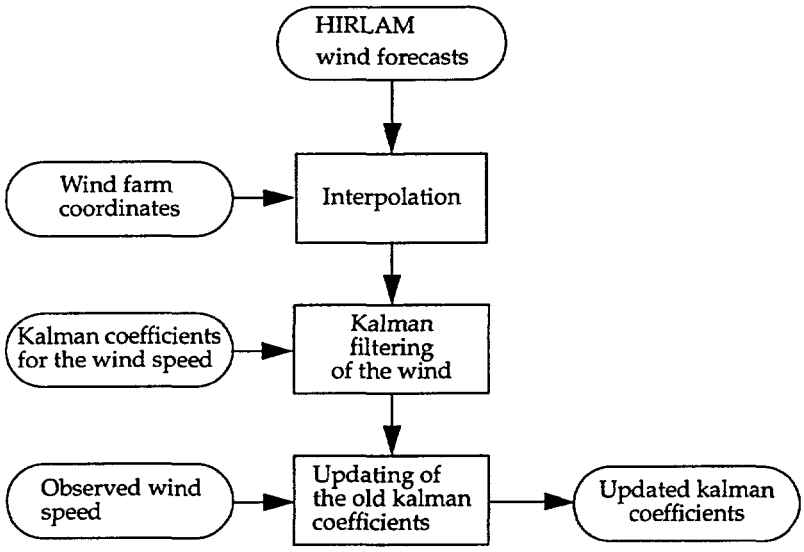

Figure 6. The data flow when updating the Kalman filter coefficients.

Why the post Kalman filtering?

Our model is constructed to have a mean error equal to zero in the value it forecasts, but since it is not the electrical power we optimize our model upon but the wind speed we cannot be sure that this is also true for the power.

In figure 7 we see the mean error and mean absolute error for the forecasted DMO wind speed for the Østermarie wind farm (oem). The left frame shows the errors when no Kalman filtering is done, and the right shows the effect of the Kalman filtering. The advantage of the Kalman filtering method is clear; we get a mean error very close to zero for all prognosis lengths and a mean absolute error between 1.1 m/s and 1.5 m/s.

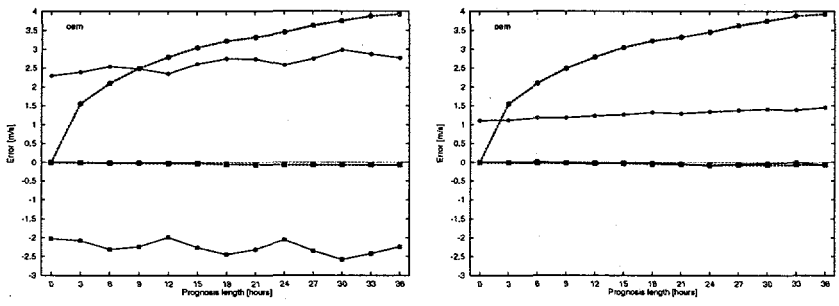

Figure 7. Mean errors (squares) and absolute mean errors (circles) for the wind forecast vs. prognosis length for the Østemarie wind farm. Open circles and squares are the persistence. Left is before Kalman filtering and right is after.

With this in mind we now turn to figure 8 to inspect what will happen when we use our approach, i.e. use a forecasted wind speed as an entry in a wind power curve. Let W_0 be the Kalman filtered wind speed forecast; dW its error, symmetric about W_0; P_0 is the derived power forecast corresponding to W_0 . If the wind-to-power relation is linear the error of P_0 is also symmetric, and will be averaged out in greater samples, but if the relation is non-linear the symmetric error interval around W_0 will not nessecarily be imaged into an symmetric interval on the power axis, and thus will not average to zero even in greater samples. When the curvature of the wind-to-power relation is positive the spread around the mean will be biased towards the higher values giving a positive bias, and if the curvature is negative it will be biased towards the lower values yielding a negative bias. The result of this is seen in the left frame of figure 9. To eliminate this effect we applied a second Kalman filtering to the end result using the forecasted electrical power as predictor and a non-biased electrical power forecast as predictand. In the right frame of figure 9 we see the effect of using an additional Kalman filter on the derived power production: the mean error is reduced while the mean absolute error is not changed. We see that we will benefit from using two Kalman filters: one for filtering the raw model wind speed, and one for filtering the derived power production. In the appendix A we list the initial and resulting Kalman coefficients for the wind speed filtering (tables 5 and 6) as well as for the post-filtering of the derived electrical power (tables 7 and 8).

5.6 Results

Verification

The forecast data is given in 3-hour resolution and the observational data is given for all hours. This means that we have a lot more data points for the persistence

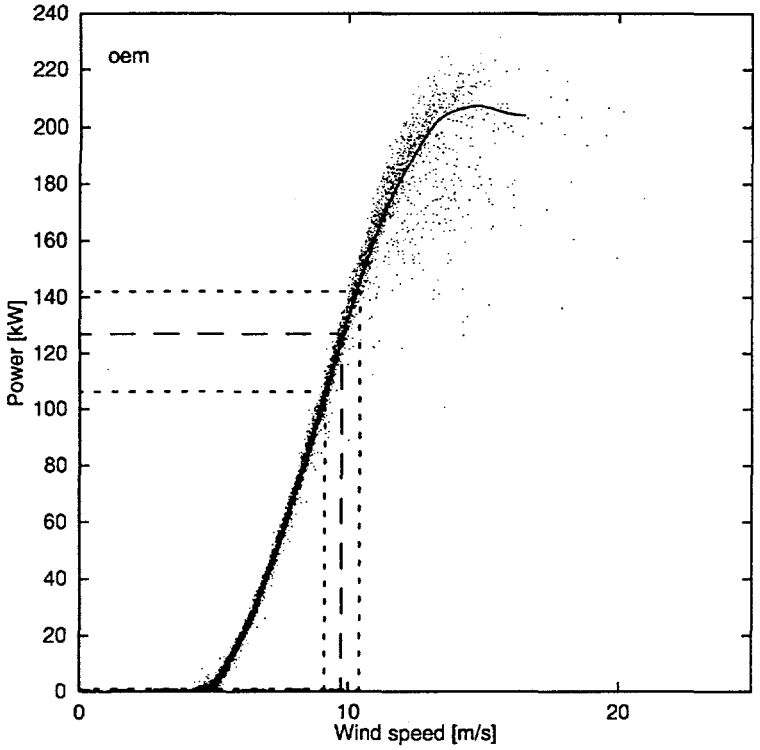

Figure 8. The wind-power relation for the Østermarie wind farm used as an example showing the effect of the non-linear imaging.

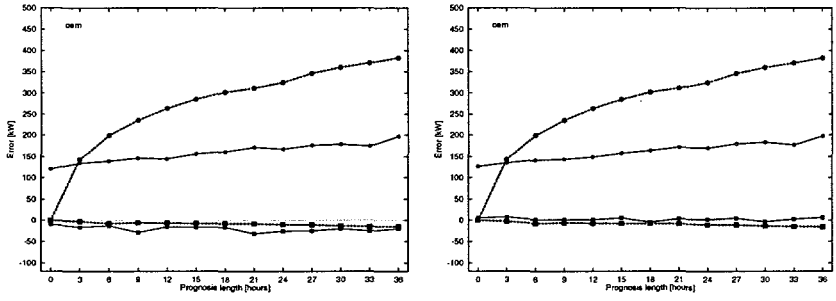

Figure 9. Mean errors (squares) and absolute mean errors (circles) for the electric power forecast vs. prognosis length for the Østemarie wind farm. Open circles and squares are the persistence. Left is before Kalman filtering and right is after.

approach than for the model approach. The forecasts is always stated on the hour while the observations most often is somewhere in between two hours. This means that we have to decide whether we will use the nearest data point or apply some interpolation scheme - we chose the latter. The interpolation was simply linearly in both the wind and the power production. A draw-back of this method is the greater data loss because we for the interpolation to work need to have 2 adjacent data points, while we in the "nearest point" scheme just needs one within one hour. We only interpolate if the two data points lie within one hour from the interpolation time.

The total power production

We define the total power produced as the sum of the production in all farms in the sample that are producing power at the precise moment. For the error-measures to be justified in the total power production we cannot tolerate missing farms at any time, so in the verified production time series we only include those observation times for which all farms are reporting. With this restrictive approach the total data cover only sums to about a few percent of the time, so in order to increase the data coverage of the total sum we exclude those wind farms that have too small a data cover. Table 3 in the appendix A lists the data coverages for all farms; we see that the coverage range from 24% to 76% (see also the figure 46 in appendix A). If we place a limit at 60% we get 10 wind farms in the restricted sample (table 4) excluding Prejehøj (pre) which lacked data prior to the project. The total itself is not postfiltered.

In figure 10 we see the performance for the prediction of the total power production.

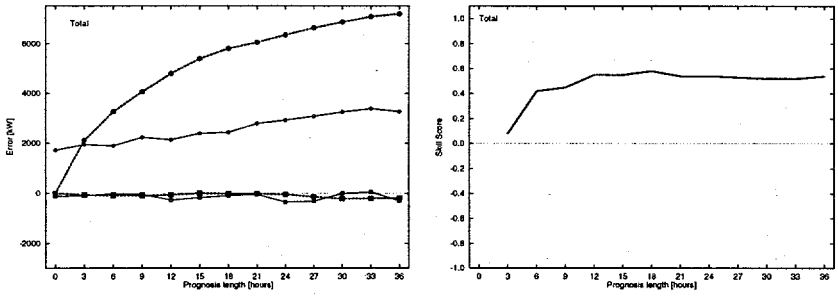

Figure 10. The ability of the model to predict the total power produced by the wind farms compared to the performance of the persistence model. In the left frame is shown the errors, where open symbols and dashed lines refer to persistence and filled symbols and solid lines to the model. Square symbols are the mean error (in kW) and round symbols are the mean absolute error (also in kW). The forecast length (in hours) is along the apsis. In the right frame is shown the skill score of the model over the persistence.

We see from the MAE that already from +3 hours the model wins over the persistence. This is also seen in the skill score frame.

In figures 11 and 12 we compare the scatter plots of the total for the model and persistence for both short and long term predictions. From these scatter figures we see that the model performs slightly better than the persistence in the short term predictions, but that there for the longer terms are no doubt about the usefulness of incorporating the weather forecast in the power prediction; the scatter for +24 hours is still along the ideal line for the model, but for the persistence the scatter looks more or less random. In the appendix A the scatter plots for the prognosis lengths +3, +6, +12, +24 and +36 hours is shown in figures 62 and 63.

From the appendix's figures 56 and 57 showing the relative error versus farm id we identify the best and the poorest farms as kvp (Kyndby) and skv (Skovlænge) respectively. The errors and skill score for kvp is shown in figure 13, and in figure 14 for skv. In the appendix A the scatter plots for the prognosis lengths +3, +6, +12, +24 and +36 hours is shown in figures 58 and 59 for kvp and in figures 60 and 61 for skv.

The errors and skill score for 16 of the 17 wind farms is shown in the appendix A in figures 50 to 57.

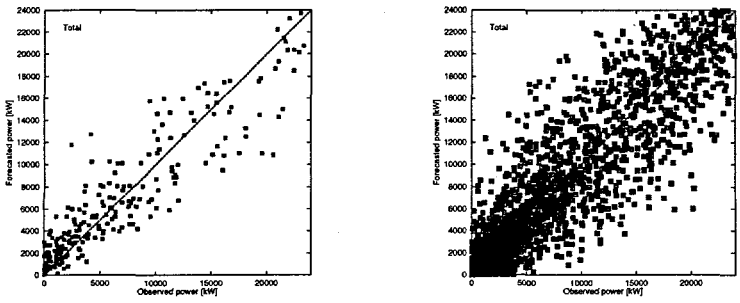

Figure 11. +3 hour forecast scatter plots for the total. At left the model and at the right the persistence.

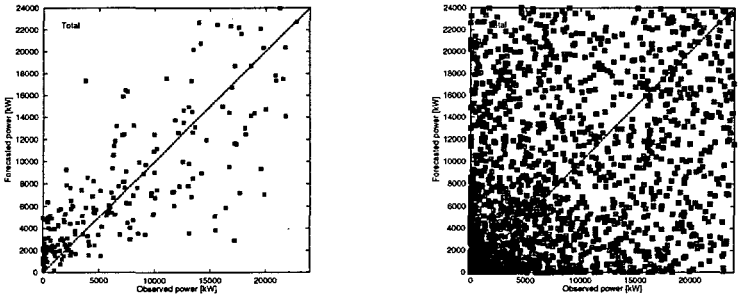

Figure 12. +24 hour forecast scatter plots for the total. At left the model and at the right the persistence.

5.7 Expanding to entire population

In this project we focussed on 17 wind mill farms belonging to the ELKRAFT population. From these 17 we choose 10 well behaved wind farms to construct a total power production forecast. But neither these 17 individual wind farms nor the total of the restricted sample have any practical use for the end user. What he needs to know for the forecast information to have any practical use is the predicted total production from all the wind farms in the ELKRAFT population. To this end we gained observations from the total wind mill farm system for the year

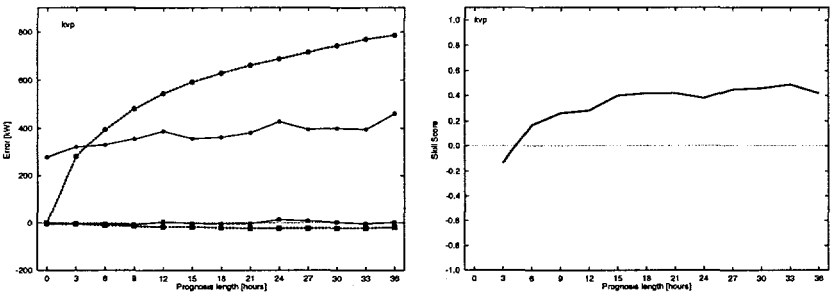

Figure 13. The performance of the model described here for the Kyndby wind mill farm. Left frame shows the errors, and right shows the skill score. The rated power of the Kyndby wind farm is 3780 kW. Open symbols and dashed lines refer to the persistence and filled symbols and solid lines to the model. Square symbols are the mean error (in kW) and round symbols are the mean absolute error (also in kW). The forecast length (in hours) is along the apsis.

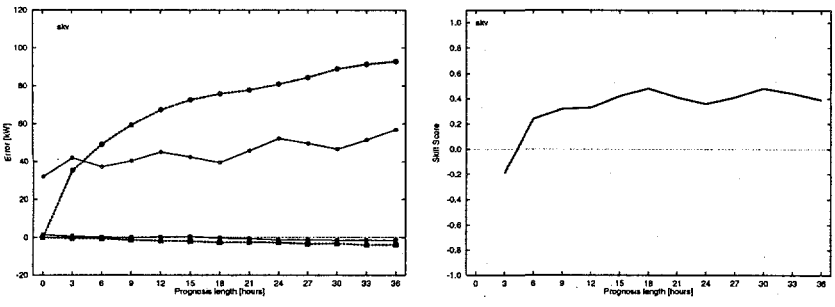

Figure 14. The performance of the model described here for the Skovlænge wind farm. Left frame shows the errors, and right shows the skill score. The rated power of the Skovlænge wind farm is 300 kW. Open symbols and dashed lines refer to persistence and filled symbols and solid lines to the model. Square symbols are the mean error (in kW) and round symbols are the mean absolute error (also in kW). The forecast length (in hours) is along the apsis.

1995 and used our restricted sample's forecast as predictor in yet another Kalman filtering yielding the predicted power production from the entire population as the predictand. This approach gives the result as seen in figure 15. We see that we perform better than the persistence from +6 hours and on. This is maybe more clearly seen in the skill score frame. The scatter plots is shown in the figures 64 and 65 in the appendix A. The initial and final Kalman coefficients are shown in the tables 9 and 10, respectively.

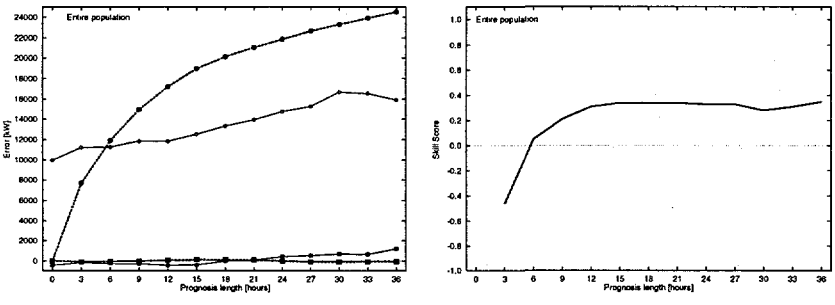

Figure 15. The performance of the model described here for the entire wind farm population. Left frame shows the errors, and right shows the skill score. The rated power of the entire population is 130 MW. Open symbols and dashed lines refer to persistence and filled symbols and solid lines to the model. Square symbols are the mean error (in kW) and round symbols are the mean absolute error (also in kW). The forecast length (in hours) is along the apsis.

6 The Risø Model

In this section the physical model of Risø National Laboratory is described. Each step, from selecting the HIRLAM wind to the final MOS corrections, will be described in turn. An overview of the model is given in Figure 16.

6.1 Overview

The forecasting system from the output from HIRLAM to the final forecast at the utility is sketched in Figure 16.

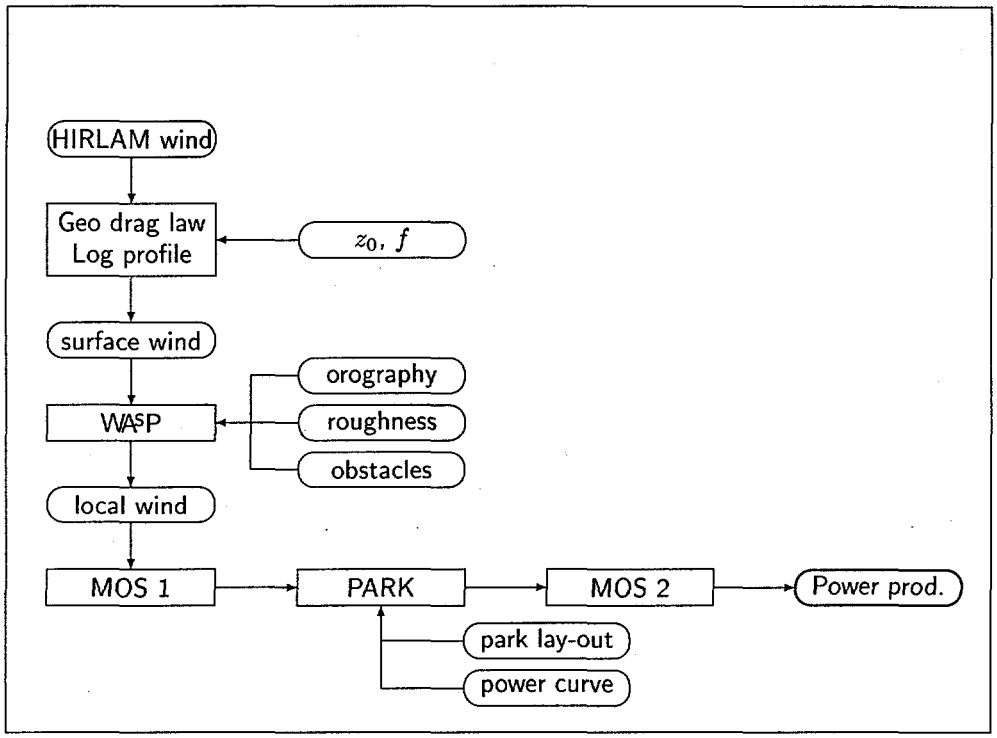

Figure 16. Flow chart of the model complex from the HIRLAM wind to the final prediction of the power output from a wind farm.

6.2 HIRLAM

The large-scale flow of the atmosphere is modelled by HIRLAM (DKV) of the Danish Meteorological Institute. The model has a horizontal resolution of 23 km and it is run twice a day at 00 and 12 UTC. For further details, see Section 4.

Finding the right HIRLAM level

Since HIRLAM has a vertical grid of 31 levels it is necessary to investigate which level gives the wind that best approximates the geostrophic wind (a theoretical wind). To do this an analysis has been carried out on a subset of the wind farms: Kappel, Kyndby, Vindeby, and Østermarie, where the model has been run with HIRLAM winds from level 1 (65 m) to level 7 (1050 m). The results are shown in Figures 17 and 18.

Analysing these two plots, a number of observations can be done:

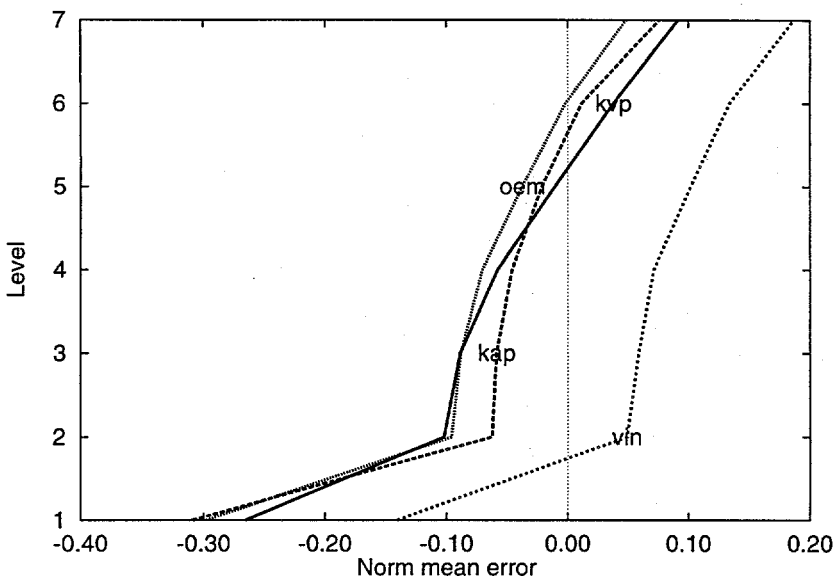

Figure 17. The mean of the error for the 12 hour prediction normalised with the total capacity of the wind farm as a function of the level.

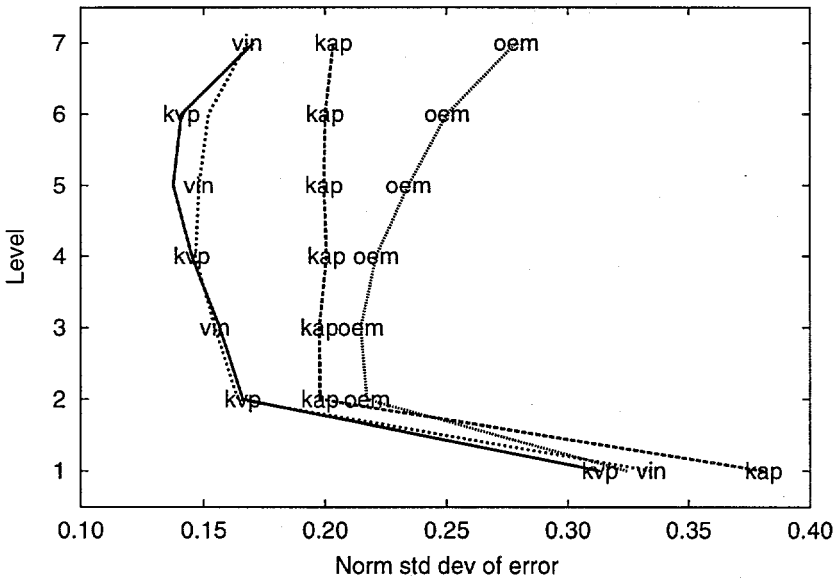

Figure 18. The standard deviation of the error for the 12 hour prediction normalised with the total capacity of the wind farm as a function of the level.

- Vindeby seems to be very different from the others, we will return to this in a later section. Here, we will not put emphasize on this station when drawing our conclusions.
- The mean error is closest to zero at levels 5 and 6.
- The std. dev. of the error is smallest again for levels 5 and 6

These observations lead to a choice between either level 5 or level 6. Level 5 have been chosen, because it has the overall smallest error and most stations have the smallest or second smallest std. dev. of the error. In the following, therefore, *the geostrophic wind, G, will be set equal to the wind obtained from level 5 (ie*

at 550 m agl) of HIRLAM. Note, that it is the *actual* HIRLAM wind which is used, not the geostrophic HIRLAM wind. It was found that this wind gave too high standard deviations of the error. This is in agreement with the findings in Landberg et al, 1993.

6.3 Surface transformation

The idea behind the physical model is that the predicted wind from HIRLAM, which is a wind specific to a gridcell of 23×23 km^2, is transformed to the surface using the geostrophic drag law (cf Blackadar and Tennekes, 1968),

$$G = \frac{u_*}{\kappa}\sqrt{\left[\ln\left(\frac{u_*}{f z_0}\right) - A\right]^2 + B^2} \tag{20}$$

where G is the geostrophic wind, here set equal to the HIRLAM wind at level 5, u_* the friction velocity, κ the Von Kármán constant (=0.4), f the Coriolis parameter, and z_0 the aerodynamic roughness length. A and B are constants here set equal to 1.8 and 4.5, respectively, in accordance with Troen and Petersen (1989).

The geostrophic drag law gives the friction velocity which can be used to get a velocity in the surface boundary layer by using the logarithmic wind profile

$$u(z) = \frac{u_*}{\kappa}\ln\left(\frac{z}{z_0}\right) \tag{21}$$

where $u(z)$ is the velocity at height z. These equations are in their neutral form. For further details, see Landberg and Watson (1994).

6.4 WA^{S}P

The wind calculated so far is still valid for quite a big area and it must be corrected to take local effects into account. This is done using WA^{S}P (Wind Atlas Analysis and Application Program, Mortensen et al, 1993). WA^{S}P is taking the following local effects into account:

- Shelter from obstacles (houses, wind breaks etc).
- Effects of roughness and changes in roughness.
- Effects of the orography, speed-up/down.

Note, that this list does not include thermally-driven effects as e.g. sea-breezes and katabatic winds. In most of Northern Europe (including Denmark) these latter effects will not be of any importance, and can thus be left out without any loss of accuracy. The problem of thermally-driven effects must be addressed, however, if the model is to be used in areas where those effects prevail (eg the Meditrainian).

From the previous study (Landberg and Watson, 1994 and Landberg et al, 1993) an estimate of the RMS error gave around 1.5 ms^{-1} for a typical station in Northern Europe. The study also showed that implementing MOS (Model Output Statistics) greatly improved the predictions for some of the stations, and as a consequence this method will also be used in this study to explain the effects not explained by the physical models.

The parameters in the MOS model will be estimated using detailed measurements from the 17 wind farms and model output from HIRLAM. The measurements consist of data from the individual turbines plus a number of meteorological parameters at each farm taken at one-hourly intervals.

A further refinement of the method could be to include time dependent roughness descriptions, this is due to the fact that roughness is actually a time-varying

quantity (eg trees have leaves in the the summer and none during winter), the only one in the list above. The time-variance of roughness is not taken into account in WASP because WASP is estimating climatological quantities (eg the yearly production), and therefore it would be wrong to let the roughness vary; in the present approach, on the other hand, we look at individual times, making it necessary to examine the inclusion of this time dependence. The time variability of the roughness could be included by making four different roughness descriptions: one for each season.

6.5 Model Output Statistics (MOS)

To correct for all effects not explained by the models, Model Output Statistics (MOS) is used. A number of different approaches can be taken.

Firstly, the functional form of the MOS filter must be chosen. Studying the behaviour of the error (cf Figure 19) it can be seen that the only reasonable candidate is the simple linear function:

$$y(\text{final}, \text{sector}) = y(\text{model}, \text{sector})a(\text{sector}) + b(\text{sector}) \tag{22}$$

where $y(\text{final}, \text{sector})$ is the final forecast, $y(\text{model}, \text{sector})$ the forecast from the physical models, $a(\text{sector})$ and $b(\text{sector})$ are the direction dependent constants of the linear function.

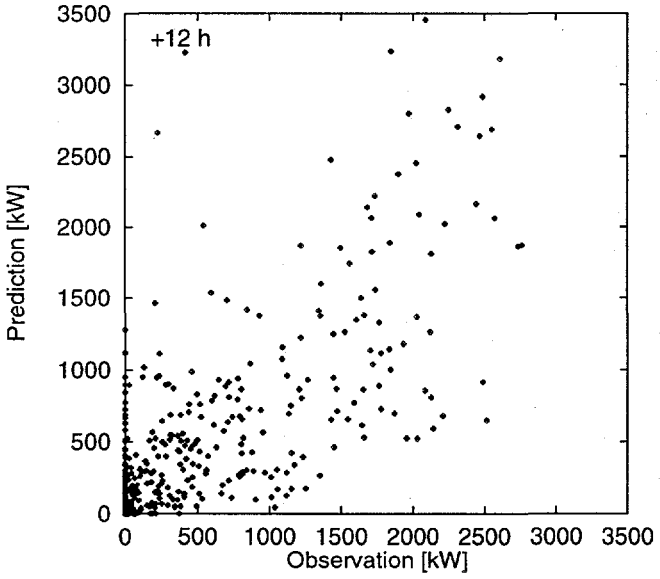

Figure 19. Scatter plot of the raw physical prediction vs the observation for the Kyndby wind farm for the 12 hour prediction length.

The second choice concerns the point at which the MOS filter is to be applied. Here a number of possibilities present themselves:

1. the output could be corrected right after the local wind has been calculated (and before the application of the power curve and the park effects).
2. to correct after the power has been calculated
3. to correct the end product of the model.

It has also to be decided whether MOS should be applied to the predictions as a whole or whether it should be applied to the predictions sector by sector. All these possibilities have been looked into and the findings are described in the following.

Before any MOS is applied it is necessary to determine whether any of the input to the physical models can be improved: is there eg a station which is consistently under-predicted, and is this station located in a flat area, then it is more than likely that the roughness assigned to the area is too high. It was found that if corrections are applied sector by sector (see later) they did not consistently stay under/over 1.0 for any one station. This means that the roughnesses most likely has been assigned the correct values. It could, however, also just mean that the signal for the effect of roughness is overwritten by signals from other error sources. It is therefore decided not to change the roughness for any of the stations.

Another reason for not changing the roughness lengths is that the values used are the standard values for the Danish landscape (cf Table 2).

Table 2. Standard roughness lengths, z_0, for typical Danish landscapes.

Type	z_0 [m]
Sea	10^{-4}
Village	0.35
City	0.4-0.5
Forrest	0.35-0.4
Farmland	0.1

MOS applied to the wind speed

There can be no doubt that the best place to apply MOS is as early as possible, namely, at the predicted local wind.

One could also apply MOS to the geostrophic wind itself, but this would make the statistical corrections the dominating part, and overshadow the abilities of the physical models to explain the local variation of the wind. This latter approach would therefore be more like a statistical approach, than a physical one. Since we have set out to use the available physical models as far as possible, correcting the geostrophic wind will not be done.

The observed wind is unfortunately measured *on* the nacelle of the wind turbines, causing severe flow distortion. On top of this the anemometers were never meant as precision devices for measuring the wind, so it has been decided not to use the speed measurements. Another very unfortunate thing is the fact that wind direction is not measured at all. We know, however, from a previous study (Landberg and Watson, 1994) that the direction is predicted fairly well. All this leads to the conclusion that MOS should not be applied directly to the wind speed.

MOS applied to the power

Taking the above findings into account, it is found that MOS must be applied to the power prediction. Since the power curve distorts the wind speeds quite significantly, leaving small variations in wind speed very important in some places and completely unimportant in others, the following procedure has been devised.

It is assumed that the real wind speed (of which we have no reliable measurement), $\hat{u}$, is connected to the predicted wind speed by the following simple relation:

$$\hat{u} = a_i u_{\text{pred}} \tag{23}$$

where a_i is the factor for the i'th sector and u_{pred} is the predicted wind speed.

Folding this back through the power curve, we get:

$$P_{\text{obs}} \simeq P_{\text{pred}} = p(a_i u_{\text{pred}}) \times T \times E \tag{24}$$

where P_{obs} and P_{pred} are the observed and predicted power, respectively, of a given wind farm, $p(u)$ is the power a given turbine will produce at speed u (ie the power curve), T is the number of turbines operating, and E the efficiency of the wind farm as calculated by PARK (see Section 6.6).

It is then possible to find that a which for a certain sector gives the smallest value of the error:

$$e = |P_{\text{obs}} - P_{\text{pred}}| \tag{25}$$

The functional shape of e as a function of a can be seen in Figure 20. It can be seen that the function is well behaved, which means that simple methods for minimising e can be used.

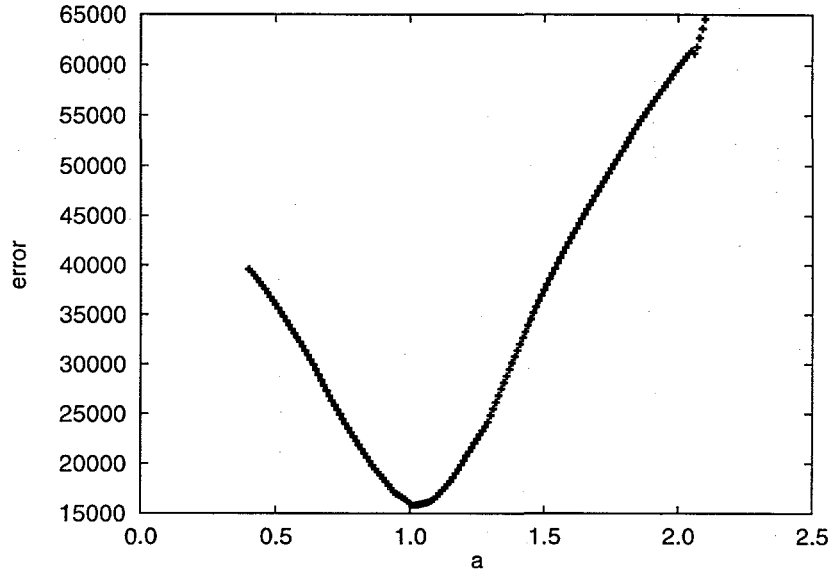

Figure 20. Typical example of the error, e, plotted as a function of the MOS parameter a.

Estimating the final a's

Following the above procedure a value for a can be calculated for each sector and for each forecast length. Doing this, a typical example of the calculated values is found in Figure 21. As can be seen from this figure, most of the calculated a's do not vary with the forecast length. This is also to be expected, since it is hypotesised that the effects, that the a's correct for, are *physical* effects, which are independent of the forecast length. Some sectors, however, display quite a large variation (in the figure, sectors 1, 2 and 11), this is explained by the fact that the number of samples in these sectors is down to only 25% of the average number of samples for all sectors, and these sectors are thus not statistically stable.

To calculate one a per sector (ie to collapse the a's in the forecast length direction) the weighting function shown in Figure 22 is applied to the a's from each forecast length. The weighting function is biased towards the important range of forecast lengths, ie from 12 to 27 hours. The initial forecasts from 0 to 6 hours are given low weights and the long-range ones are given medium weight. The factors

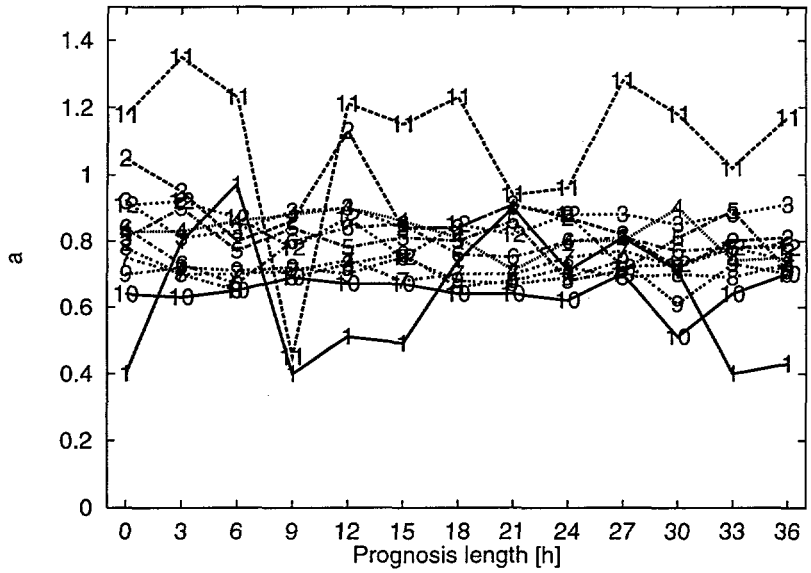

Figure 21. The MOS-correction factor for each of the twelve 30 degree sectors for the different prognosis lengths.

calculated in this way are listed in the tables for each of the selected wind farms in Appendix B.

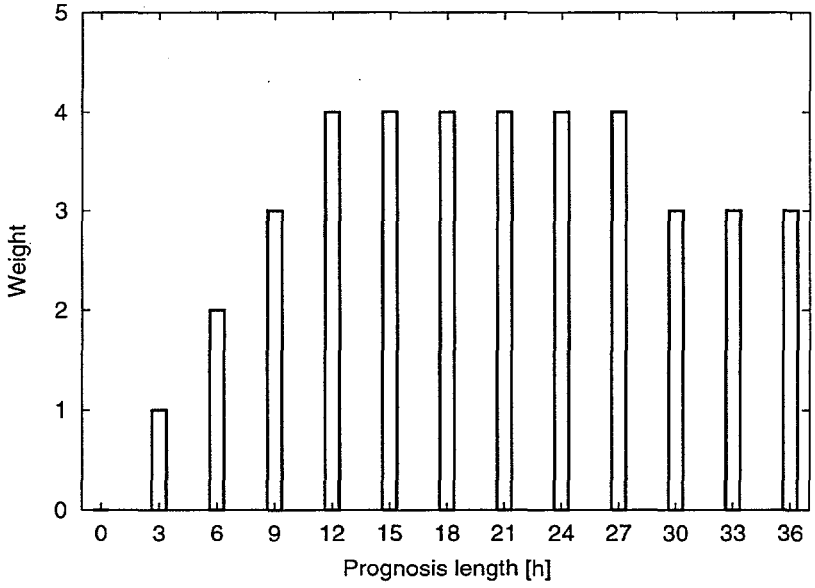

Figure 22. The weighting function used to weight the a's calculated for each forecast length.

A final question pertaining to the sector-wise corrections is the constancy with time of the estimates, ie for how long must one wait until the factors have stabilised. A typical example of this is given in Figure 23. Studying this figure it can be seen that most factors are stable after only a few months, except of course seldomly visited sectors (1, 2 and 12 in the figure). Sector 3 stands out in that the total amount of observations over the year is large enough, but during the first few months very few observations are present, explaining the marked swing after two months. The pattern found for this wind farm is repeated for the other wind

farms as well.

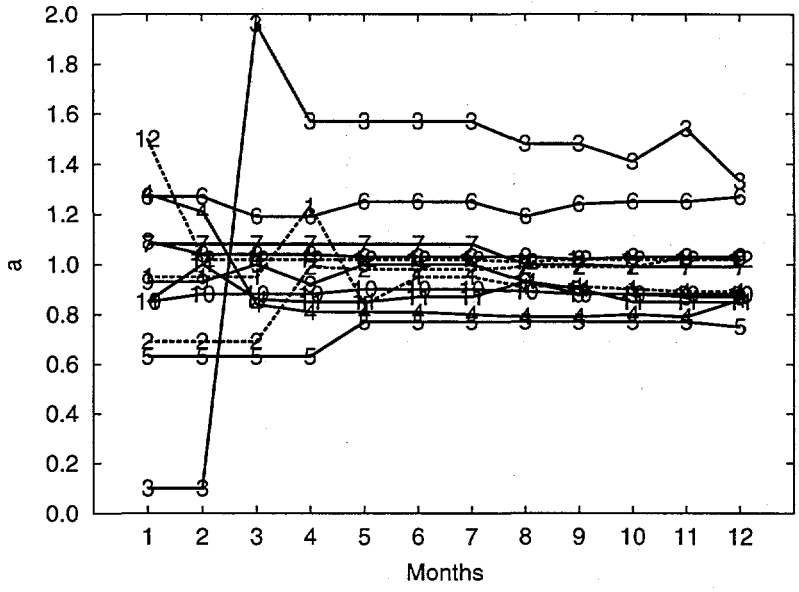

Figure 23. The variation with time of the estimate of the sector-wise MOS correction factor. Sectors with very few observations are marked with dashed lines. The data are taken from the Nøjsomhedsodde Wind Farm.

MOS applied to the final output

To correct for any *bias* another simple MOS model has been chosen to correct the *final* output of the model, ie the actual production of the park. A simple linear version of MOS is again used

$$P_{\mathrm{MOS}} = P_{\mathrm{model}} + b \tag{26}$$

where P_{MOS} is the MOS-corrected production of a given wind farm (ie the final result of the model), P_{model} the production predicted by the physical model, and b the bias. Note that b is not dependent on the sector, since it is assumed that the first MOS module took care of any directional differences.

6.6 PARK

To take into account the influence of wakes hitting other turbines in the park the PARK program (Sanderhoff, 1993) has been used to create a park efficiency rose (ie a sector-wise list of the actual production seen relative to the rated production). This rose is listed for each of the wind farms in Appendix B.

6.7 Input to the model

To be able to predict the power output of a wind farm the following input is needed:

- HIRLAM wind field (Geo. drag law)
- description of orography (WAsP)
- description of roughness (WAsP)
- description of obstacles (WAsP)

- power curve (PARK)
- thrust curve (PARK)
- wind farm lay-out (PARK)
- measurements of actual power production (MOS)

Note that this information, except for the HIRLAM forecast, is needed only for the initial analysis of the wind farm, once the farm is analysed the prediction model uses only the results of the analysis. To have a truly operational model information about the status of each turbine in each wind farm is needed in order to be able to scale the wind farm productions correctly.

HIRLAM wind field

An example of the HIRLAM wind field is given in Figure 24.

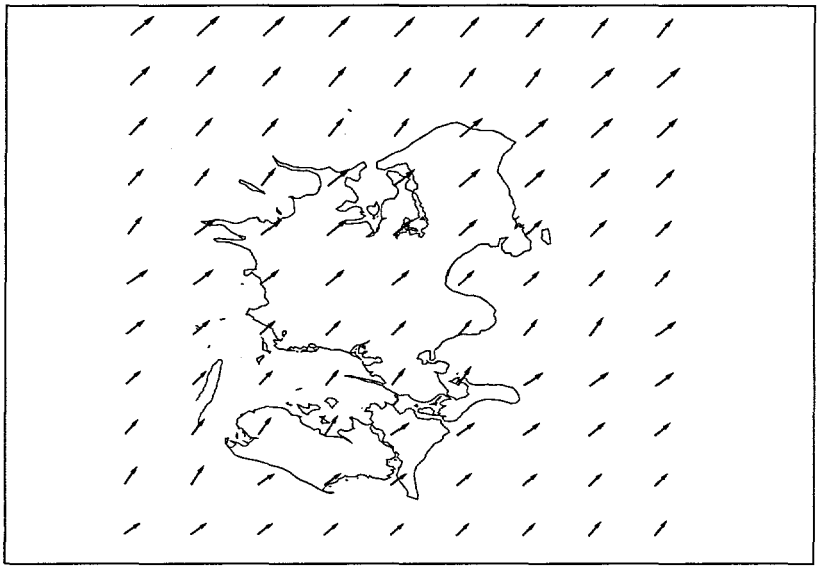

Figure 24. An example of the wind field from HIRLAM. A similar field is generated for Bornholm.

Input to WA^{S}P

For WA^{S}P to be able to simulate the local effects, input of the orography, roughness and obstacles are needed. In Figure 25 the orography and roughness of the surroundings of the Kyndby wind farm are shown and in Figure 26 the obstacles of the Avedøre 1000 wind turbine are shown. The orography is taken from the digital terrain database of the Danish National Cadastre, with a resolution of 2 m. The roughness has been assigned manually from 1:25,000 scale maps using the values given in Table 2.

Input to PARK

The PARK program needs as input the power and thrust curves (see Figure 27 and the wind farm lay-out (see Figure 28).

In the beginning of the project the standard powers curve given by the manufacturer were used, but referring to Figure 29 it can be seen that the actual

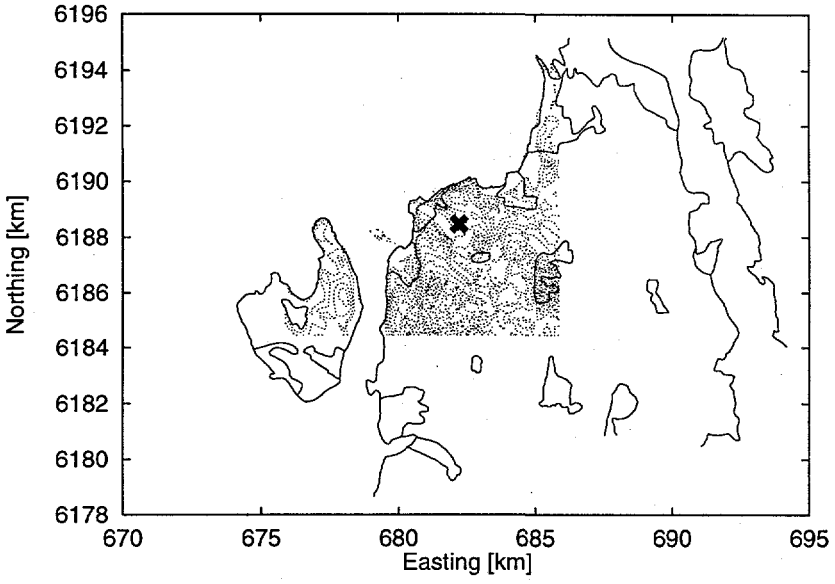

Figure 25. The orography (dotted lines, thinned) and the roughness (thick lines) for Kyndby wind farm. This digital information is given as input to WA^{S}P. The cross marks the location of the wind farm.

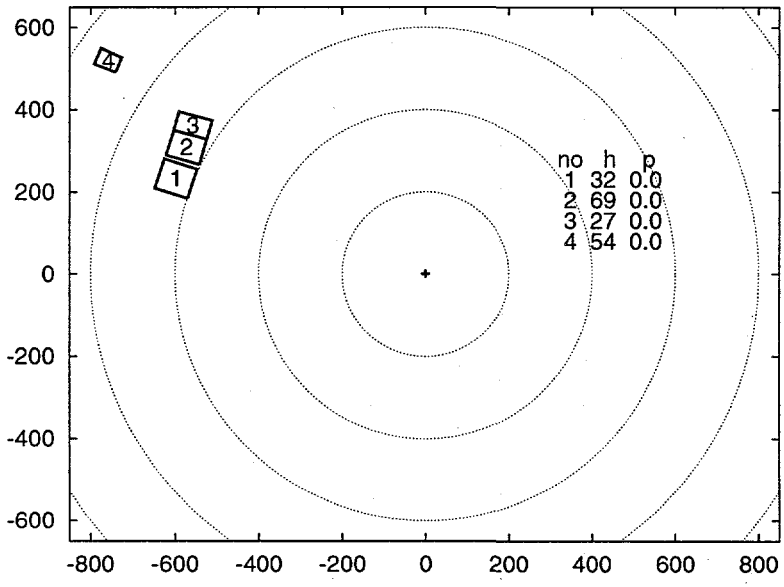

Figure 26. The obstacles input to WA^{S}P for the Avedøre 1000 turbine. The table embedded in the figure gives the height, h, in m and the porosity, p, (0=solid) for each of the obstacles.

performance of the turbine is somewhat different. This led to that, for each of the wind farms, the power curve was reassessed. Unfortunately, this introduces an additional error source, since the wind speed measurements on which the new power curves are based are somewhat incorrect.

In Appendix B the orography, roughness, wind farm lay-out, and the power curve are shown for each of the 17 wind farms.

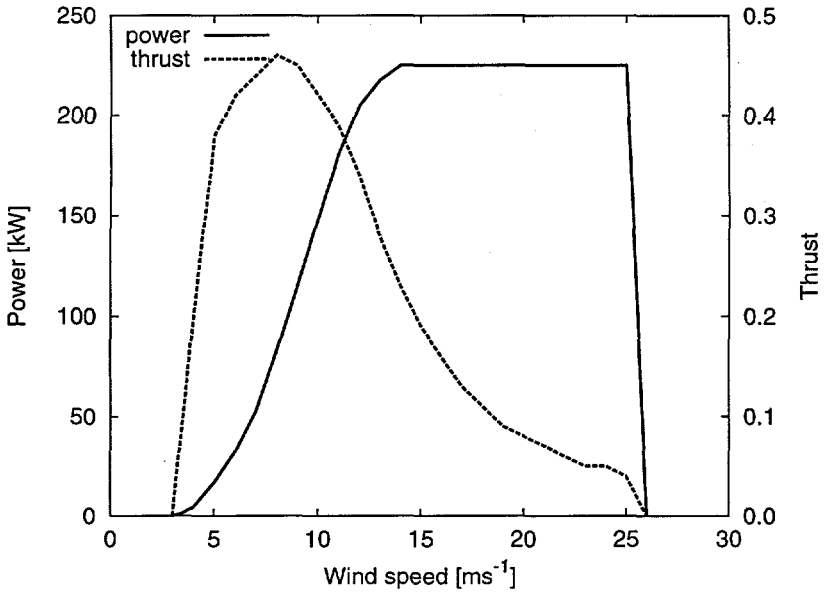

Figure 27. The power (solid line) and thrust curve (dashed line) of the Vestas V27 wind turbine.

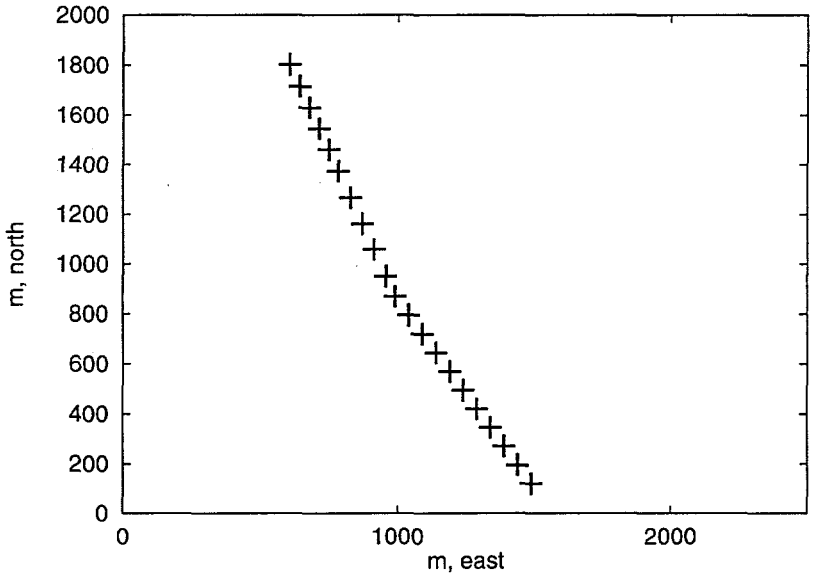

Figure 28. The lay-out of the Kyndby wind farm.

6.8 Output from the model

For ease of electronic transfer, the model output is sent as plain ASCII text files via a modem connection. An example of such a text file is given in Figure 30.

The files contain the 13 forecasts (from +0 to +36 hours ahead) for the total production and for each wind farm. It is imagined that the utility then have a program which displays the forecasts in a user-friendly form. An example of this is given in Figure 31.

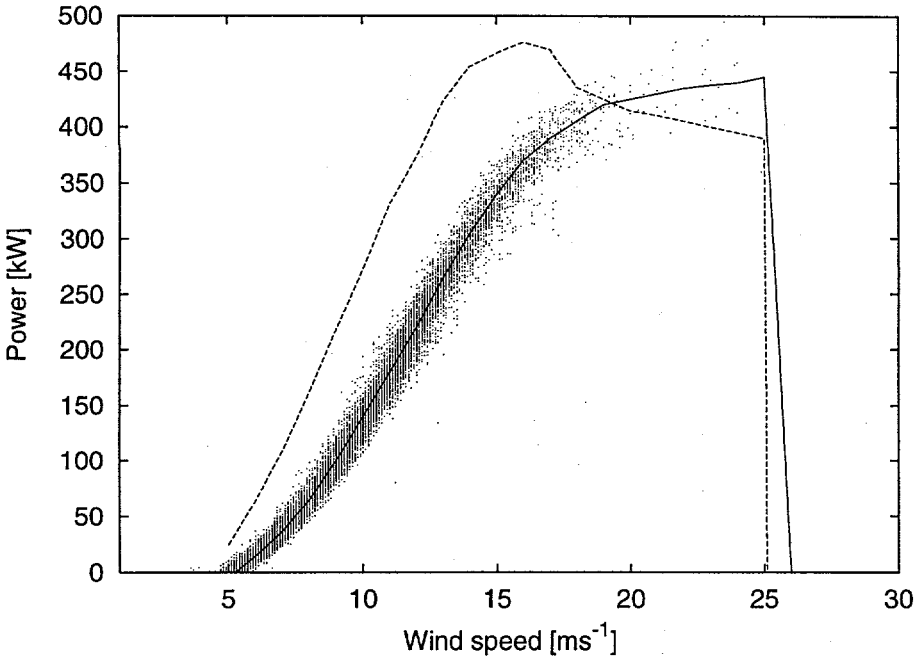

Figure 29. The observed power plotted against the observed wind speed. The solid curve is the power curve used in the project, the dashed the power curve supplied by the manufacturer (taken from the European Wind Turbine Catalog).

6.9 Results

This section will give a description of the results obtained. A few aspects of the model and the data will be discussed in some detail in the next section.

The model has now run for an entire year and it is possible to draw some firm conclusions as to its performance. Two aspects will be focused on: the ability of the model to predict the power output of individual wind farms and the ability of the model to predict the total wind-farm-produced power.

To get an estimate of the skill of the method the predictions are compared to the those of the *persistence* model, described in Chapter 3.

A comparison between the predictions for the Kyndby wind farm of the two models is shown in Figure 32. It can be seen from this that in the first four hours the persistence model performs better than the developed model, after that the model is superior. It can also be seen that – as was the case with the model predicting the wind only (Landberg and Watson, 1994) – that the standard deviation of the error seems to be rising only very slowly with time.

The qualitative results found for the other wind farms are much like the ones found for Kyndby. There does not seem to be any explanation why some stations perform better and some worse, other than natural variations. A complete overview of the performance of the model for all the wind farms is given in Appendix B.

Turning now to the prediction of the *total* power, a subset of the 17 wind farms have been chosen. The reason for not including all the wind farms is that the number of observations for some of the farms is quite low, due to technical problems with the data acquisition system. The subset consists of 10 wind farms (8 on Zealand and 2 on Bornholm), totalling 24.0 MW, which all have an around 70% recovery rate (cf Table 1).

Comparing the result of the model to that of the persistence model the results plotted in Figure 33 are found.

To compare the results of the model to that of the persistence model the *skill*

```
------------------------------------------------------------
                    EFP prognose
------------------------------------------------------------

  Prognose ID: HIRLAM/Risoe

  TOTAL PRODUCTION:

    Time     Prod    Error  Runtime
  -------------------------------
  95042600  11084        0 95042600
  95042603   8406        0 95042600
  95042606   8095        0 95042600
  95042609   6542        0 95042600
  95042612   7077        0 95042600
  95042615   5579        0 95042600
  95042618   6645        0 95042600
  95042621   5820        0 95042600
  95042700   4219        0 95042600
  95042703   2843        0 95042600
  95042706   2647        0 95042600
  95042709   2056        0 95042600
  95042712   1781        0 95042600


Individual forecasts for 95042600:
 95042600                Avedoere_1000_kW   1   393      0 95042600   6.4   47.5
 95042600                           Kyndby  21   199      0 95042600   4.9   47.3
 95042600                        Kolleroed   1   140      0 95042600   7.0   48.6
 95042600                       Oestermarie  7  1054      0 95042600  11.0   33.7
 95042600                     Sose_Vindfarm  2   271      0 95042600  12.1   27.9
 95042600                        Rosendale   3   620      0 95042600  12.0   35.6
 95042600                             MAV82  1    40      0 95042600   2.1   48.9
 95042600                           Vindeby  11  3392     0 95042600  13.9   54.8
 95042600                  Kappel_Vindfarm  24   829      0 95042600   0.9   45.2
 95042600                       Flakkebjerg  1    28      0 95042600   5.8   41.3
 95042600         Noejsomhedsodde_Vindfarm  23  1258     0 95042600   6.4   54.9
 95042600                        Tystofte   3   195      0 95042600   6.2   41.8
 95042600                           Sprove   2   149      0 95042600   7.9   49.5
 95042600                       Skovlaenge   2   193      0 95042600   8.0   39.3
 95042600                        Prejehoej   1   197      0 95042600   7.8   53.8
 95042600                     Nyboelle_Hede  2   632      0 95042600  10.1   52.1
 95042600                     Avedoere_Holme 12  1495     0 95042600   9.5   45.8
```

Figure 30. A sample of the contents of the plain ASCII text file containing the forecasts. A complete listing of a file is given in Appendix B.

score

$$S = 1 - \frac{\mathrm{MAE}_{\mathrm{model}}}{\mathrm{MAE}_{\mathrm{persist}}} \tag{27}$$

is used. MAE is the mean absolute error. The performance of the model for individual farms and the total is shown in Figure 34. It can be seen from the figure that the skill of the model predicting the total is slightly smaller than that

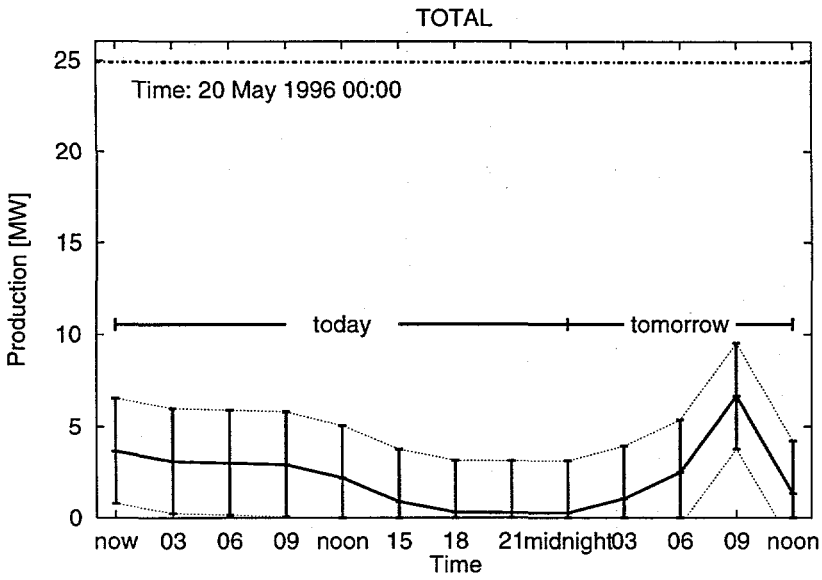

Figure 31. Example of the forecasts as could be seen at the dispatchers desk. The figure shows: the total rated power (dot-dash line at the top), the prediction (solid line), and the expected error (dotted line on both sides of the prediction). The plot is originally in colour.

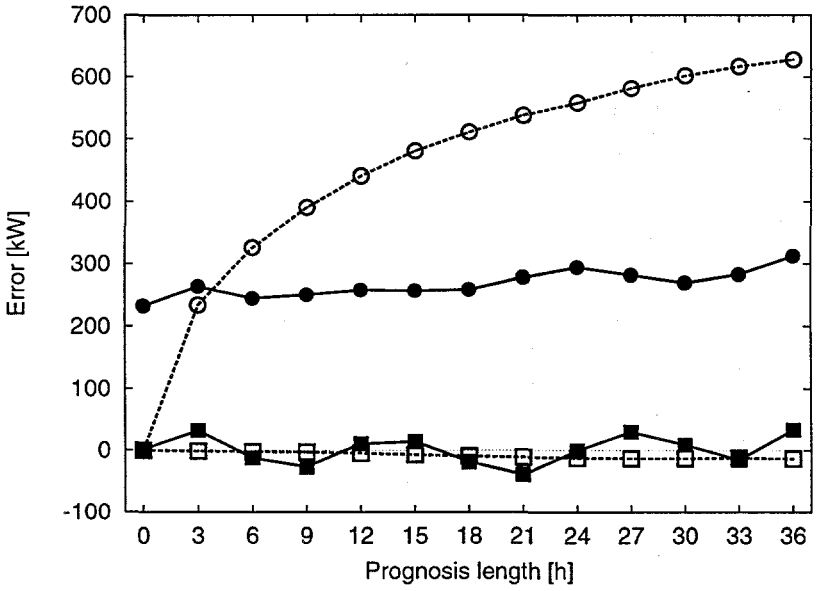

Figure 32. The performance of the model, compared to the persistence model for the Kyndby wind farm. Data from an entire year are used. The rated power of the wind farm is 3780 kW. Open symbols and solid lines refer to the method and filled symbols and dashed lines to persistence. Square symbols are the absolute mean of the error (in kW) and round symbols are the mean error (also in kW). The forecast length (in hours) is along the x-axis.

of the well predicted wind farms, but also that it is not reduced significantly by the not-so-well performing wind farms.

A thorough discussion of the possible error sources is given in the next section.

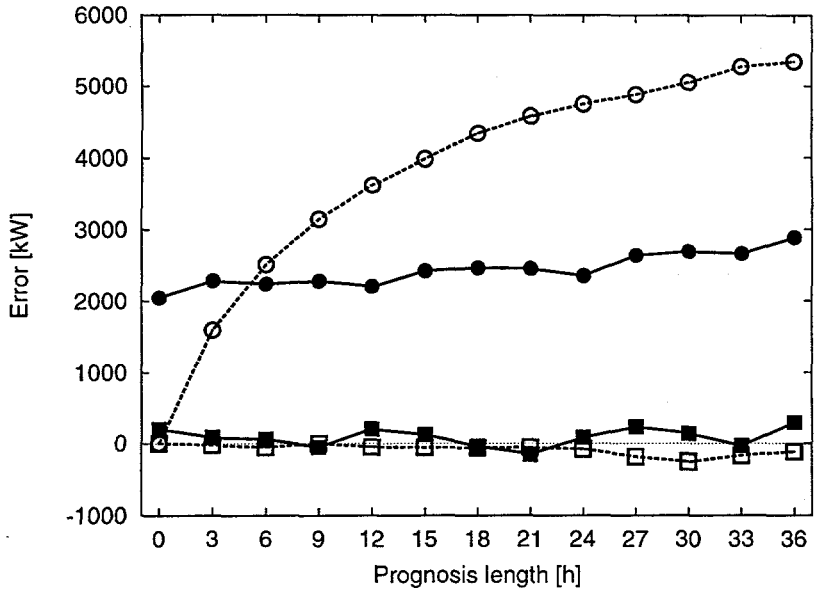

Figure 33. The ability of the model to predict the total power produced by the wind farms compared to the performance of the persistence model. Total capacity 24.93 MW. Legend as in Figure 32.

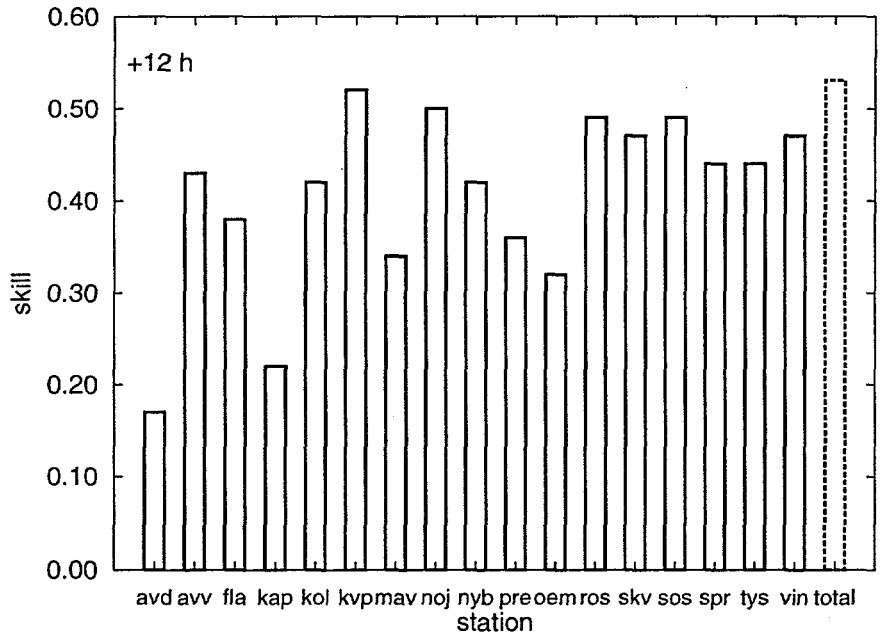

Figure 34. Comparison between the skill of the +12 hour predictions for each of the wind farms and the total using one year of data.

The error

It is interesting to realise how many different error sources there are. Basically, each sub-model will have its own error, so the error is a sum of

- *HIRLAM errors* which depend on the kind of weather system being predicted; some systems are easier to predict than others, eg blocked situations.
- *Geostrophic approx. & log. wind profile* assumes that the atmosphere is barotropic, so no baroclinic effects are taken into account. Furthermore, neutral condi-

tions are assumed, which will mainly be erroneous for low wind sites.

- *WA^{S}P errors* the main source of error is the orographic model which assumes gently sloping terrain, this is the case all over Denmark, so in the Danish case this will not constitute a problem.
- *Power curve error* it is well known that it is hard to measure the power curve, and as a consequence the production of a turbine given the wind speed is also subject to some uncertainty.
- *PARK program errors* the program assumes a very simple model of the wake, which in some cases (especially when turbines are situated close to each other) may cause errors.

Returning to Figure 32 it can be seen that there is no bias in the error, and furthermore, that the standard deviation is significantly smaller than that of the persistence model. So, despite these many possible sources of errors, the resulting error is small, amounting to typically around 8% of the total installed capacity of the wind farm.

6.10 Discussion

Intra-wind farm variability of WA^{S}P calculations

In the model – as it stands now – one WA^{S}P-matrix is calculated for each wind farm. This might constitute a problem if the wind farm is big and therefore covering a large area, since the local effects and as a consequence the WA^{S}P-matrix will vary from turbine to turbine. As an example of this consider the Kappel wind farm which runs along a more than 2 km long line. The normalised power production (taking only local effects into account) is shown in Figure 35. It can be seen from this figure that significant variability (more than 15%) can be found within a wind farm. This leads to the conclusion that to estimate the local effects better it is not sufficient to look at only one point in a wind farm, but instead to look at all the turbines and then calculate an average WA^{S}P correction. In the present model these differences are absorbed by the MOS filter.

Prediction of changes

In the previous section we analysed the error of the predictions, that is comparing the forecast production with the observed at a certain time. Another matter of interest is how well the model can predict *changes*, ie how well is the change from eg 3 to 6 hours ahead predicted. This is interesting mostly because of the fact that when a frontal system crosses an area, it is important to be able to predict exactly when and of what size the change will be. Looking at Figure 36 it can be seen that the model predicts the changes rather well, especially when the production rises. Comparing to the ability of the persistence model, it is obvious from its definition that the model is not able to predict any changes at all, so compared to the persistence model, the HIRLAM/WA^{S}P-model performs extremely well.

Correlations with distance

Addressing now the issue of how many wind farms it is necessary to predict for to generate valid predictions covering all of a certain area, the inter-correlations of the production from all the wind farms in this study are shown in Figure 37. From the figure it can be seen that after only 50 km the correlation coefficient has dropped to 0.75, this means that to cover an area the size of Zealand six to seven prediction sites are needed. For Bornholm the similar number would be one

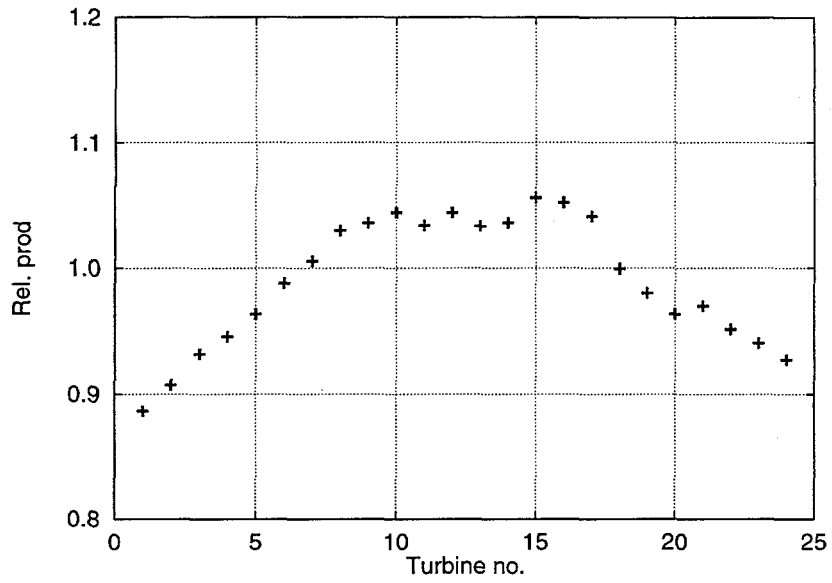

Figure 35. The relative production of the turbines in the Kappel wind farm. The productions are calculated using WA^{S}P and are normalised with the value used in the HIRLAM/WA^{S}P-model.

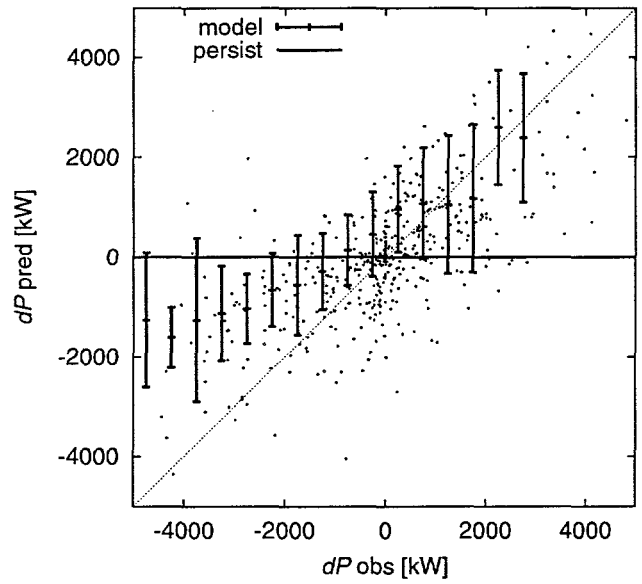

Figure 36. The observed change of the +6 to the +33 hour forecast for Nøjsomhedsodde Wind Farm (noj) plotted against the predicted change. The small dots are the actual data points and the high-close-low bars are the mean of the data plus and minus the standard deviation of the data. In the ideal case all the points should lie on the $x = y$-line. For reference the result of the persistence model is also plotted (the horizontal line).

to two. In the present study 14 are used on Zealand and 3 on Bornholm, leading to the conclusion that both areas are covered well with respect to forecasts.

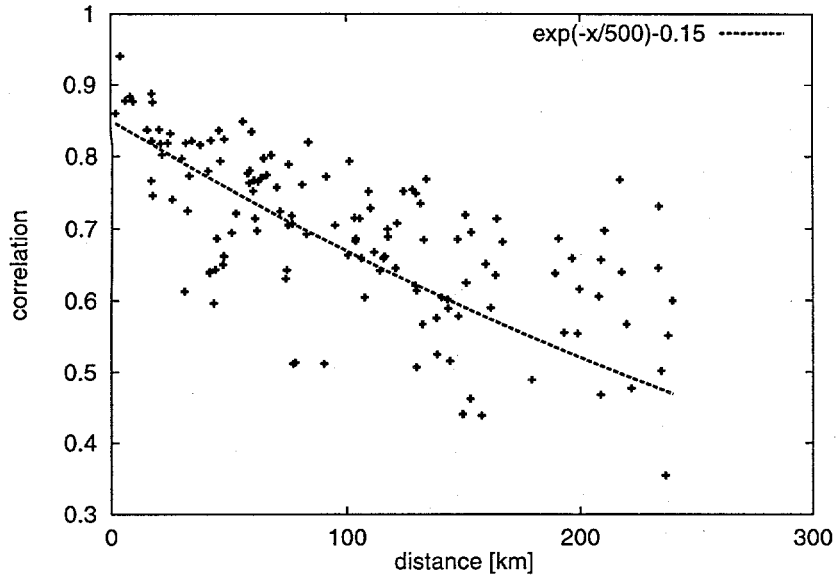

Figure 37. The inter-correlation between all the wind farms as a function of distance.

Sub-3 hour variability

Because of the resolution of the output of the HIRLAM model forecasts can only be given every 3 hours. To try to shed some light on what happens between the 3 hours forecasts the observations have been processed to give the interval the minimum and maximum production within a specified period (here 1, 2, 3 hours). This has been analysed to give the accumulated distributions shown in Figure 38. As can be seen from this figure there is indeed a difference between the different time-windows: the smaller the time difference between forecasts, the smaller the spread in the variability in the production. For the 3 hour time steps used in this study it can be seen that for the Nøjsomhedsodde wind farm more than 80% of the variabilty is smaller than 20% of the total installed power.

Opening the black-box

In this section the physical model will be analysed in a mathematical sense, since this will give us an understanding of the differences between the physical model and statistical model. The analysis will also end up with a recommended statistical model, based on the properties of the physical model.

The physical model is made up of the following:

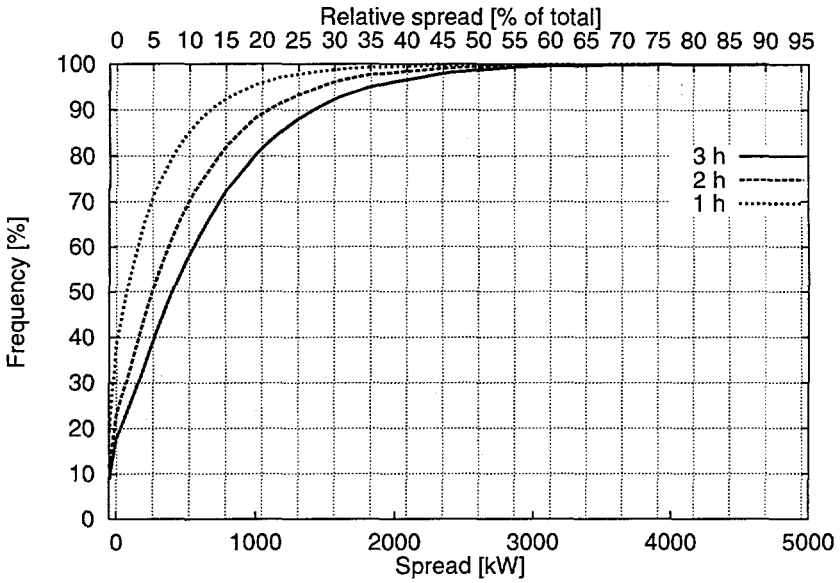

Figure 38. The accumulated frequency (in %) of the spread of the production for three different time intervals: 1, 2 and 3 hours. The bottom x-axis shows the spread in kW and the top the with the total installed power (5.2 MW) normalised spread.

	Forecast HIRLAM	$\rightarrow$	$\vec{G}$
$\rightarrow$	Surface transformation Geo. drag + log. profile	$\rightarrow$	$u(G,\theta)$, since $z_0 = z_0(\theta)$
$\rightarrow$	Local corrections WAsP	$\rightarrow$	$w_i u(G,\theta)$
$\rightarrow$	Production	$\rightarrow$	$N\text{pow}(w_i u(G,\theta))$
$\rightarrow$	Park influence PARK	$\rightarrow$	$p_i N\text{pow}(w_i u(G,\theta))$

As can be seen, the total production can be written in the following way

$$P = p_i N\text{pow}(w_i u(G,\theta)) \tag{28}$$

Studying Figure 39 it can be seen that the relation between the geostrophic wind and the wind at the surface is to a first approximation linear. As a consequence of this u can be written

$$u(G,\theta) \approx d_i \vec{G} \tag{29}$$

which leads to that the total production can be written in the following way

$$P = p_i N\text{pow}(w_i d_i G) = A_i \text{pow}(B_i G) \tag{30}$$

where it can be seen that the total production can to a first approximation be written as a scaling, B_i, of the geostrophic wind, G, put into the power-curve, pow(u), and then scaled, A_i.

This means that a simple non-physical model, should contain two factors for each direction sector.

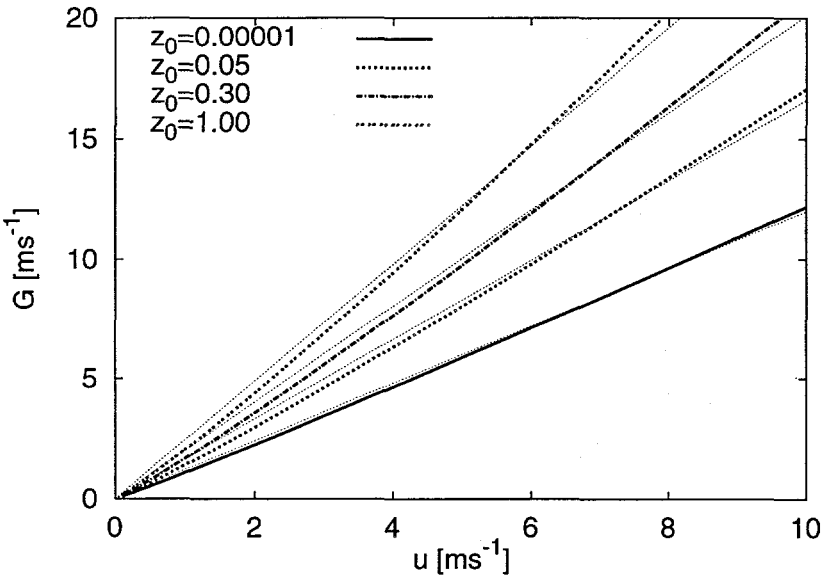

Figure 39. The relation between the geostrophic wind and the wind at the surface (here at 30 m agl) assuming different roughnesses. $f = 10^{-4}$. For each roughness a straight line is also plotted.

7 Intensive test period

In September 1995 we coordinated a test setting encompassing all members of the project. The goal was to compare the results from a short period of simultaneously made forecasts from all 3 parties: DMI-model, Risø-model and the experience/intuition of the engineers from ELKRAFT. The two models just went on as they had done since February 1995, but for the engineers there was a new task to fulfill. A number of persons volunteered to fill in a slip with his/hers guess for the next 36 hours. The values were not fully compatible with the values that the two automated models gave, because the engineers could only talk about the entire power production from all the wind farms belonging to ELKRAFT, while the models concerned only a smaller sample. So we could not actually compare values, instead we had to consider trends and relative measures.

In figures 40 to 44 we show the scatter plots for the 2 model, the ELKRAFT-guesses and the persistence. Comparing the models (figures 40 and 41) with the persistence in their regime (figure 43) and the ELKRAFT-guesses (figure 42) with the persistence in its regime (figure 44) it is clear that they all perform better than the persistence from at least +6 hours. Comparing the three prediction approaches with each other we see that two weather based prediction approaches perform better than the ELKRAFT intuition approach, and that between these two models the DMI model has the highest score for all prediction hours. This is most easily seen in the skill score figures. The reason why the Risø model did not perform so well was that a bug was identified and corrected during the test period. This has – of course – an effect on the results for the 14-day test period. Comparing the results at the end of this report it can be seen that with the error corrected, the two models perform equally well.

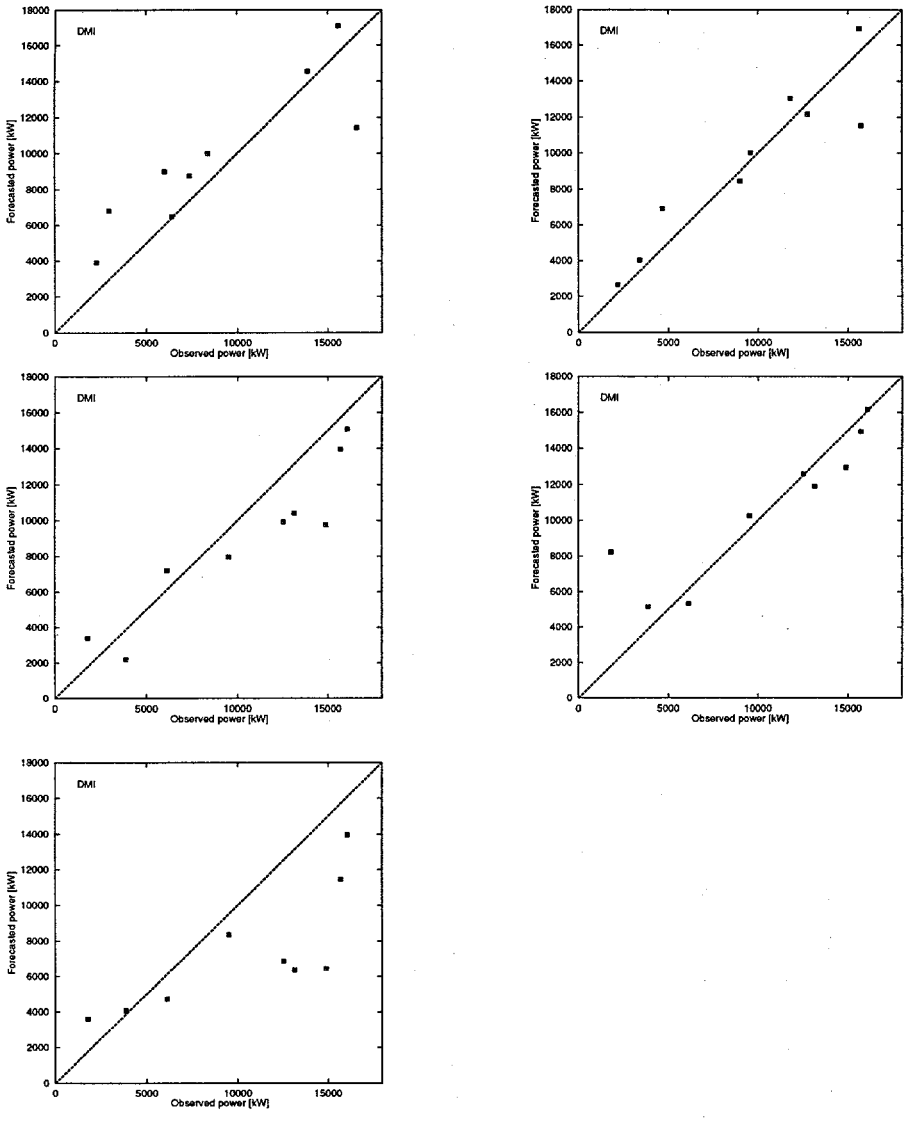

Figure 40. The scatter plots for the DMI model. The prognosis lengths increase from left to right following the series: +3, +6, +12, +24, +36 hours.

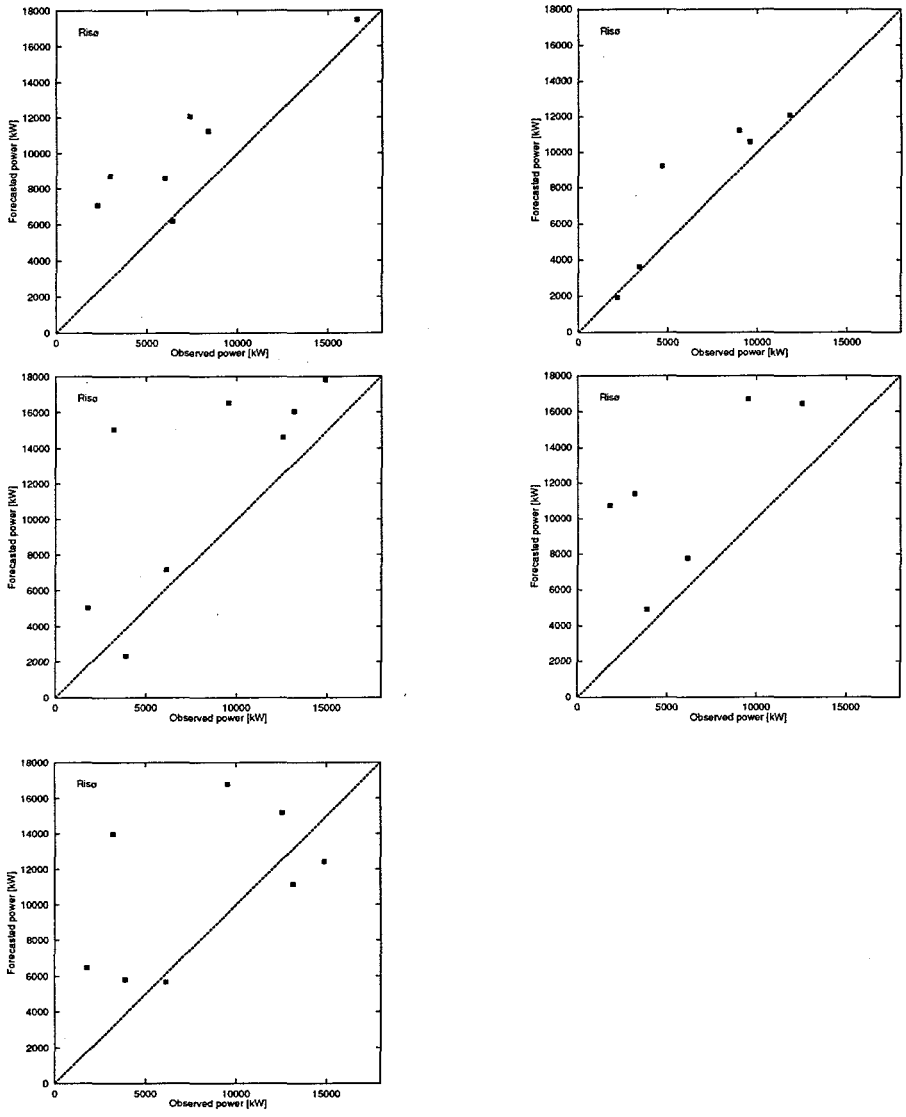

Figure 41. The scatter plots for the Risø model. The prognosis lengths increase from left to right following the series: +3, +6, +12, +24, +36 hours.

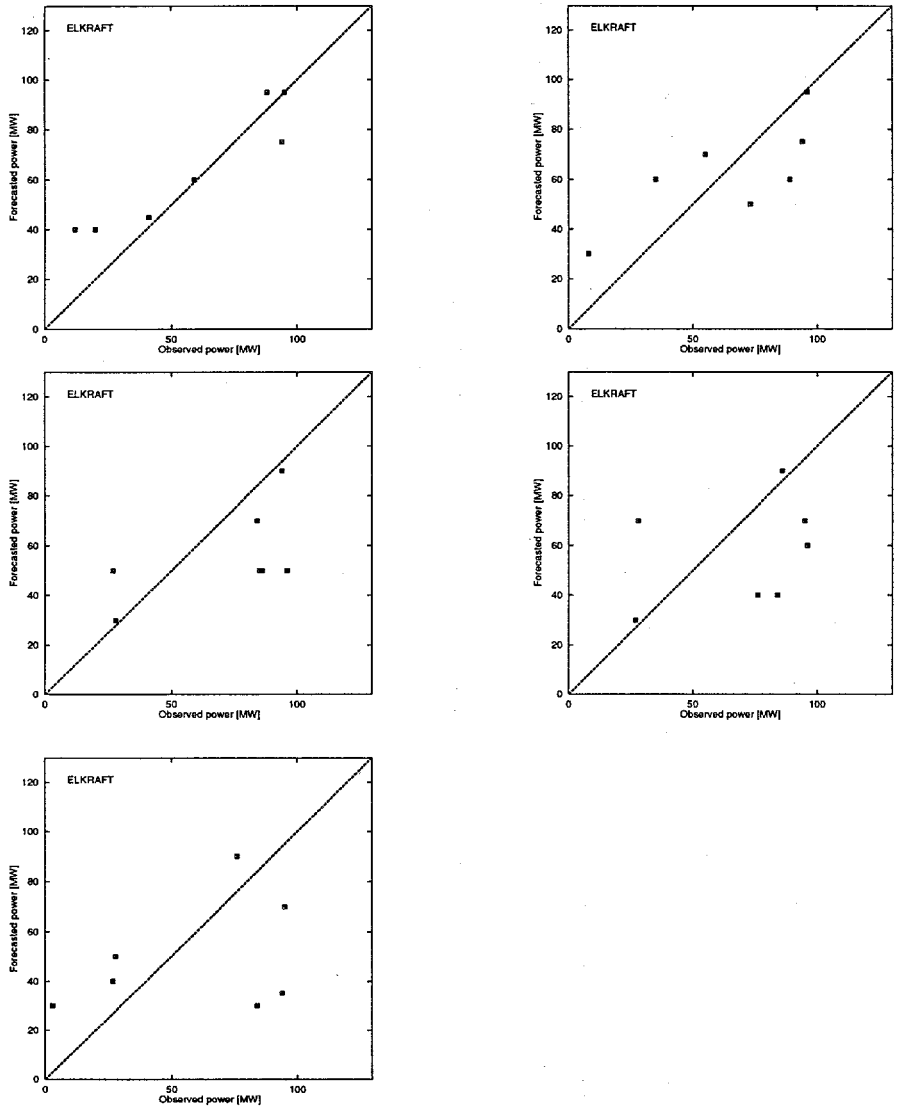

Figure 42. The scatter plots for the ELKRAFT model. The prognosis lengths increase from left to right following the series: +3, +6, +12, +24, +36 hours.

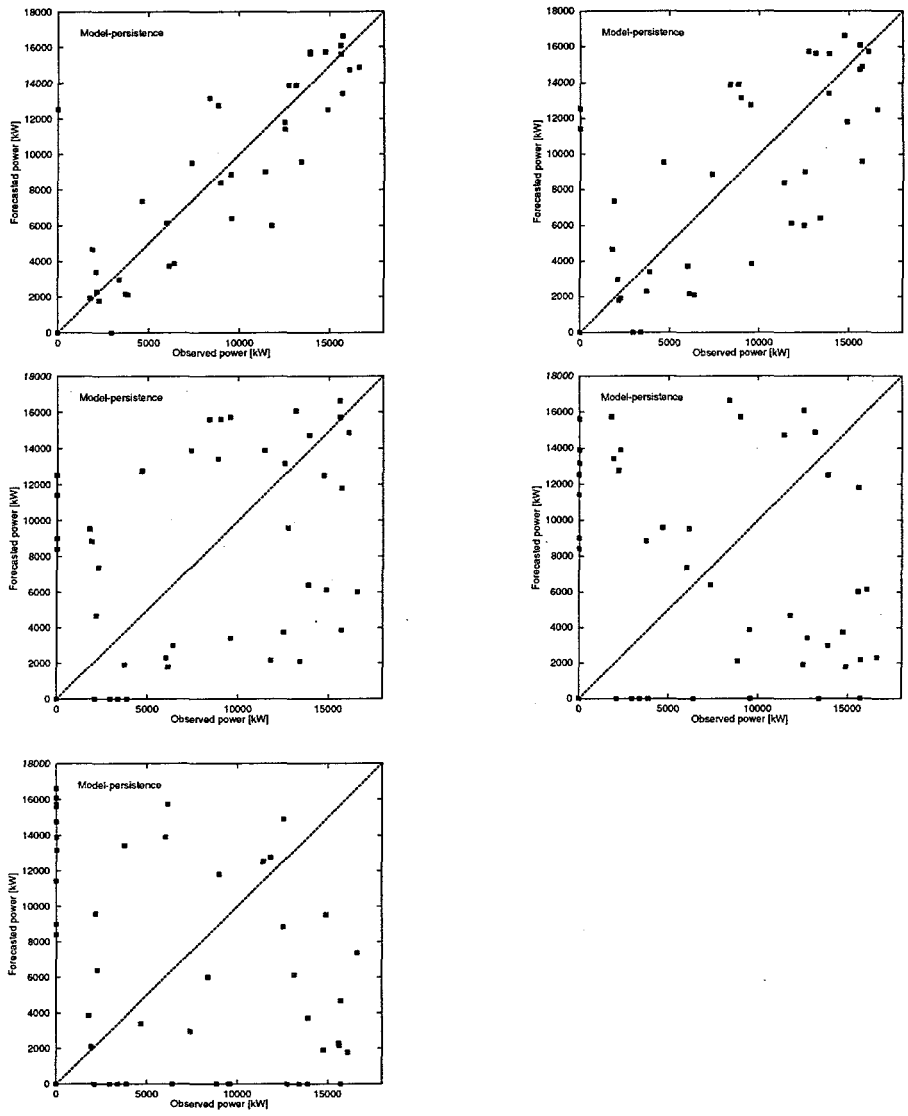

Figure 43. The scatter plots for the persistence (in the DMI and Risø regime). The prognosis lengths increase from left to right: +3, +6, +12, +24, +36 hours.

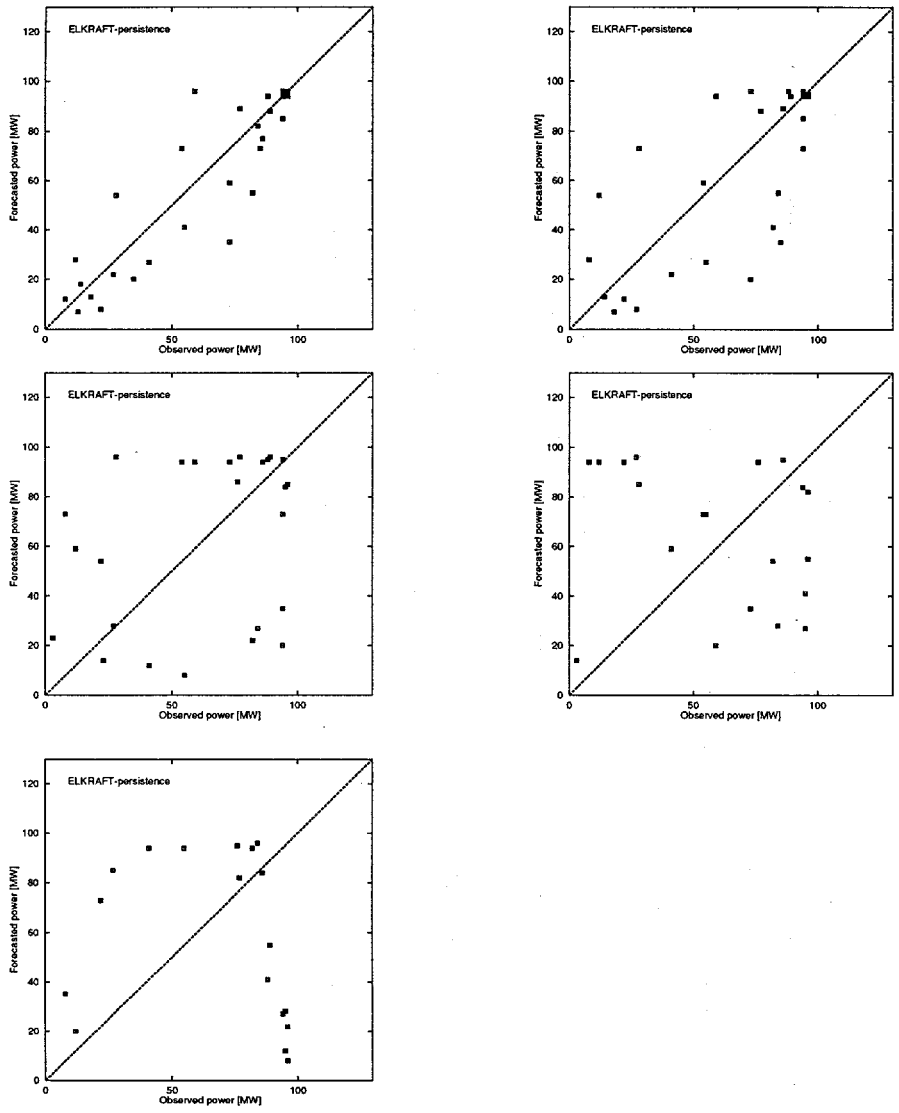

Figure 44. The scatter plots for the persistence (in the ELKRAFT regime). The prognosis lengths increase from left to right: +3, +6, +12, +24, +36 hours.

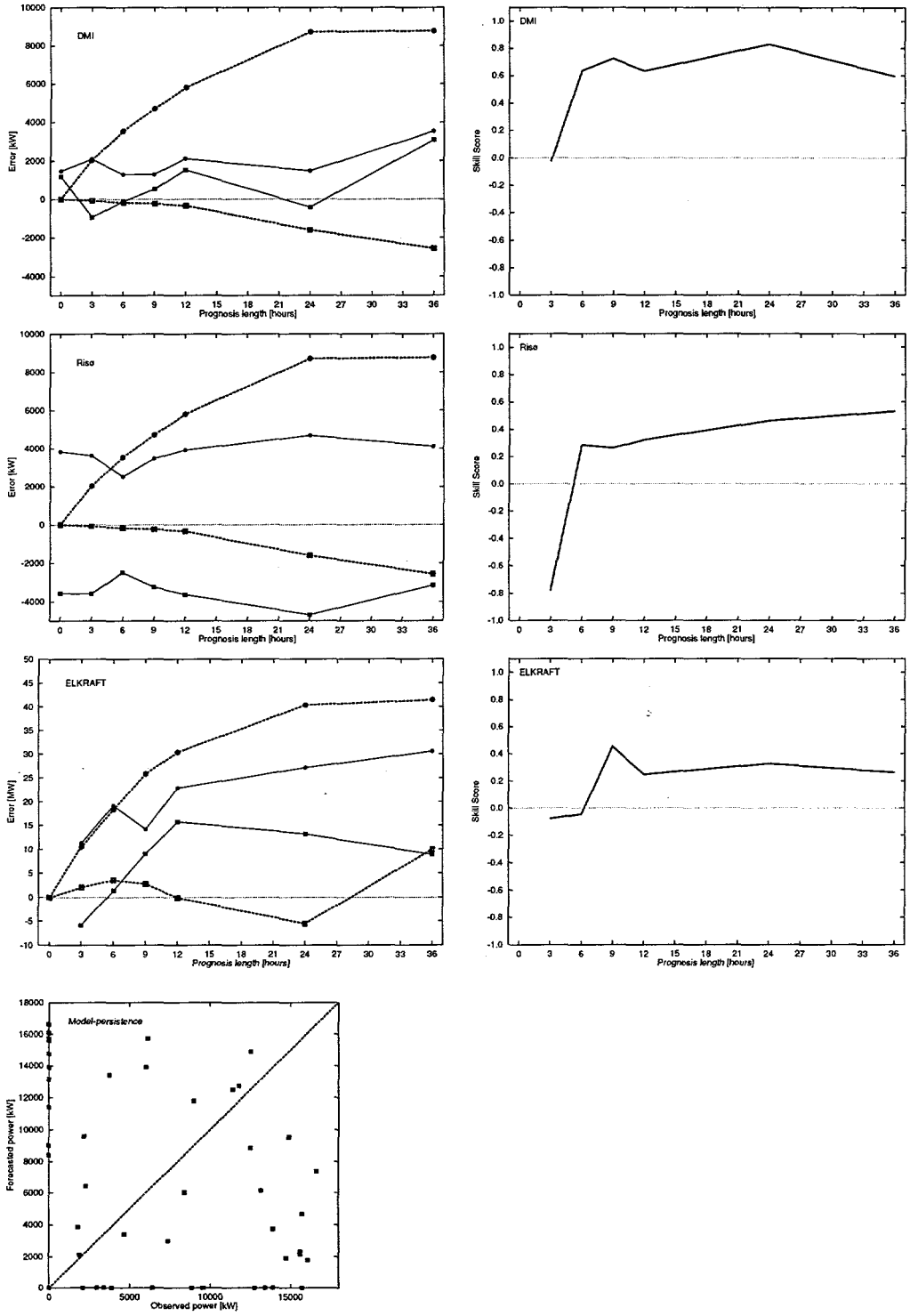

Figure 45. The performance of the models and ELKRAFT-guesses, compared to the persistence model. Left column shows the errors and right the skill scores. Open symbols and dashed lines refer to persistence and filled symbols and solid lines to the models. Square symbols are the mean error and round symbols are the mean absolute error. The forecast length is along the apsis. The sample was very small (9 data points) thus leading to the rather clumsy look of the curves.

8 Operational use of models

8.1 Background

As coordinator for Eastern Denmark's electricity and cogenerated heat supply, Elkraft seeks to achieve balance between supply security, environmental protection and competitiveness. This objective guides all the company's activities including the tasks performed in the control centre, i.e. short-term planning, load dispatch as well as import and export of electricity.

In this context, the wind power production has a considerable - and ever increasing - importance.

By the end of 1995 the total wind power capacity in the Elkraft region amounted to about 150 MW, including the privately owned wind turbines. In relation to this, the total production capacity in the region was 4,300 MW electricity. In Denmark as a whole, wind power accounts for 600 MW of the total production capacity, which is approx. 10,000 MW electricity.

The wind power capacity, both at regional and national level, will be considerably expanded during the next decade.

Apart from the wind turbines and some units using biomass, electricity production in Denmark is based on fossil-fired power plants.

8.2 Main tasks in the control centre

The system operation at Elkraft constitutes a main task in the control centre. System operation means optimisation and coordination of the electricity and heat production as well as power transmission and power exchange.

As regards production, the staff's primary task is to take care of the dispatching function, i.e.:

- unit commitment (which units in operation)
- placing generation scale instructions (set points) for the power stations.

The aim of the above-mentioned work is to:

- meet the demand for power and heat
- achieve optimal economy
- secure sufficient reserves.

8.3 Production planning, power exchange and load dispatching

The production planning in the control centre is a weekly (or even more frequent) task based on the current situation of operations. In principle all the production possibilities and combinations are estimated to find the least expensive which at the same time meets the demand for security of supply and which is within the current technical limits.

The planning ensures an optimum production plan for delivery of the necessary heat and power, the latter in combination with agreements about power exchange/trade with foreign partners.

Based on the plans of operations drawn up, a close follow-up and adjustment to the current situation take place.

Minor short-term discrepancies between the plans of operations and the current situation are corrected manually by the dispatcher ensuring that entered agreements are kept, while major and long-term discrepancies require elaboration of

new plans of operations and possibly entering into new/additional agreements on production and exchange with foreign utilities.

8.4 Load dispatching in a power supply system including wind power

In a simplified model we can assume that the dispatcher has three basic groups of units at his disposal:

	Start-up time	Start-up costs [DKK]	Production cost [DKK/MWh]
Group 1	10 min.	5,000	300
Group 2	30 min.	10,000	200
Group 3	6 hours	30,000	100

The production capacity of the different units may range from 20 to 600 MW, the largest units belonging to group 3.

This table clearly indicates that a reliable wind power forecast for a horizon of one or two days can be an important parameter in the dispatcher's basis for decisions.

Basically, there is a need for a prediction covering the total region, including information about expected errors. Operational use requires that the predicted data should be received on line with automatic update of the future database, which is attached to the planning applications.

8.5 Implementation

In the graphic MMI, the forecast data shall be available as curves with the look-ahead time along the x-axis, and the time for completion of the shown prediction. This will make it possible to integrate wind power forecasts into the graphic planning tools which are being prepared for the system operation staff.

It is essential to the success of the operator support that the tools are integrated in the existing system in the control centre. A deep analysis of these aspects has been done by Anders Persson, Sweden, and the findings are described in Persson (1996).

8.6 Further aspects

A special need for wind power prediction occurs when electricity from wind turbines ("green power") is offered to the customers at a special rate (more expensive). To manage this situation satisfactorily, credible forecasts as well as reliable measurements from wind farms are necessary.

Another aspect is that the ongoing expansion of wind farms will result in an increasing load on the power grid. This problem is accentuated by the fact that the wind turbines, especially the off-shore units, are often sited in areas with rather limited transmission capacity. Consequently, the power grid monitoring must be intensified, and to handle this problem in the control centre, a need may arise for detailed forecasts for groups of wind turbines located in critical areas. The involved utilities are aware of the increasing demands on power transmission capacity, but a way to defer a grid extension could be to build local energy stores (e.g. flywheels) and coordinate the utilization of the stores with the above-mentioned detailed predictions for selected wind farms.

9 Conclusions

This project has shown that it is indeed possible to predict the production from wind farms as far into the future as 36 hours. The project has further shown that it is practically possible to implement the models at a utility. Unfortunately, it has not been possible to gain real operational experience due to technical problems at the utility. An operational system was set up, however, where predictions – via modem connections – on a daily basis twice a day, were sent from the Danish Meteorological Institute to the utility ELKRAFT. The production from the 17 wind farms was predicted operationally for one full year (February 1995 up to and including January 1996). This part of the project ran very smoothly with a data coverage of close to 100%.

The one major reason for the fact that the predictions were as successful as they were is the HIRLAM model. Had it not been for HIRLAM's ability to predict the weather patterns well, the project should not have met success.

On the practical side, it is important for a utility that as many parts of the model run at their premises, because of the strict operational constraints imposed on the utility. This means that in this case it will be the raw HIRLAM forecasts that will be transmitted from the meteorological institute to the utility.

Turning now to the history of this project, the ideas of this project were first developed under a JOULE 1 project, were a comprehensive test of the model – used to predict the wind speed – was carried out. The ideas were then build in to a model complex for predicting the power output from wind farms. This complex was then tested operationally under this project. The latest development is that because of the results found in this project a JOULE 3 project has been granted where the model complex is to be used at the two Danish utilities, in the UK, Greece and USA.

To sum up the conclusions, the project has been successful in that is has

- Demonstrated that it is possible to make models which can predict the power from grid-connected wind farms up to 36 hours ahead. The quality of the models is such that in power fossil fuel and economic terms there are major savings to be obtained.
- Set up an operational framework, such that the utility could – on a twice daily basis – get new predictions of the power of the grid connected wind farms up to 36 hours ahead.
- Demonstrated that the predictions are significantly better than anything that the dispatcher could have come up with, without these models.

Acknowledgements

The work described in this report is funded by the Danish Ministry of Energy and the Environment, under contract EFP 1363/94-0005. Rasmus Paulsen is thankfully acknowledged for having digitised the maps for the Risø analysis of the wind farms.

References

Blackadar, A.K. and H. Tennekes, 1968: *Asymptotic Similarity in Neutral Barotropic Planetary Boundary Layers.* J. Atmos. Sci., **25**, 1015–1020.

European Wind Turbine Catalogue, 1995. Energy Centre Denmark, Thermie programme. 63pp.

Gustafsson, N. (editor) 1993: *HIRLAM 2 Final Report.* HIRLAM Tech. Report no. 9, available from SMHI S-60176, Norrköping, Sweden.

Harrison, P.J., and C.F. Stevens, 1976: *Bayesian Forecasting.* Journal of the Royal Statistical Society, Ser. B, **38**, 205–247.

Kalman, R.E., 1960: *A New Approach to Linear Filtering and Prediction Problems.* Journal of Basic Engineering, **82**, 34–45.

Kalman, R.E., and R.S. Bucy, 1961: *New Results in Linear Filtering and Prediction Theory.* Journal of Basic Engineering, **83**, 95–108.

Landberg, L., S.J. Watson, J. Halliday, J.U. Jørgensen, A. Hilden, 1993: *Short-term prediction of local wind conditions.* Report to the Commission of the European Communities, JOULE programme.

Landberg L. and S.J. Watson, 1994: *Short-term prediction of local wind conditions.* Boundary-Layer Meteo. **70**, 171–195.

Machenhauer, B. (ed), 1988: *HIRLAM final report.* HIRLAM Technical Report 5, Copenhagen, Denmark. 116 pp.

Meinhold, R.J., and N.D. Singpurwalla, 1983: *Understanding the Kalman Filter.* The American Statistician, **37**, 123–127.

Mortensen, N.G., L. Landberg, I. Troen and E.L. Petersen, 1993: *Wind Atlas Analysis and Application Program (WA^{S}P), User's Guide.* Risø-I-666(EN)(v.2), Risø National Laboratory, Roskilde, Denmark. 133 pp.

Persson, A, 1996: "Helhetssyn vid utformning av operatörstöd för drift av komplexa energisystem" (in Swedish), PhD-thesis, Technical University of Lund, 215pp.

Sanderhoff, P, 1993: *PARK – User's Guide. A PC-program for calculation of wind turbine park performance.* Risø-I-668(EN), Risø National Laboratory, Roskilde, Denmark. 8 pp.

Troen and Petersen, 1989: *The European Wind Atlas.* Published for the CEC by Risø National Laboratory, Roskilde, Denmark. 656 pp.

A The DMI model

A.1 Data coverage

Table 3. Datacoverages (in %) for all the wind farms.

avd	58.2	kvp	76.1	pre	68.1	tys	71.1
avv	57.8	mav	42.8	ros	75.0	vin	46.6
fla	72.4	noj	73.9	skv	75.8		
kap	62.5	nyb	70.5	sos	23.9		
kol	36.3	oem	66.0	spr	62.9		

A.2 The total rated power

The total production is defined as the sum of the power from all the farms which are producing electrical power at the moment. Times for which one or more of the wind farms are missing are omitted from the sample. In order to yield the highest datacoverage for the total power we exclude the farms which have the poorest data cover rate. Placing a limit at 60% we end up with the 10 wind farms listed in table 4.

Table 4. Listing the restricted sample yielding the total.

Farm ID	Rated power [kW]
fla	225
kap	9600
kvp	3780
noj	5175
nyb	1000
oem	1575
ros	675
skv	300
spr	300
tys	1350
Total	23980

The testing period started February 2, 1995, i.e. right after the big void in the data flow. The two farms sos and pre lacked data prior to the project start so these two are omitted from the sample eventhough pre has a rather high data coverage.

A.3 Figures showing wind-power relations

These figures show the empirical relations between the observed wind and the observed electrical power. We see that they all show rather sharp cutoffs in the low-speed end. This is because each mill needs a minimum wind force to over win the inertia. The mill actually uses a little energy to start propelling when the wind exceeds the specific lower limit. This edge in the wind-to-power relation causes some boundary effects in the fitting process. This is most clearly seen in the

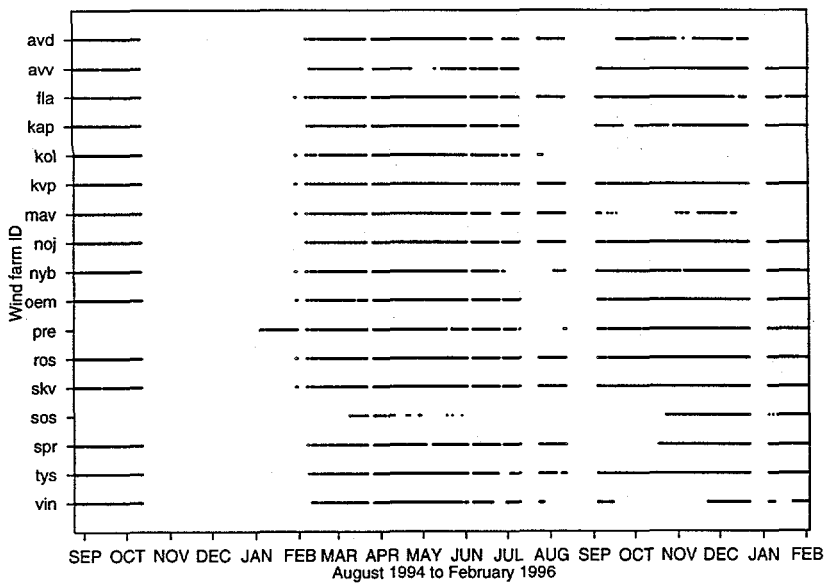

Figure 46. The data coverage for the whole period for all wind farms.

Prejehøj (pre) figure (lower left frame of figure 48). The lower limit is implemented in the Kalman updating and forecasting processes, hence no error is caused by these boundary effects.

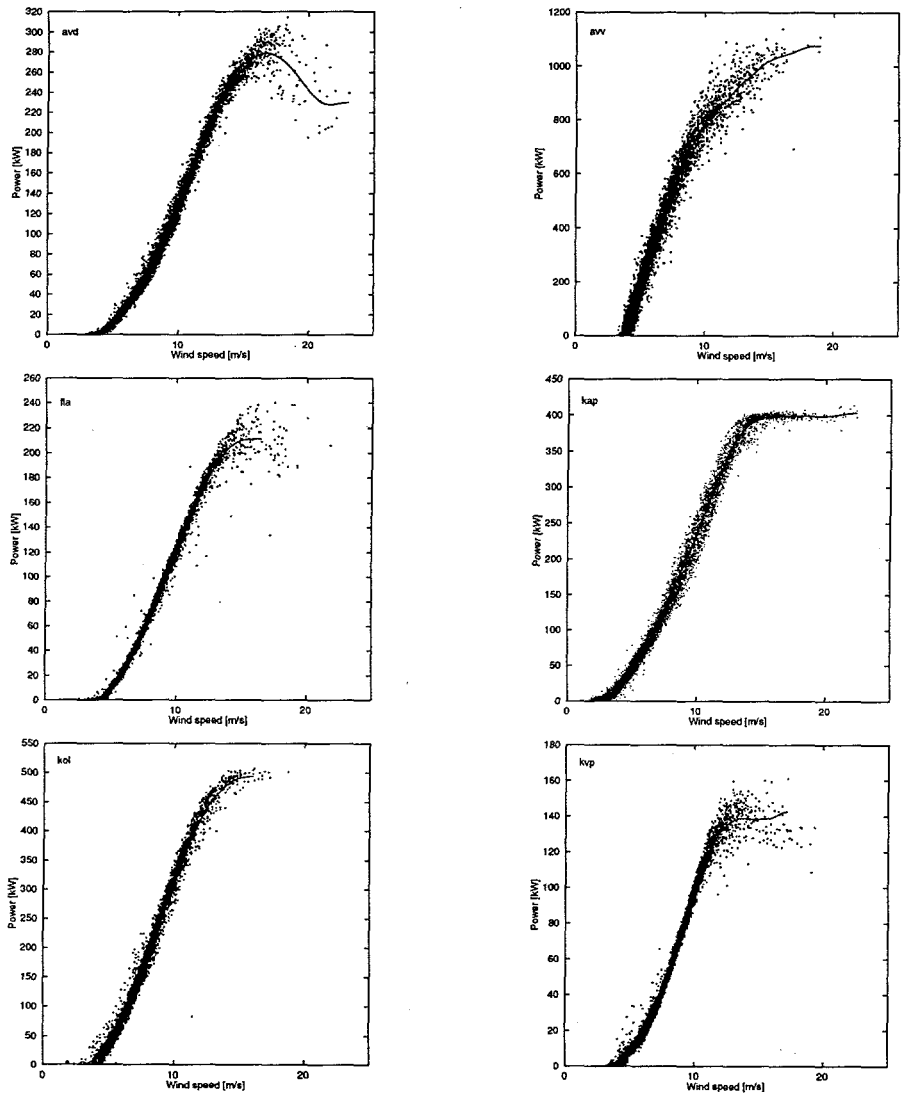

Figure 47. The observed wind-to-power relation with the used fit shown superposed.

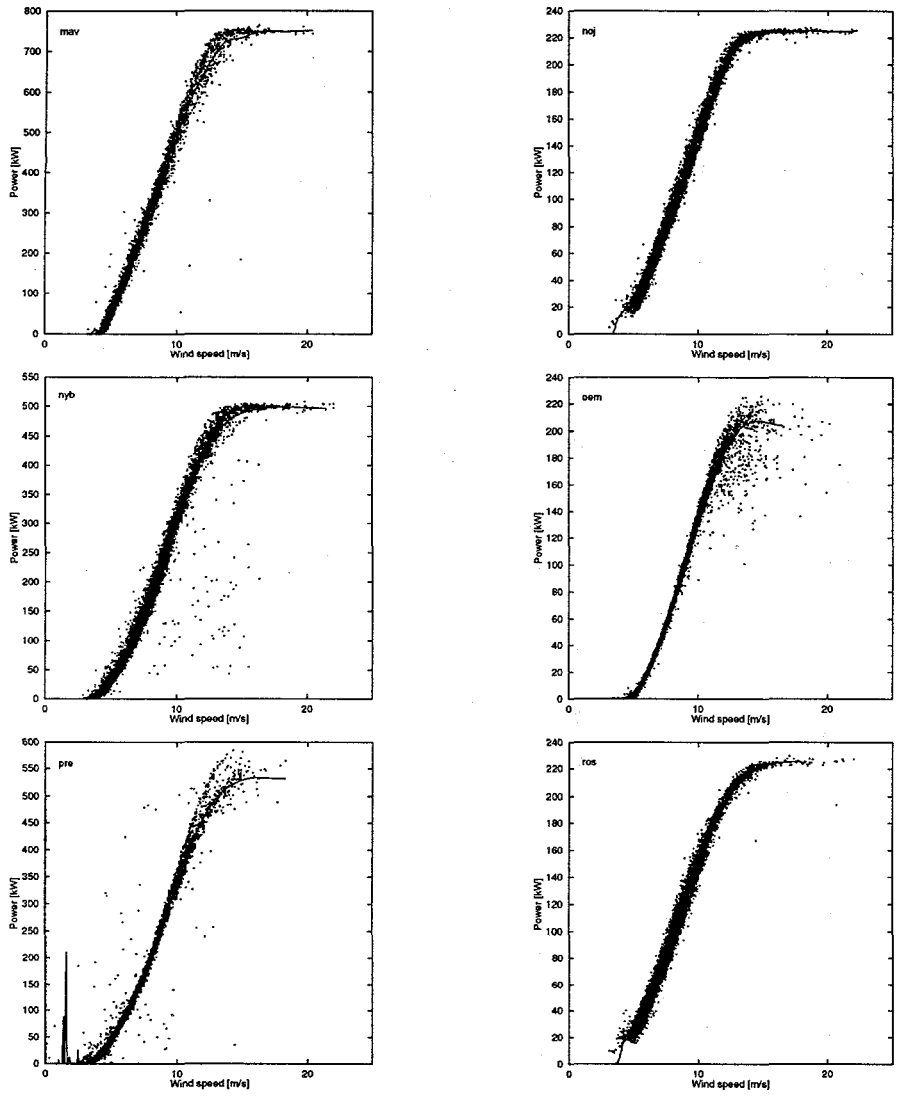

Figure 48. The observed wind-to-power relation with the used fit shown superposed.

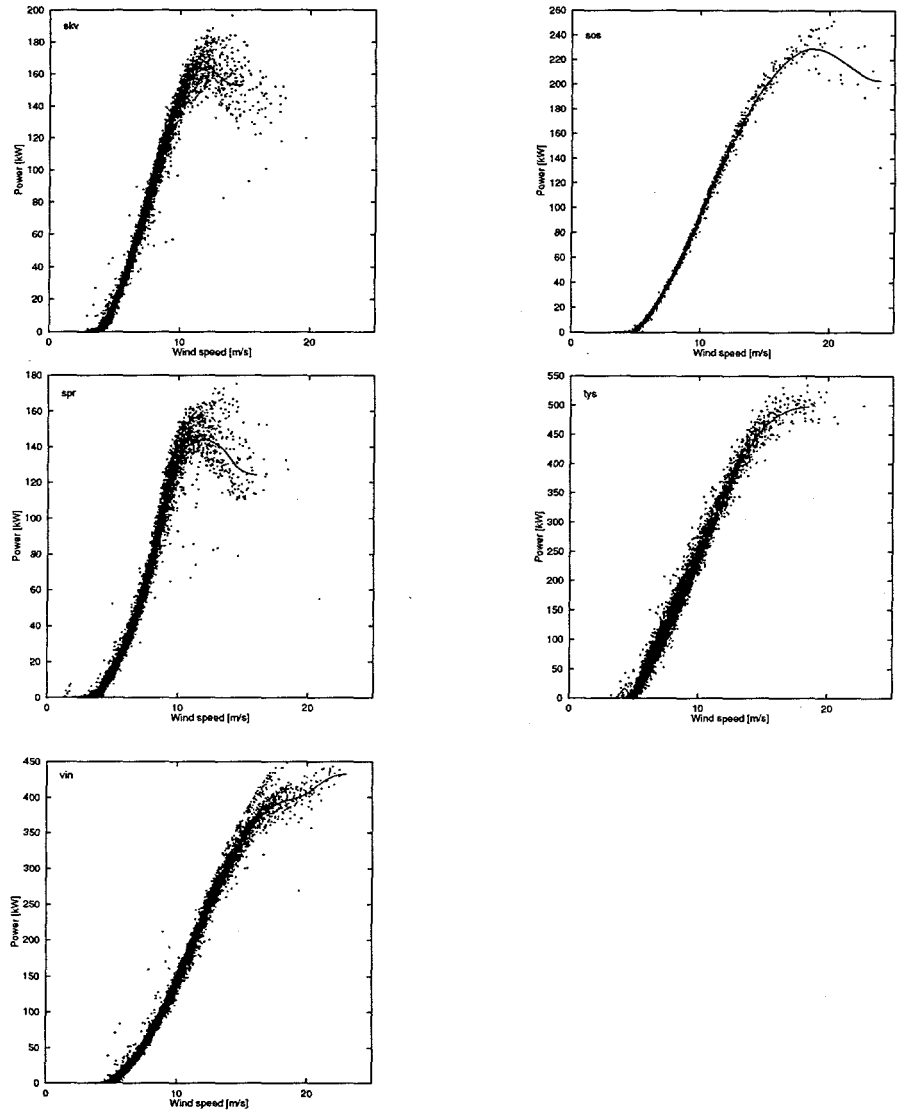

Figure 49. The observed wind-to-power relation with the used fit shown superposed.

A.4 Figures showing error and skill score vs. prognosis lengths

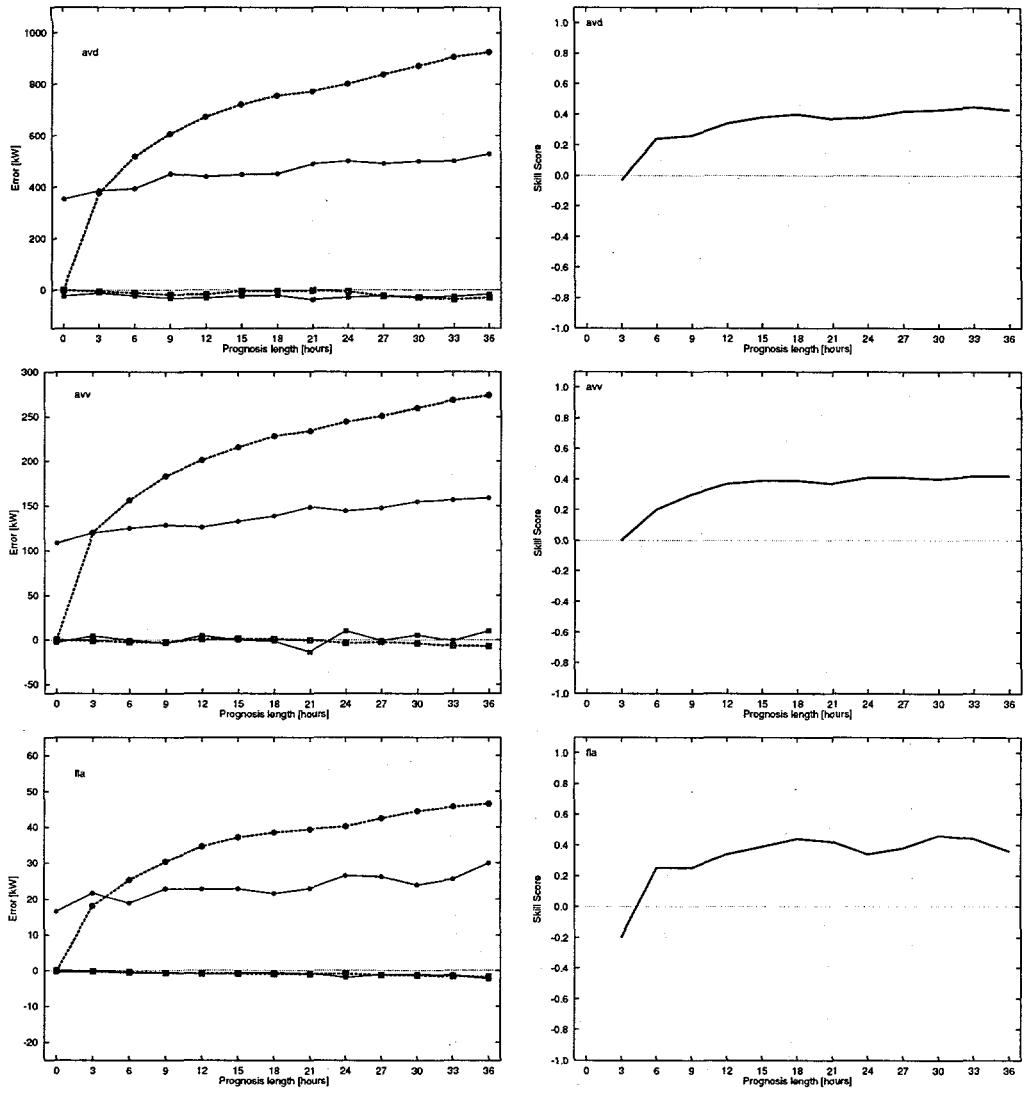

Figure 50. The ability of the model to predict the power produced by the wind farms compared to the performance of the persistence model. In the left frames the open symbols and dashed lines refer to persistence and the filled symbols and solid lines to the model; square symbols are the mean error (in kW) and round symbols are the mean absolute error (also in kW). Right frames shows the skill score. In all frames the forecast length (in hours) is along the apsis.

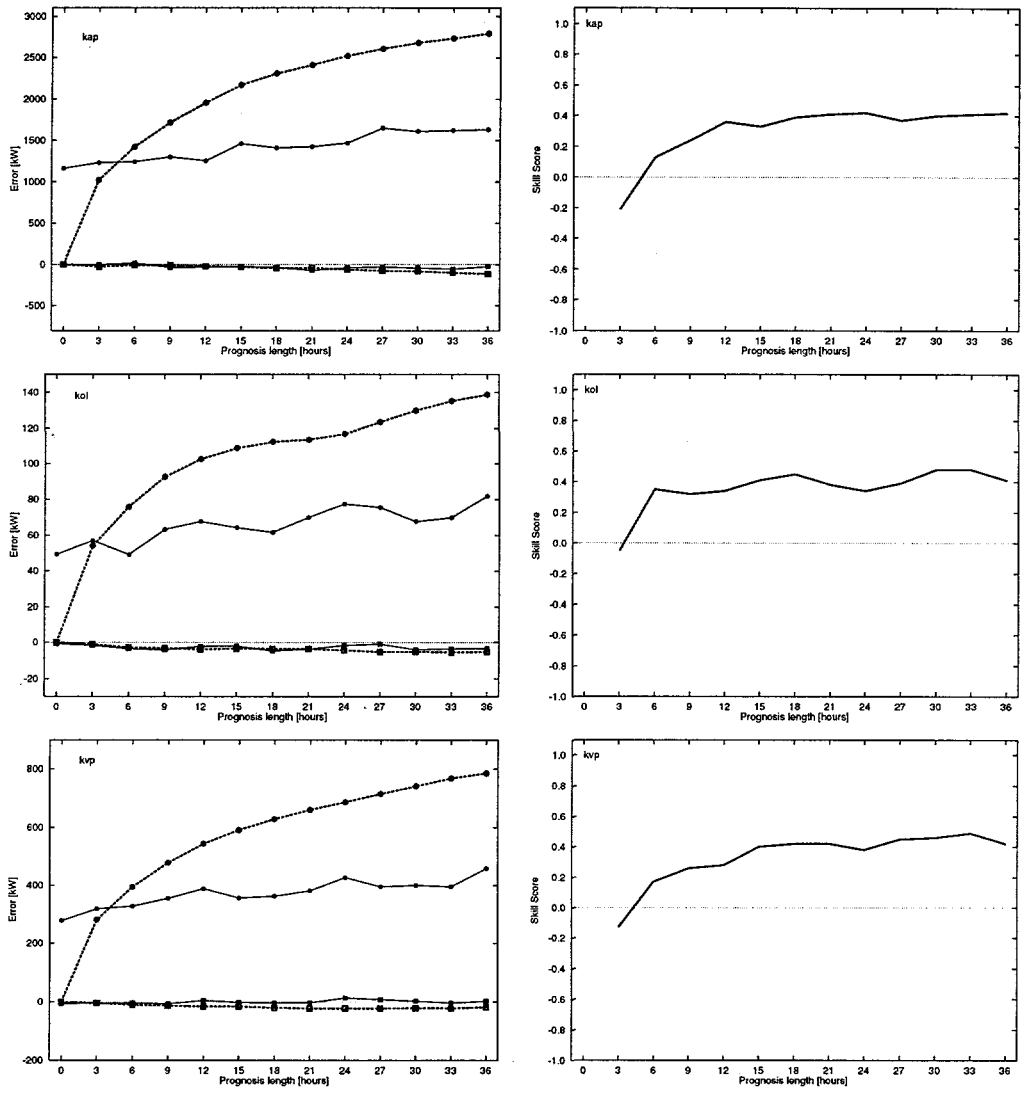

Figure 51. The ability of the model to predict the power produced by the wind farms compared to the performance of the persistence model. In the left frames the open symbols and dashed lines refer to persistence and the filled symbols and solid lines to the model; square symbols are the mean error (in kW) and round symbols are the mean absolute error (also in kW). Right frames shows the skill score. In all frames the forecast length (in hours) is along the apsis.

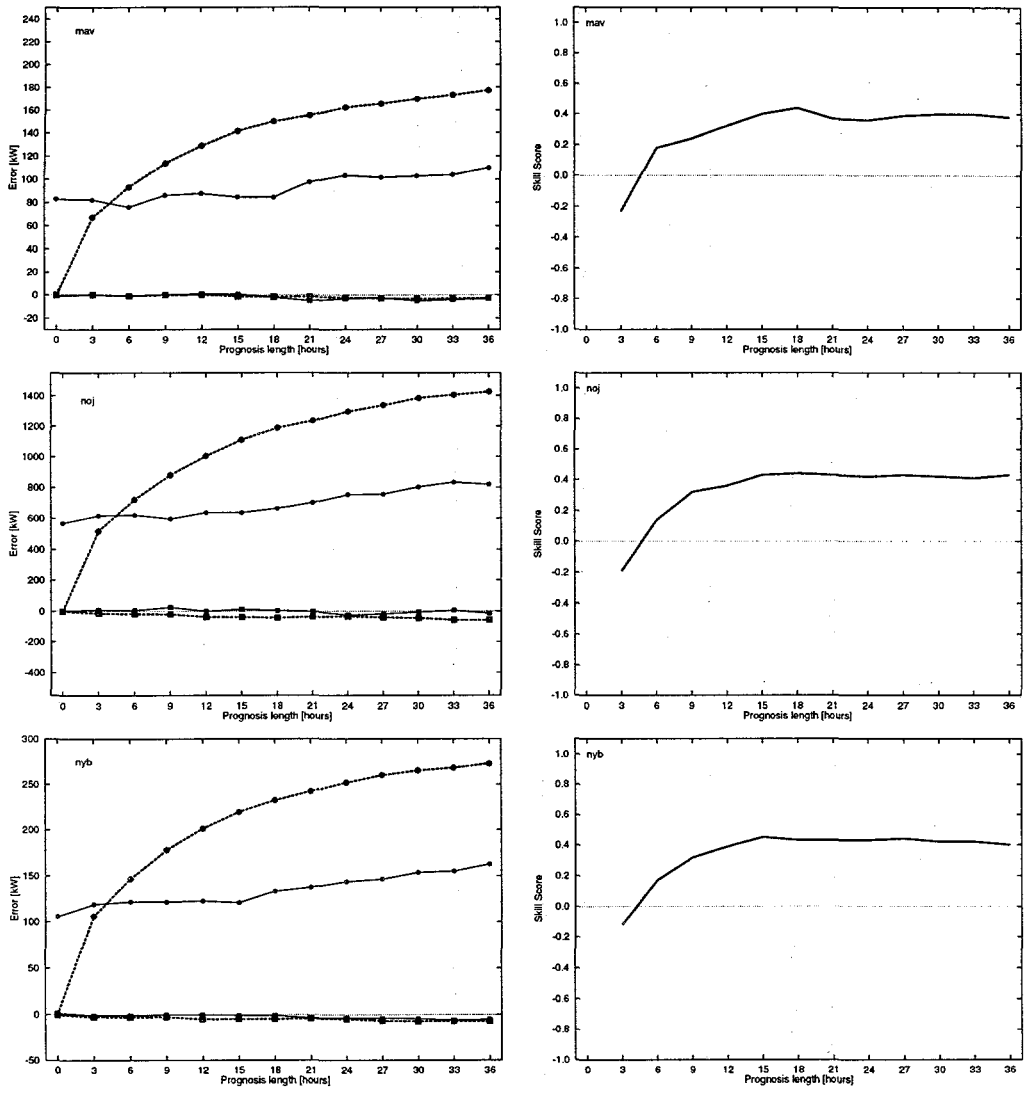

Figure 52. The ability of the model to predict the power produced by the wind farms compared to the performance of the persistence model. In the left frames the open symbols and dashed lines refer to persistence and the filled symbols and solid lines to the model; square symbols are the mean error (in kW) and round symbols are the mean absolute error (also in kW). Right frames shows the skill score. In all frames the forecast length (in hours) is along the apsis.

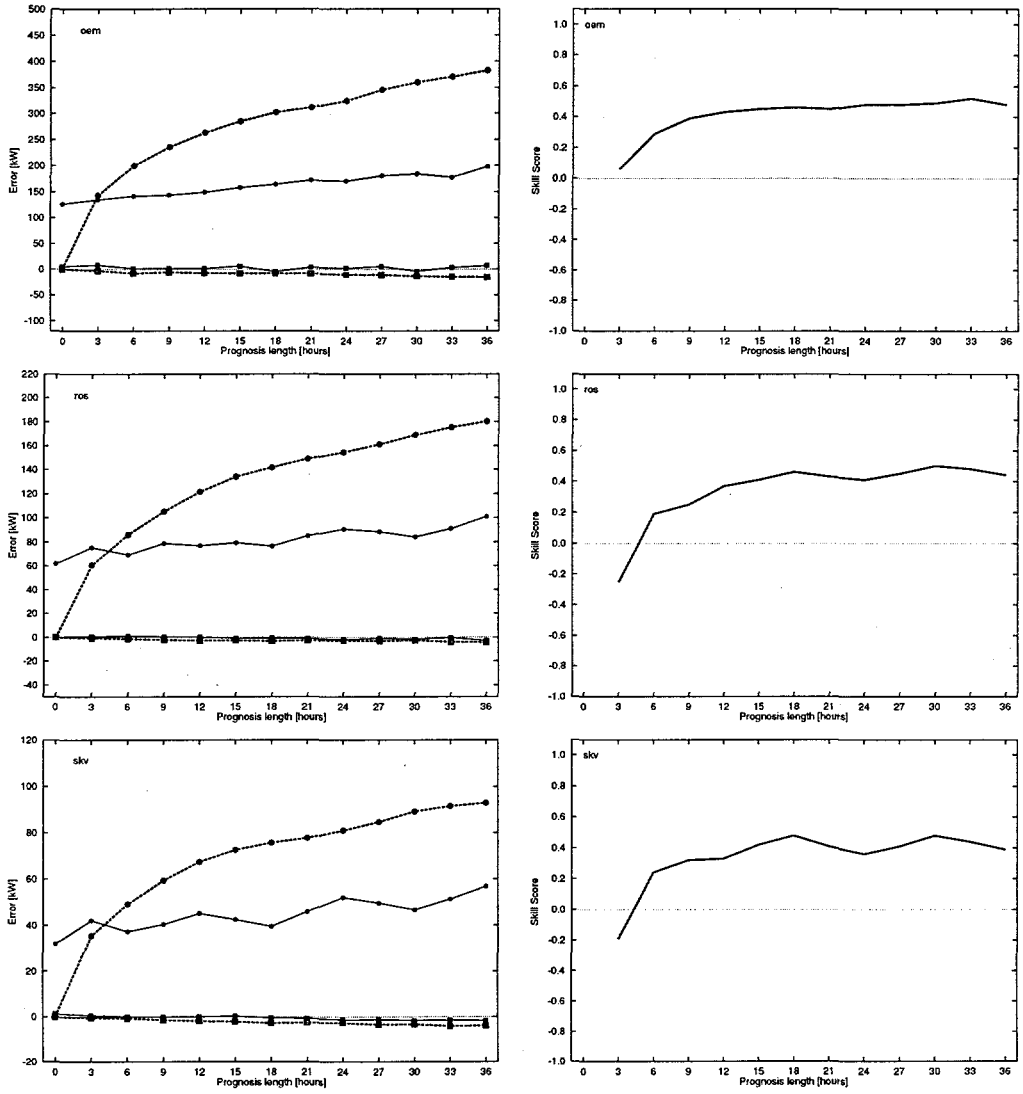

Figure 53. The ability of the model to predict the power produced by the wind farms compared to the performance of the persistence model. In the left frames the open symbols and dashed lines refer to persistence and the filled symbols and solid lines to the model; square symbols are the mean error (in kW) and round symbols are the mean absolute error (also in kW). Right frames shows the skill score. In all frames the forecast length (in hours) is along the apsis.

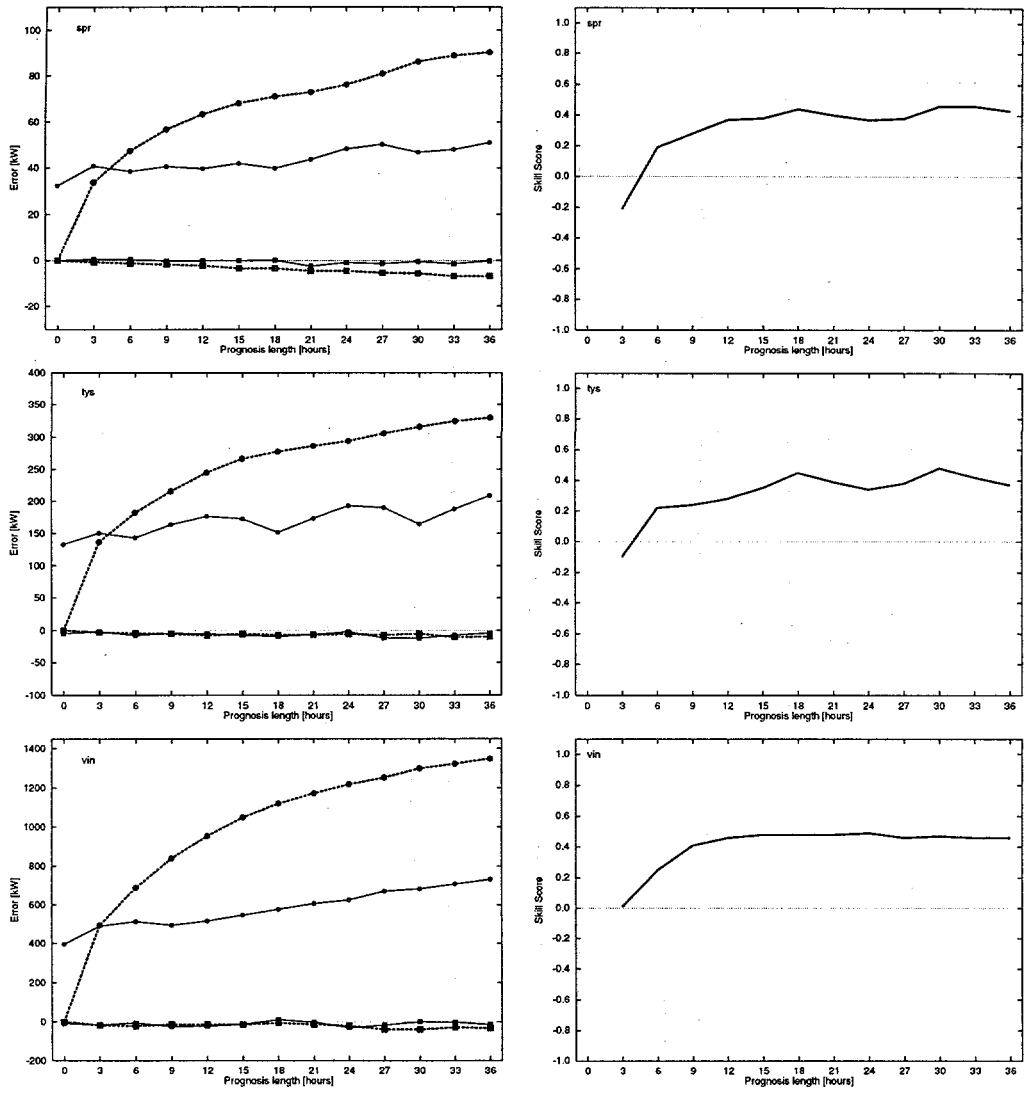

Figure 54. The ability of the model to predict the power produced by the wind farms compared to the performance of the persistence model. In the left frames the open symbols and dashed lines refer to persistence and the filled symbols and solid lines to the model; square symbols are the mean error (in kW) and round symbols are the mean absolute error (also in kW). Right frames shows the skill score. In all frames the forecast length (in hours) is along the apsis.

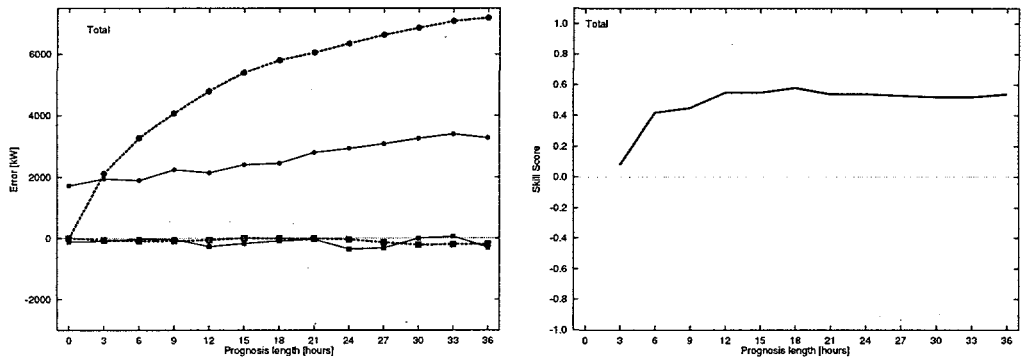

Figure 55. The ability of the model to predict the total power produced in the restricted sample compared to the performance of the persistence model. In the left frame the open symbols and dashed lines refer to persistence and the filled symbols and solid lines to the model; square symbols are the mean error (in kW) and round symbols are the mean absolute error (also in kW). Right frame shows the skill score. In all frames the forecast length (in hours) is along the apsis.

A.5 Figures showing error vs. wind farm id

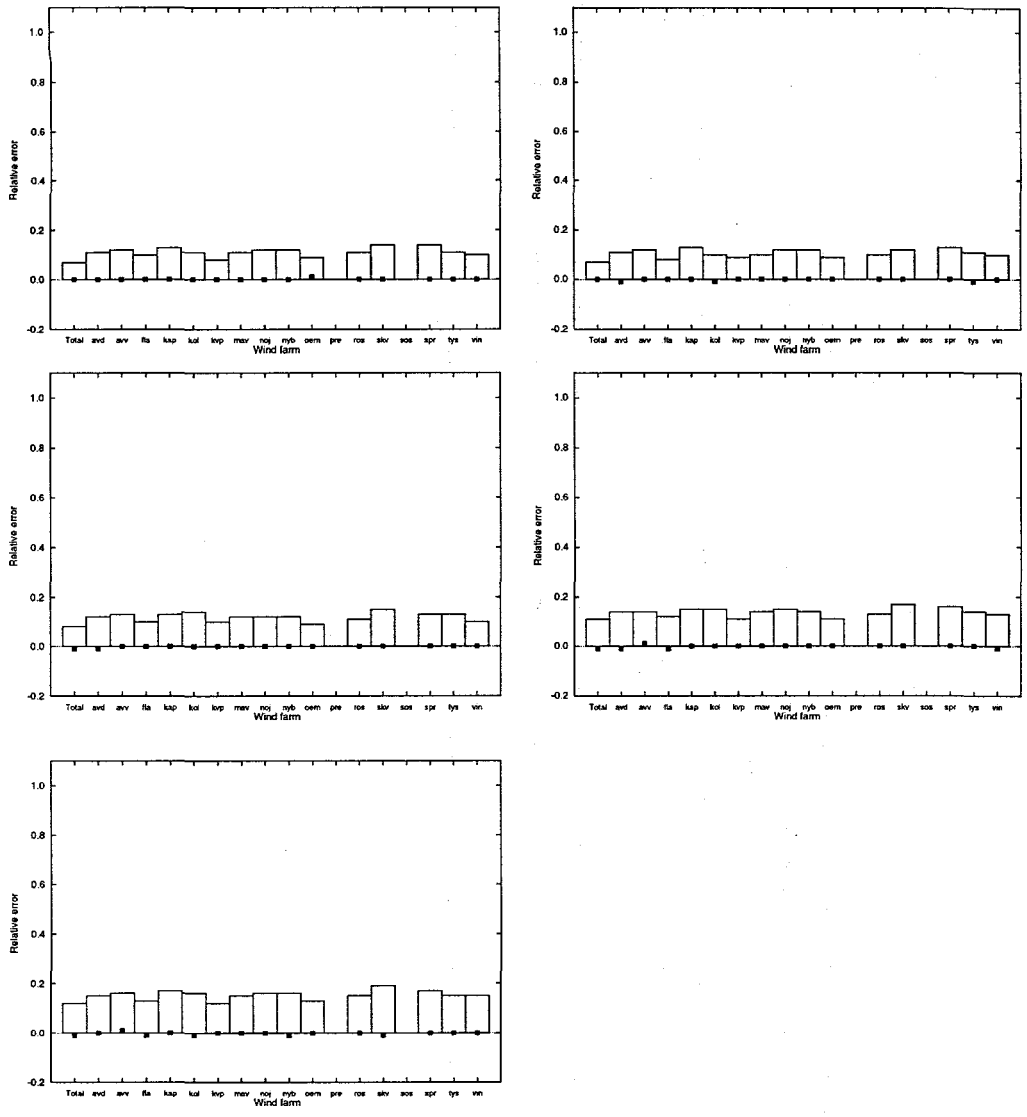

Figure 56. The errors for all wind farms and the total constructed from the restricted sample compared using the DMI model. The boxes are the mean absolute error and the filled squares are the mean errors. The prognosis length increases from left to right in the series: +3, +6, +12, +24 and +36 hours.

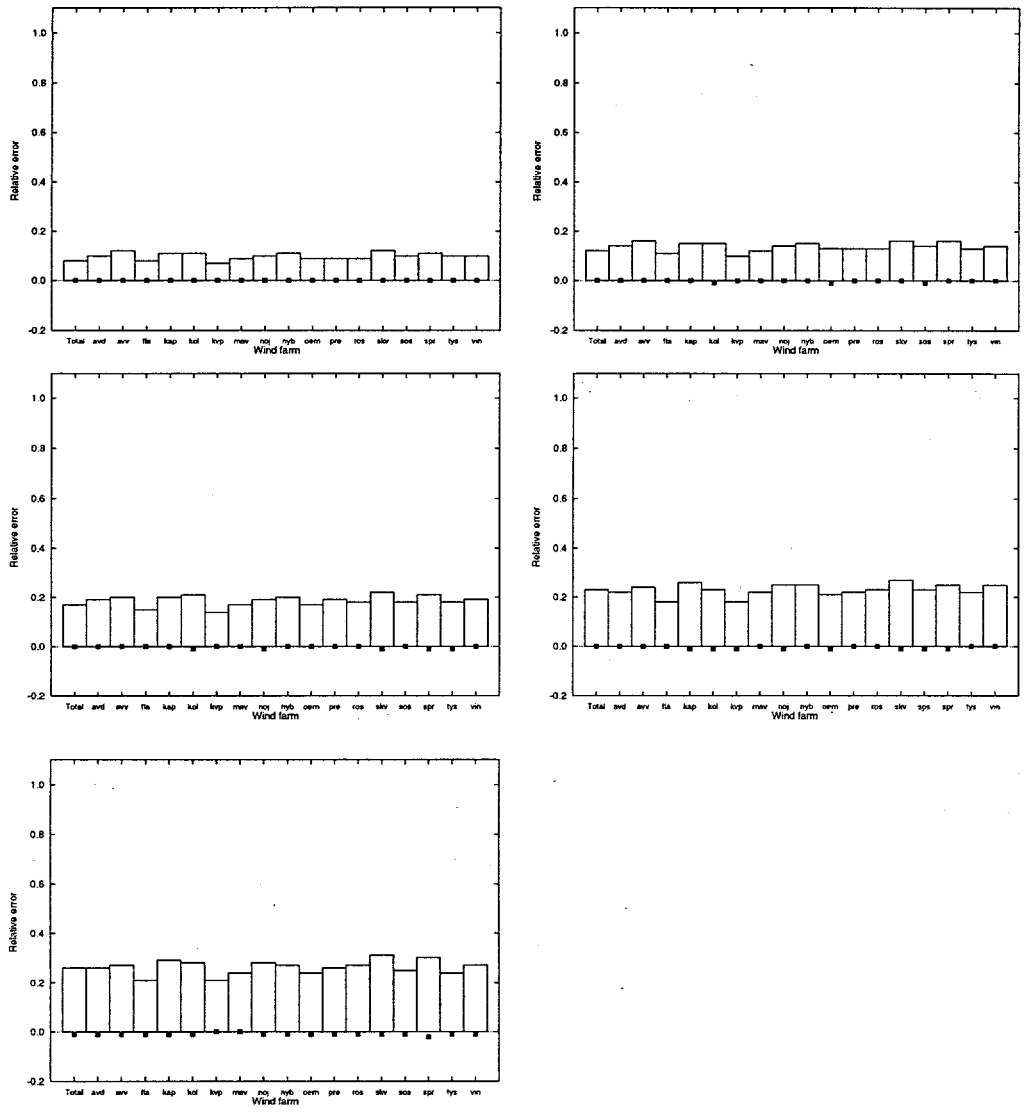

Figure 57. The errors for all wind farms and the total constructed from the restricted sample compared using the persistence approach. The boxes are the mean absolute error and the filled squares are the mean errors. The prognosis length increases from left to right in the series: +3, +6, +12, +24 and +36 hours.

A.6 Scatter plots for the best, the poorest and the total

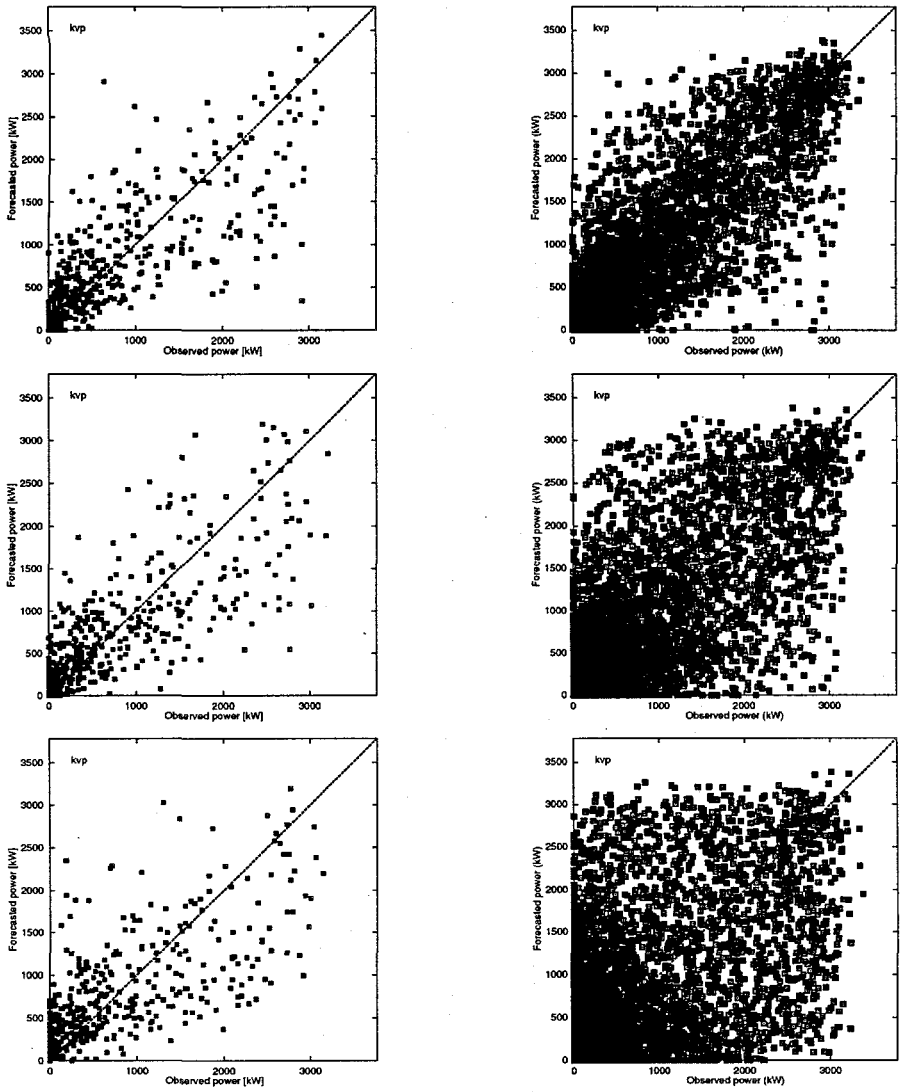

Figure 58. Scatter plots for the wind mill farm performing best (Kyndby- kvp). DMI model is shown on the left and the persistence approach on the right. The prognosis length increases from top down in the order +3, +6 and +12 hours.

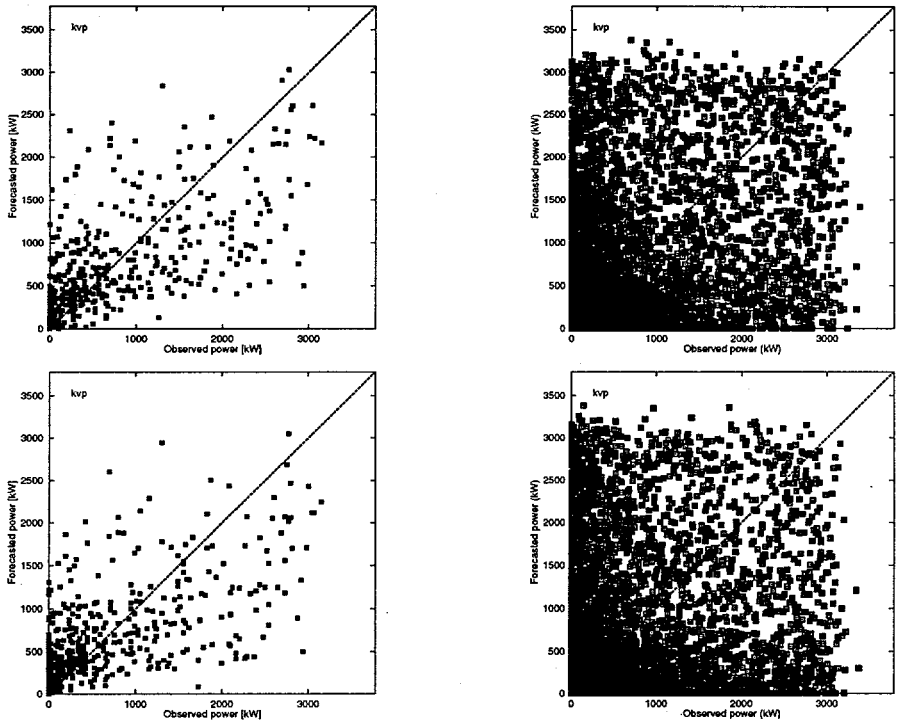

Figure 59. Scatter plots for the wind mill farm performing best (Kyndby-kvp). DMI model is shown on the left and the persistence approach on the right. The prognosis length increases from top down in the order +24, and +36 hours.

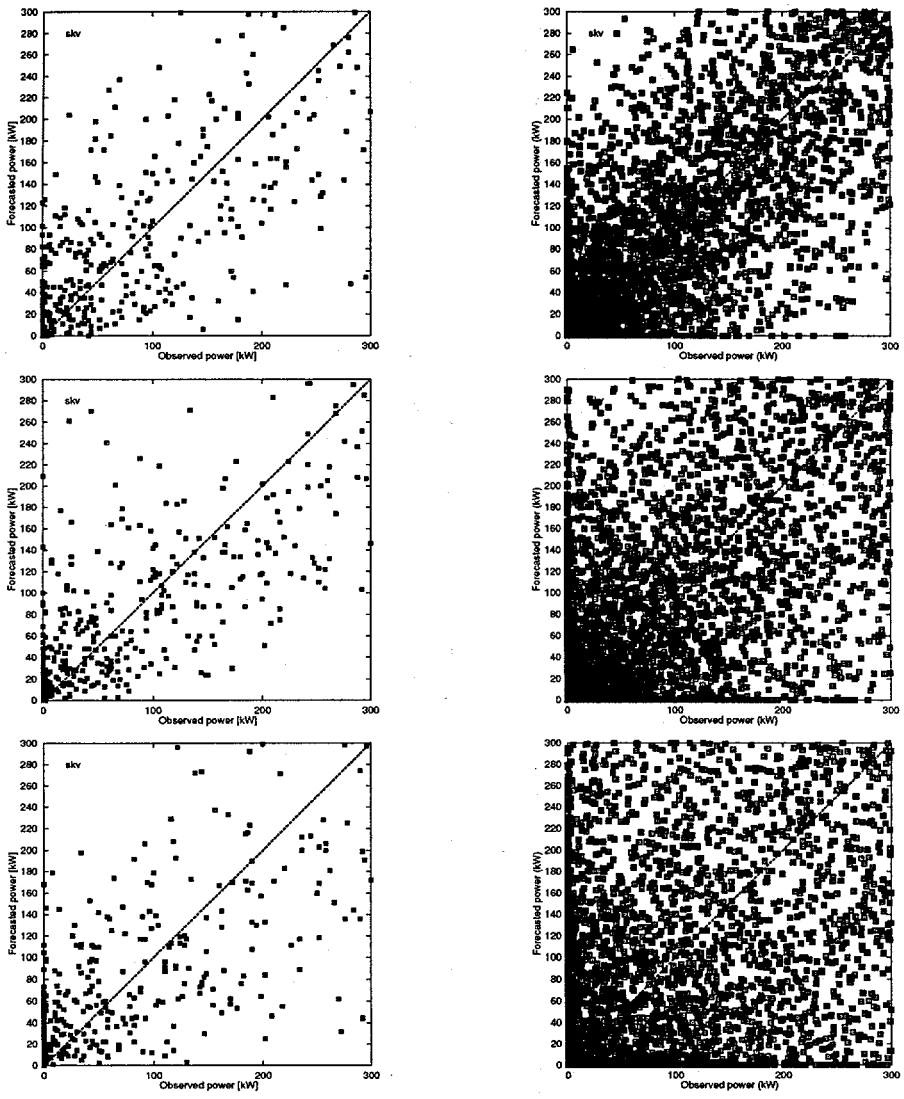

Figure 60. Scatter plots for the wind mill farm performing poorest (Skovlængeskv). DMI model is shown on the left and the persistence approach on the right. The prognosis length increases from top down in the order +3, +6 and +12 hours.

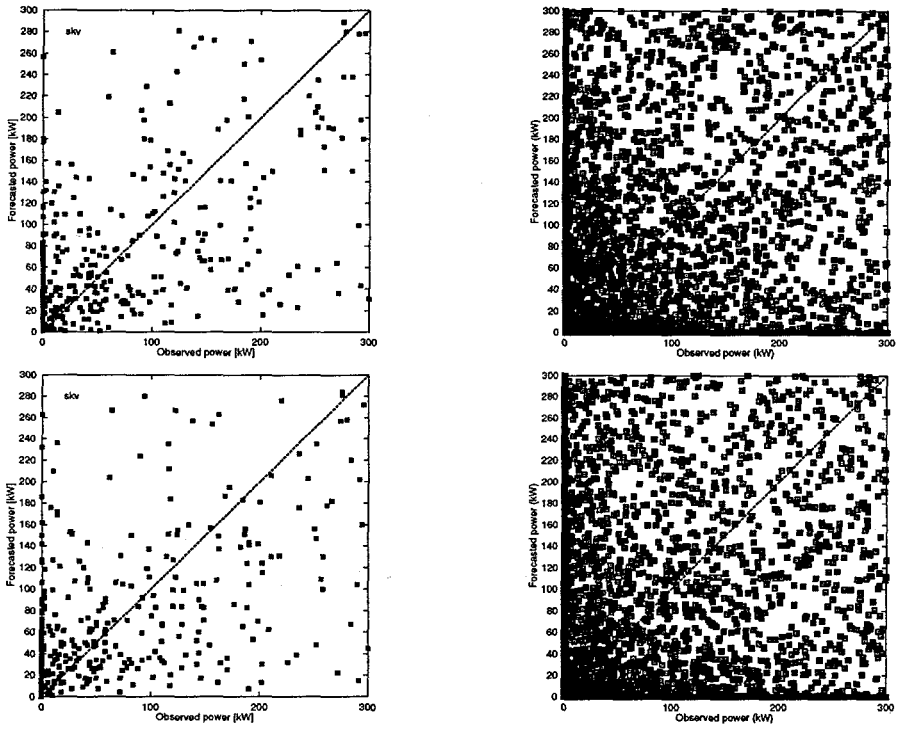

Figure 61. Scatter plots for the wind mill farm performing poorest (Skovlængeskv). DMI model is shown on the left and the persistence approach on the right. The prognosis length increases from top down in the order +24, and +36 hours.

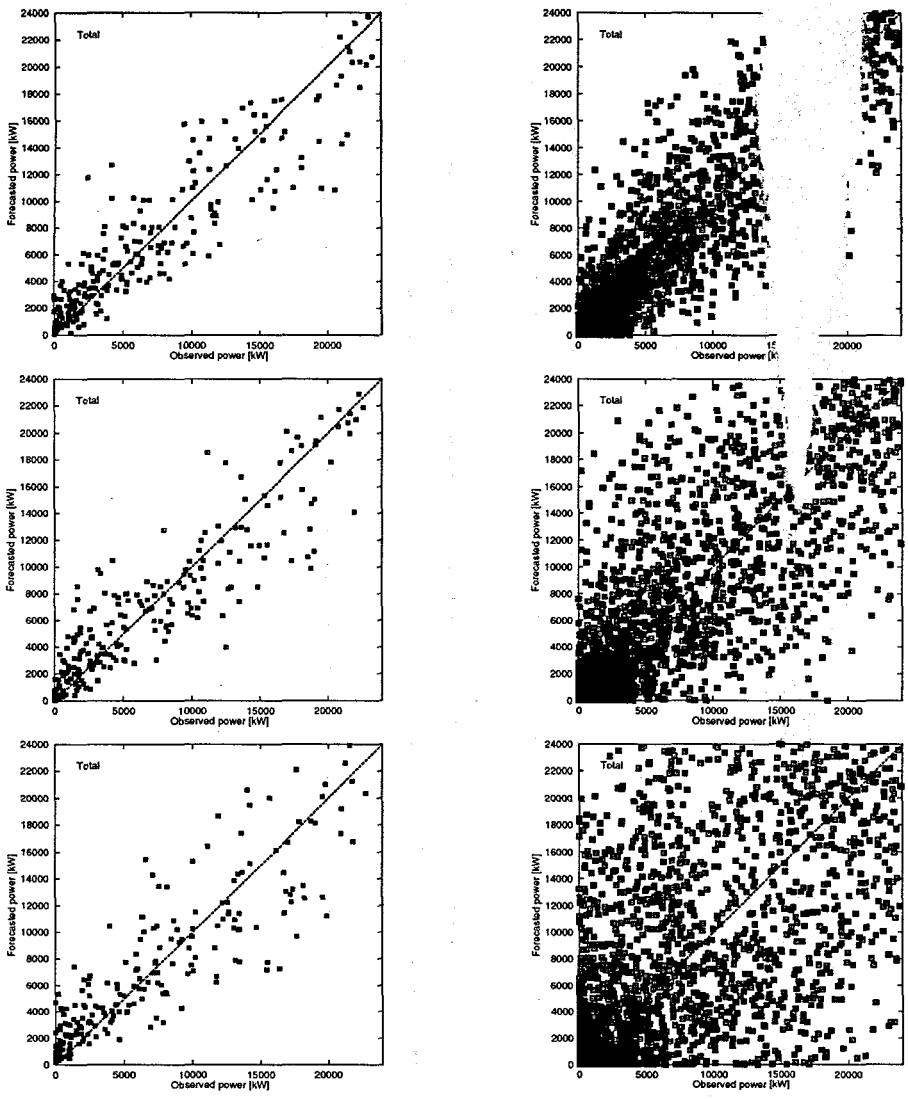

Figure 62. Scatter plots for the total. DMI model is shown on the left and the persistence approach on the right. The prognosis length increases from top down in the order +3, +6 and +12 hours.

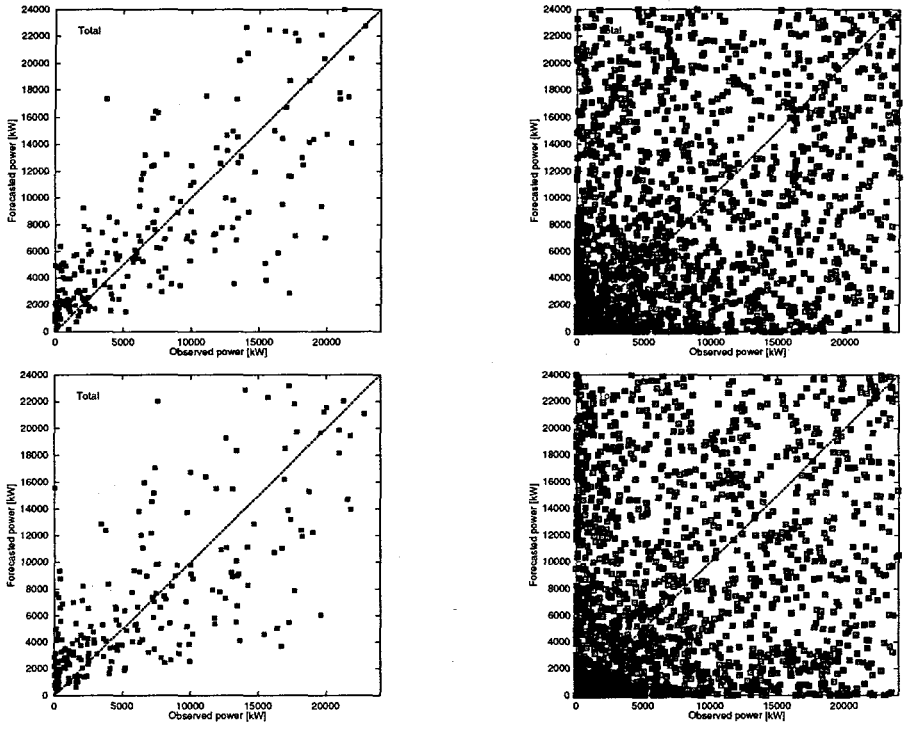

Figure 63. Scatter plots for the total. DMI model is shown on the left and the persistence approach on the right. The prognosis length increases from top down in the order +24, and +36 hours.

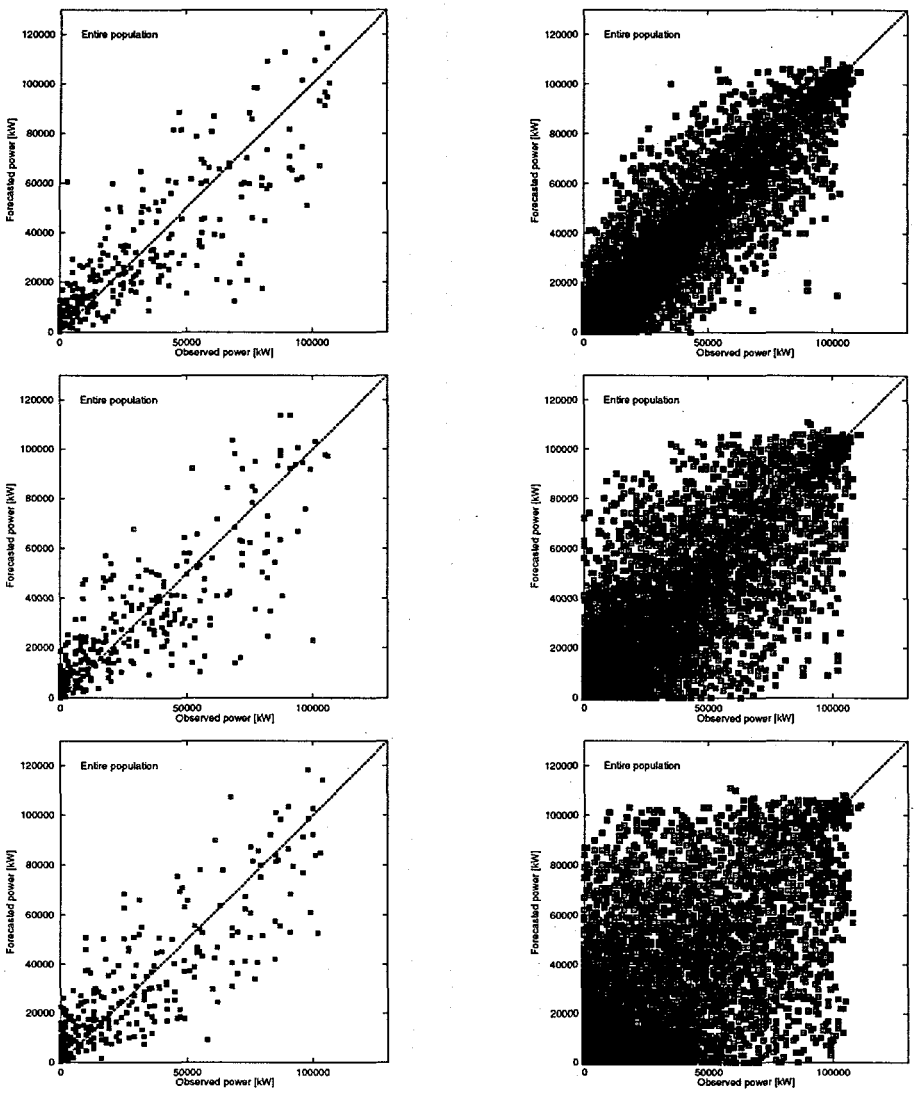

Figure 64. Scatter plots for the entire population. DMI model is shown on the left and the persistence approach on the right. The prognosis length increases from top down in the order +3, +6 and +12 hours.

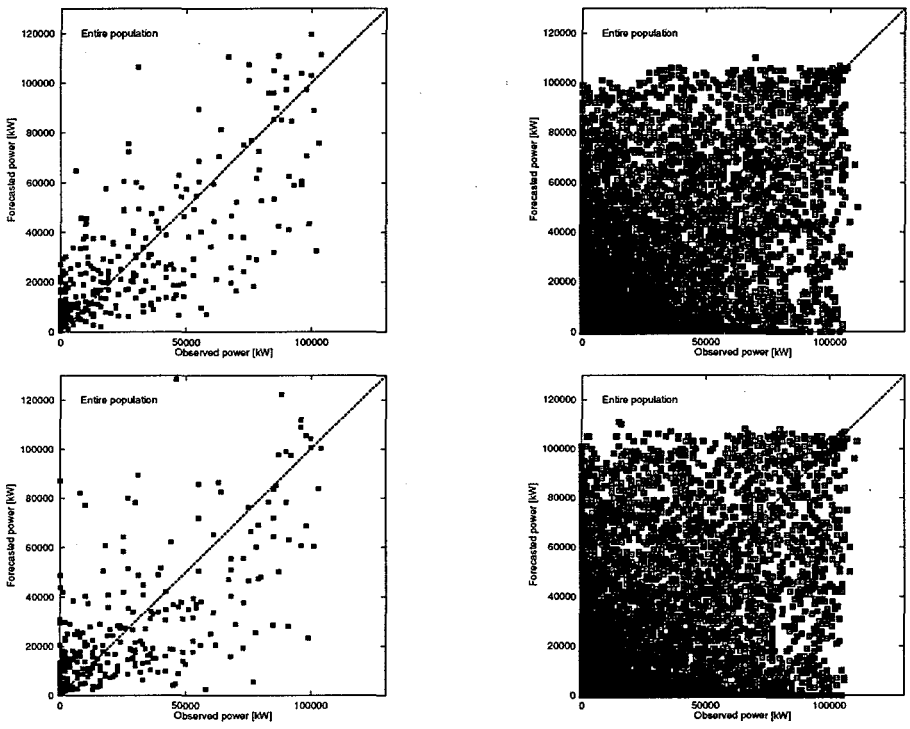

Figure 65. Scatter plots for the entire population. DMI model is shown on the left and the persistence approach on the right. The prognosis length increases from top down in the order +24, and +36 hours.

A.7 Kalman coefficients

Here we present the initial and resulting coefficients in the Kalman filtering of the wind speed and the derived electrical power. The columns V and $E_{\max}$ in the tables showing the initial values is the variance of the observation equa- equation and the maximum error tolerated respectively. These two values are set to be constant all the time, and are therefore omitted from the tables showing the resulting Kalman coefficients.

The Θ's filter the wind speed or derived electrical power like this:

$$\text{Kalmanfilteredvalue} = \Theta_1 + \Theta_2 \times \text{Rawvalue} \tag{A.31}$$

Table 5. Initial Kalman coefficients for the wind speed filtering. The initial coefficients are the same for all prognosis lengths, and for all farms.

Θ_1	Θ_2	$\sum_1$	$\sum_2$	$\sum_3$	$\sum_4$	V	$E_{\max}$
0.0	1.0	4.0	0.0	0.0	0.1	4.0	10.0

Table 6. Kalman coefficients for the wind filtering resulting from one year of updating. ID is wind farm identification, PL is prognosis length (hours).

PL	Θ_1	Θ_2	$\sum_1$	$\sum_2$	$\sum_3$	$\sum_4$
avd						
0	2.49	0.77	0.536	-0.054	-0.054	0.012
3	1.73	0.78	0.587	-0.059	-0.059	0.012
6	2.26	0.79	0.607	-0.058	-0.058	0.011
9	3.02	0.72	0.524	-0.051	-0.051	0.011
12	3.12	0.67	0.508	-0.052	-0.052	0.012
15	2.67	0.61	0.560	-0.053	-0.053	0.010
18	2.88	0.68	0.626	-0.059	-0.059	0.011
21	3.06	0.69	0.545	-0.052	-0.052	0.010
24	3.03	0.61	0.563	-0.055	-0.055	0.011
27	2.72	0.61	0.562	-0.055	-0.055	0.011
30	3.23	0.64	0.599	-0.058	-0.058	0.011
33	3.48	0.66	0.509	-0.048	-0.048	0.010
36	3.82	0.54	0.512	-0.051	-0.051	0.011
avv						
0	1.94	0.51	0.673	-0.066	-0.066	0.012
3	1.80	0.58	0.755	-0.074	-0.074	0.012
6	1.53	0.64	0.776	-0.074	-0.074	0.012
9	2.21	0.49	0.769	-0.078	-0.078	0.013
12	2.54	0.47	0.635	-0.066	-0.066	0.013
15	2.44	0.50	0.717	-0.069	-0.069	0.012
18	2.19	0.57	0.767	-0.074	-0.074	0.012
21	2.72	0.41	0.755	-0.075	-0.075	0.013
24	2.41	0.46	0.683	-0.069	-0.069	0.013
27	2.55	0.48	0.735	-0.071	-0.071	0.012
30	2.64	0.49	0.750	-0.071	-0.071	0.012
33	3.23	0.33	0.684	-0.062	-0.062	0.010
36	3.07	0.36	0.662	-0.064	-0.064	0.012

fla						
0	0.33	0.90	0.690	-0.066	-0.066	0.011
3	0.64	0.90	0.907	-0.084	-0.084	0.012
6	0.71	0.92	0.877	-0.081	-0.081	0.012
9	2.49	0.65	0.797	-0.074	-0.074	0.011
12	1.80	0.79	0.630	-0.064	-0.064	0.012
15	1.22	0.86	0.883	-0.084	-0.084	0.012
18	1.72	0.78	0.825	-0.072	-0.072	0.010
21	2.86	0.59	0.799	-0.073	-0.073	0.011
24	1.97	0.72	0.673	-0.066	-0.066	0.012
27	2.24	0.72	0.756	-0.070	-0.070	0.011
30	2.77	0.67	0.791	-0.072	-0.072	0.011
33	3.38	0.52	0.727	-0.065	-0.065	0.010
36	3.37	0.56	0.585	-0.057	-0.057	0.011
kap						
0	0.75	0.58	0.777	-0.060	-0.060	0.008
3	0.51	0.65	0.894	-0.065	-0.065	0.008
6	1.65	0.61	0.863	-0.062	-0.062	0.008
9	1.50	0.53	0.820	-0.062	-0.062	0.008
12	0.61	0.64	0.758	-0.064	-0.064	0.009
15	1.13	0.60	0.913	-0.068	-0.068	0.008
18	1.58	0.62	0.875	-0.063	-0.063	0.008
21	2.13	0.47	0.787	-0.058	-0.058	0.008
24	1.77	0.47	0.735	-0.057	-0.057	0.008
27	2.58	0.42	0.877	-0.059	-0.059	0.007
30	2.40	0.52	0.881	-0.061	-0.061	0.007
33	3.50	0.30	0.785	-0.055	-0.055	0.007
36	3.28	0.31	0.673	-0.050	-0.050	0.007
kol						
0	2.32	0.74	0.632	-0.070	-0.070	0.014
3	2.62	0.78	0.624	-0.076	-0.076	0.017
6	2.46	0.65	0.662	-0.074	-0.074	0.015
9	2.81	0.65	0.712	-0.083	-0.083	0.017
12	3.34	0.63	0.608	-0.072	-0.072	0.016
15	3.39	0.60	0.600	-0.068	-0.068	0.015
18	3.48	0.49	0.600	-0.065	-0.065	0.014
21	3.18	0.59	0.679	-0.077	-0.077	0.015
24	3.92	0.52	0.538	-0.059	-0.059	0.014
27	3.74	0.50	0.599	-0.066	-0.066	0.014
30	3.55	0.45	0.610	-0.065	-0.065	0.013
33	3.52	0.49	0.640	-0.069	-0.069	0.014
36	4.37	0.40	0.558	-0.060	-0.060	0.013

kvp						
0	1.21	0.92	0.669	-0.070	-0.070	0.013
3	1.25	0.91	0.728	-0.077	-0.077	0.014
6	1.73	0.86	0.677	-0.071	-0.071	0.013
9	1.80	0.87	0.748	-0.080	-0.080	0.014
12	2.07	0.86	0.639	-0.070	-0.070	0.014
15	1.48	0.89	0.676	-0.073	-0.073	0.014
18	1.76	0.89	0.652	-0.069	-0.069	0.014
21	1.81	0.84	0.706	-0.073	-0.073	0.013
24	2.37	0.76	0.650	-0.069	-0.069	0.013
27	1.94	0.80	0.637	-0.067	-0.067	0.013
30	2.46	0.76	0.618	-0.064	-0.064	0.013
33	1.94	0.77	0.712	-0.072	-0.072	0.013
36	2.26	0.71	0.666	-0.068	-0.068	0.013
mav						
0	2.35	0.71	0.640	-0.069	-0.069	0.014
3	1.52	1.00	0.654	-0.067	-0.067	0.012
6	2.16	0.81	0.595	-0.066	-0.066	0.014
9	1.71	0.75	0.651	-0.067	-0.067	0.012
12	2.77	0.74	0.593	-0.070	-0.070	0.016
15	2.12	0.96	0.642	-0.069	-0.069	0.014
18	2.54	0.78	0.585	-0.066	-0.066	0.015
21	2.38	0.70	0.596	-0.063	-0.063	0.013
24	3.63	0.58	0.580	-0.068	-0.068	0.016
27	2.68	0.74	0.667	-0.074	-0.074	0.015
30	3.49	0.60	0.604	-0.069	-0.069	0.015
33	2.81	0.63	0.601	-0.064	-0.064	0.013
36	3.65	0.55	0.588	-0.065	-0.065	0.014
noj						
0	0.73	0.71	0.764	-0.063	-0.063	0.009
3	0.41	0.81	0.878	-0.077	-0.077	0.011
6	0.57	0.81	0.844	-0.074	-0.074	0.011
9	0.90	0.75	0.829	-0.075	-0.075	0.011
12	1.11	0.75	0.736	-0.069	-0.069	0.011
15	0.72	0.81	0.836	-0.076	-0.076	0.011
18	1.38	0.71	0.790	-0.067	-0.067	0.010
21	2.03	0.59	0.779	-0.067	-0.067	0.010
24	1.49	0.66	0.760	-0.067	-0.067	0.010
27	1.52	0.69	0.828	-0.072	-0.072	0.011
30	1.98	0.63	0.789	-0.066	-0.066	0.009
33	3.41	0.45	0.650	-0.052	-0.052	0.008
36	2.75	0.51	0.704	-0.060	-0.060	0.009

nyb						
0	0.16	0.90	0.808	-0.067	-0.067	0.009
3	0.15	1.06	0.743	-0.067	-0.067	0.011
6	0.18	1.03	0.864	-0.078	-0.078	0.011
9	0.86	0.91	0.758	-0.068	-0.068	0.011
12	0.65	0.95	0.800	-0.075	-0.075	0.011
15	0.56	1.04	0.720	-0.066	-0.066	0.011
18	1.30	0.90	0.786	-0.070	-0.070	0.011
21	1.94	0.75	0.706	-0.059	-0.059	0.009
24	1.36	0.82	0.780	-0.069	-0.069	0.010
27	1.65	0.89	0.701	-0.063	-0.063	0.010
30	2.29	0.76	0.779	-0.068	-0.068	0.010
33	2.83	0.64	0.637	-0.051	-0.051	0.008
36	2.44	0.69	0.750	-0.065	-0.065	0.010
oem						
0	1.87	0.63	0.664	-0.062	-0.062	0.011
3	1.78	0.70	0.631	-0.055	-0.055	0.010
6	2.31	0.63	0.650	-0.059	-0.059	0.010
9	1.83	0.65	0.738	-0.066	-0.066	0.010
12	2.04	0.58	0.677	-0.061	-0.061	0.010
15	1.70	0.68	0.683	-0.060	-0.060	0.010
18	2.43	0.58	0.690	-0.062	-0.062	0.010
21	2.52	0.55	0.737	-0.065	-0.065	0.010
24	1.94	0.58	0.695	-0.062	-0.062	0.010
27	1.91	0.62	0.698	-0.061	-0.061	0.010
30	2.86	0.53	0.658	-0.057	-0.057	0.010
33	2.72	0.51	0.716	-0.060	-0.060	0.009
36	2.86	0.47	0.634	-0.054	-0.054	0.009
pre						
0	0.00	1.00	4.000	0.000	0.000	0.100
3	0.00	1.00	4.000	0.000	0.000	0.100
6	0.00	1.00	4.000	0.000	0.000	0.100
9	0.00	1.00	4.000	0.000	0.000	0.100
12	0.00	1.00	4.000	0.000	0.000	0.100
15	0.00	1.00	4.000	0.000	0.000	0.100
18	0.00	1.00	4.000	0.000	0.000	0.100
21	0.00	1.00	4.000	0.000	0.000	0.100
24	0.00	1.00	4.000	0.000	0.000	0.100
27	0.00	1.00	4.000	0.000	0.000	0.100
30	0.00	1.00	4.000	0.000	0.000	0.100
33	0.00	1.00	4.000	0.000	0.000	0.100
36	0.00	1.00	4.000	0.000	0.000	0.100

ros						
0	1.35	0.70	0.757	-0.072	-0.072	0.012
3	1.37	0.73	0.768	-0.069	-0.069	0.011
6	1.40	0.73	0.910	-0.080	-0.080	0.011
9	2.63	0.59	0.837	-0.076	-0.076	0.011
12	1.79	0.64	0.753	-0.071	-0.071	0.011
15	1.10	0.74	0.808	-0.072	-0.072	0.011
18	2.35	0.63	0.824	-0.072	-0.072	0.011
21	3.11	0.54	0.783	-0.069	-0.069	0.010
24	2.14	0.56	0.778	-0.071	-0.071	0.011
27	1.35	0.67	0.878	-0.076	-0.076	0.011
30	2.84	0.56	0.790	-0.067	-0.067	0.010
33	3.20	0.49	0.792	-0.067	-0.067	0.010
36	3.03	0.44	0.691	-0.060	-0.060	0.009
skv						
0	1.08	0.66	0.752	-0.066	-0.066	0.010
3	0.26	0.79	0.842	-0.077	-0.077	0.012
6	1.14	0.77	0.891	-0.081	-0.081	0.012
9	1.04	0.72	0.789	-0.072	-0.072	0.011
12	1.98	0.63	0.673	-0.065	-0.065	0.012
15	0.73	0.76	0.755	-0.071	-0.071	0.012
18	1.57	0.71	0.814	-0.073	-0.073	0.011
21	2.05	0.57	0.731	-0.063	-0.063	0.010
24	2.00	0.58	0.706	-0.065	-0.065	0.011
27	1.42	0.66	0.744	-0.067	-0.067	0.011
30	1.92	0.64	0.811	-0.072	-0.072	0.011
33	2.61	0.49	0.660	-0.055	-0.055	0.009
36	3.02	0.45	0.684	-0.061	-0.061	0.010
sos						
0	0.79	0.85	0.658	-0.064	-0.064	0.012
3	1.31	0.88	0.596	-0.055	-0.055	0.011
6	0.77	0.94	0.661	-0.064	-0.064	0.011
9	1.68	0.83	0.706	-0.069	-0.069	0.012
12	0.94	0.81	0.665	-0.066	-0.066	0.012
15	0.90	0.89	0.629	-0.059	-0.059	0.011
18	1.52	0.80	0.670	-0.063	-0.063	0.011
21	2.16	0.72	0.719	-0.070	-0.070	0.012
24	0.87	0.85	0.654	-0.065	-0.065	0.012
27	0.87	0.86	0.688	-0.066	-0.066	0.012
30	2.27	0.71	0.671	-0.062	-0.062	0.011
33	2.38	0.67	0.654	-0.059	-0.059	0.010
36	1.96	0.73	0.554	-0.052	-0.052	0.011

spr						
0	1.07	0.63	0.774	-0.067	-0.067	0.010
3	1.21	0.68	0.888	-0.074	-0.074	0.010
6	1.15	0.71	0.937	-0.078	-0.078	0.010
9	1.39	0.70	0.935	-0.083	-0.083	0.011
12	1.93	0.58	0.710	-0.066	-0.066	0.011
15	1.72	0.65	0.830	-0.070	-0.070	0.010
18	1.64	0.65	0.841	-0.070	-0.070	0.010
21	2.08	0.57	0.873	-0.073	-0.073	0.010
24	2.50	0.48	0.732	-0.064	-0.064	0.010
27	2.40	0.55	0.817	-0.066	-0.066	0.009
30	2.37	0.55	0.843	-0.067	-0.067	0.009
33	2.62	0.49	0.823	-0.066	-0.066	0.009
36	2.99	0.43	0.705	-0.059	-0.059	0.009
tys						
0	1.55	0.88	0.630	-0.069	-0.069	0.014
3	1.27	1.09	0.732	-0.083	-0.083	0.016
6	1.90	0.94	0.695	-0.077	-0.077	0.015
9	2.89	0.83	0.636	-0.071	-0.071	0.015
12	1.99	0.88	0.625	-0.074	-0.074	0.016
15	2.16	0.96	0.656	-0.072	-0.072	0.014
18	2.51	0.87	0.652	-0.072	-0.072	0.015
21	2.55	0.84	0.657	-0.070	-0.070	0.014
24	2.41	0.76	0.598	-0.066	-0.066	0.014
27	2.91	0.82	0.612	-0.063	-0.063	0.012
30	3.16	0.70	0.640	-0.067	-0.067	0.013
33	3.58	0.60	0.642	-0.063	-0.063	0.012
36	2.95	0.62	0.622	-0.065	-0.065	0.013
vin						
0	1.75	0.93	0.555	-0.049	-0.049	0.010
3	1.47	1.16	0.655	-0.059	-0.059	0.010
6	1.71	1.09	0.626	-0.058	-0.058	0.011
9	0.41	1.16	0.628	-0.061	-0.061	0.012
12	2.17	0.97	0.565	-0.056	-0.056	0.012
15	2.13	1.10	0.590	-0.054	-0.054	0.010
18	2.70	1.01	0.550	-0.049	-0.049	0.010
21	2.16	0.90	0.536	-0.048	-0.048	0.010
24	2.78	0.81	0.561	-0.052	-0.052	0.011
27	2.94	0.98	0.571	-0.051	-0.051	0.010
30	3.03	0.91	0.576	-0.051	-0.051	0.010
33	3.16	0.73	0.527	-0.045	-0.045	0.009
36	3.95	0.63	0.531	-0.047	-0.047	0.009

Table 7. : Initial Kalman coefficients for the post-filtering of the derived electrical power. The coefficients are the same for all prognosis lengths.

Farm ID	Θ_1	Θ_2	$\sum_1$	$\sum_2$	$\sum_3$	$\sum_4$	V	$E_{\max}$
avd	0.0	1.0	10.0	0.0	0.0	0.1	10000	5000
avv	0.0	1.0	10.0	0.0	0.0	0.1	5000	500
fla	0.0	1.0	10.0	0.0	0.0	0.1	200	5000
kap	0.0	1.0	10.0	0.0	0.0	0.1	10000	10000
kvp	0.0	1.0	10.0	0.0	0.0	0.1	160000	20000
mav	0.0	1.0	10.0	0.0	0.0	0.1	50	5000
noj	0.0	1.0	10.0	0.0	0.0	0.1	640	10000
nyb	0.0	1.0	10.0	0.0	0.0	0.1	100	5000
oem	0.0	1.0	10.0	0.0	0.0	0.1	5000	5000
ros	0.0	1.0	10.0	0.0	0.0	0.1	100	5000
skv	0.0	1.0	10.0	0.0	0.0	0.1	10	5000
sos	0.0	1.0	10.0	0.0	0.0	0.1	2500	5000
spr	0.0	1.0	10.0	0.0	0.0	0.1	10	5000
tys	0.0	1.0	10.0	0.0	0.0	0.1	500	5000
vin	0.0	1.0	10.0	0.0	0.0	0.1	250000	5000

Table 8. : Resulting Kalman coefficients for the post-filtering of the derived electrical power after one year of updating.

PL	Θ_1	Θ_2	$\sum_1$	$\sum_2$	$\sum_3$	$\sum_4$
avd						
0	-3.33	0.95	16.996	-0.020	-0.020	0.003
3	-0.07	0.69	17.694	-0.019	-0.019	0.002
6	-7.94	0.63	18.185	-0.016	-0.016	0.002
9	-6.68	0.66	17.690	-0.016	-0.016	0.002
12	-3.45	0.86	17.296	-0.019	-0.019	0.002
15	-0.53	0.58	17.975	-0.018	-0.018	0.002
18	-2.26	0.52	18.385	-0.015	-0.015	0.002
21	-5.23	0.59	17.778	-0.015	-0.015	0.002
24	-0.31	0.70	17.481	-0.018	-0.018	0.002
27	3.71	0.61	17.967	-0.021	-0.021	0.002
30	-4.49	0.59	18.662	-0.019	-0.019	0.002
33	-1.92	0.64	17.782	-0.018	-0.018	0.002
36	0.57	0.54	17.788	-0.020	-0.020	0.002
avv						
0	0.43	1.03	14.763	-0.035	-0.035	0.005
3	1.29	1.13	15.140	-0.036	-0.036	0.005
6	-3.55	1.09	15.367	-0.036	-0.036	0.004
9	-4.99	0.95	15.555	-0.041	-0.041	0.005
12	1.58	0.94	15.106	-0.042	-0.042	0.005
15	-1.89	1.10	15.605	-0.040	-0.040	0.005
18	-5.95	0.86	15.892	-0.046	-0.046	0.005
21	-3.55	0.94	15.809	-0.044	-0.044	0.005
24	2.59	0.99	15.434	-0.043	-0.043	0.006
27	-1.79	1.00	15.894	-0.041	-0.041	0.004
30	-0.66	0.72	16.206	-0.049	-0.049	0.005
33	-1.46	0.85	16.301	-0.044	-0.044	0.005
36	-0.57	0.92	16.277	-0.048	-0.048	0.005

fla						
0	-2.10	0.51	2.958	-0.027	-0.027	0.006
3	-3.96	1.18	3.092	-0.037	-0.037	0.006
6	-1.89	0.91	3.245	-0.027	-0.027	0.004
9	-3.91	0.85	3.262	-0.040	-0.040	0.006
12	-5.30	0.79	3.193	-0.047	-0.047	0.008
15	-3.46	1.12	3.163	-0.038	-0.038	0.006
18	-1.06	0.89	3.275	-0.028	-0.028	0.004
21	-4.35	0.85	3.315	-0.041	-0.041	0.006
24	-4.99	0.64	3.268	-0.039	-0.039	0.007
27	-1.63	0.88	3.190	-0.035	-0.035	0.006
30	-2.51	0.85	3.442	-0.033	-0.033	0.005
33	-6.50	0.87	3.630	-0.052	-0.052	0.007
36	-5.38	0.51	3.727	-0.046	-0.046	0.006
kap						
0	-10.81	0.36	17.642	-0.009	-0.009	0.001
3	-12.89	0.13	18.069	-0.008	-0.008	0.001
6	1.81	0.18	18.574	-0.008	-0.008	0.001
9	-29.26	0.38	18.345	-0.009	-0.009	0.001
12	-24.82	0.34	17.800	-0.008	-0.008	0.001
15	-22.53	0.15	18.429	-0.008	-0.008	0.001
18	-22.94	0.29	18.992	-0.009	-0.009	0.001
21	-26.43	0.40	18.413	-0.009	-0.009	0.001
24	-19.92	0.39	18.191	-0.009	-0.009	0.001
27	-9.29	0.11	18.620	-0.008	-0.008	0.001
30	-15.59	0.11	19.359	-0.008	-0.008	0.001
33	-8.42	0.25	18.916	-0.009	-0.009	0.001
36	3.19	0.21	18.562	-0.010	-0.010	0.001
kol						
0	-8.51	0.67	2.710	-0.021	-0.021	0.002
3	-0.25	0.69	2.907	-0.026	-0.026	0.002
6	2.60	0.68	2.622	-0.025	-0.025	0.002
9	-14.72	0.83	3.167	-0.032	-0.032	0.002
12	-4.35	0.59	3.350	-0.030	-0.030	0.002
15	-0.51	0.64	3.128	-0.027	-0.027	0.002
18	-5.69	0.69	3.153	-0.031	-0.031	0.002
21	-3.77	0.65	3.078	-0.028	-0.028	0.002
24	0.83	0.47	3.499	-0.030	-0.030	0.002
27	6.70	0.58	3.443	-0.030	-0.030	0.002
30	-0.22	0.58	3.278	-0.030	-0.030	0.002
33	-3.02	0.58	3.233	-0.029	-0.029	0.002
36	7.19	0.34	3.947	-0.032	-0.032	0.002

kvp						
0	-0.40	1.12	22.647	-0.017	-0.017	0.008
3	0.29	1.06	23.560	-0.017	-0.017	0.007
6	-0.03	1.06	23.863	-0.018	-0.018	0.007
9	-0.26	1.06	23.556	-0.018	-0.018	0.007
12	0.19	1.12	22.673	-0.020	-0.020	0.009
15	0.19	1.05	23.554	-0.017	-0.017	0.007
18	0.08	1.07	23.882	-0.018	-0.018	0.007
21	0.01	1.00	23.534	-0.017	-0.017	0.007
24	0.47	1.09	22.722	-0.020	-0.020	0.009
27	0.58	1.06	23.529	-0.018	-0.018	0.008
30	0.19	1.08	23.887	-0.019	-0.019	0.008
33	0.16	0.95	23.520	-0.017	-0.017	0.007
36	0.24	0.97	22.677	-0.018	-0.018	0.008
mav						
0	6.51	-0.02	1.878	-0.006	-0.006	0.000
3	4.40	-0.01	2.106	-0.003	-0.003	0.000
6	3.15	-0.02	2.030	-0.010	-0.010	0.000
9	-5.71	0.02	1.870	-0.007	-0.007	0.000
12	8.73	-0.03	2.125	-0.007	-0.007	0.000
15	0.04	-0.00	2.194	-0.004	-0.004	0.000
18	2.67	-0.01	2.082	-0.004	-0.004	0.000
21	2.09	-0.01	1.911	-0.005	-0.005	0.000
24	8.14	-0.03	2.583	-0.008	-0.008	0.000
27	5.73	-0.01	2.318	-0.005	-0.005	0.000
30	7.87	-0.02	2.638	-0.007	-0.007	0.000
33	-1.25	0.00	2.198	-0.007	-0.007	0.000
36	9.15	-0.03	2.545	-0.009	-0.009	0.000
noj						
0	-71.68	0.31	8.025	-0.012	-0.012	0.002
3	-48.20	0.43	8.304	-0.016	-0.016	0.001
6	-103.41	0.28	8.568	-0.012	-0.012	0.001
9	-142.74	0.72	8.868	-0.016	-0.016	0.001
12	-123.86	0.33	9.206	-0.017	-0.017	0.001
15	-62.67	0.51	8.376	-0.014	-0.014	0.002
18	-130.08	0.31	9.138	-0.014	-0.014	0.001
21	-125.83	0.65	9.730	-0.019	-0.019	0.001
24	-94.59	0.26	9.893	-0.020	-0.020	0.001
27	-81.68	0.32	9.206	-0.015	-0.015	0.001
30	-104.04	0.21	10.093	-0.017	-0.017	0.001
33	-117.88	0.19	11.368	-0.018	-0.018	0.001
36	-44.99	0.08	11.503	-0.017	-0.017	0.001

nyb						
0	-6.92	0.72	2.478	-0.007	-0.007	0.003
3	-19.37	0.53	2.737	-0.015	-0.015	0.002
6	-15.50	0.41	2.734	-0.013	-0.013	0.001
9	-21.97	0.63	2.932	-0.016	-0.016	0.002
12	-16.57	0.57	2.643	-0.013	-0.013	0.002
15	-19.57	0.50	2.634	-0.012	-0.012	0.002
18	-11.52	0.36	2.768	-0.012	-0.012	0.002
21	-24.56	0.54	3.111	-0.019	-0.019	0.002
24	-8.68	0.39	2.696	-0.014	-0.014	0.002
27	-19.20	0.29	2.841	-0.014	-0.014	0.001
30	-25.82	0.28	3.070	-0.015	-0.015	0.002
33	-22.11	0.31	3.253	-0.019	-0.019	0.002
36	-13.40	0.22	3.075	-0.012	-0.012	0.002
oem						
0	3.46	1.00	14.171	-0.028	-0.028	0.005
3	7.10	1.20	14.058	-0.024	-0.024	0.004
6	-0.52	1.20	14.234	-0.027	-0.027	0.004
9	2.23	0.95	14.471	-0.024	-0.024	0.003
12	1.48	0.96	14.464	-0.030	-0.030	0.004
15	8.61	1.12	14.240	-0.023	-0.023	0.004
18	-2.88	1.09	14.504	-0.028	-0.028	0.004
21	5.87	1.00	14.730	-0.029	-0.029	0.004
24	4.74	1.05	14.565	-0.031	-0.031	0.005
27	9.92	1.01	14.475	-0.023	-0.023	0.003
30	-1.57	0.94	14.670	-0.024	-0.024	0.004
33	7.70	0.89	14.737	-0.025	-0.025	0.004
36	10.17	0.89	14.843	-0.031	-0.031	0.005
ros						
0	-14.68	1.01	2.719	-0.016	-0.016	0.002
3	-26.21	0.90	2.686	-0.012	-0.012	0.001
6	-25.14	1.02	2.908	-0.012	-0.012	0.001
9	-35.65	0.92	3.246	-0.014	-0.014	0.001
12	-11.46	0.76	2.871	-0.013	-0.013	0.001
15	-31.06	1.03	2.729	-0.013	-0.013	0.001
18	-41.47	0.98	3.252	-0.014	-0.014	0.001
21	-51.63	1.11	3.563	-0.018	-0.018	0.001
24	-18.77	0.97	2.959	-0.018	-0.018	0.002
27	-28.35	0.96	2.801	-0.013	-0.013	0.002
30	-31.77	0.74	3.213	-0.014	-0.014	0.001
33	-44.46	1.01	3.429	-0.015	-0.015	0.001
36	-19.11	0.79	3.320	-0.017	-0.017	0.001

skv						
0	-4.57	0.43	0.651	-0.004	-0.004	0.003
3	-4.38	0.36	0.673	-0.006	-0.006	0.003
6	-6.97	0.38	0.771	-0.009	-0.009	0.002
9	-7.53	0.59	0.701	-0.008	-0.008	0.002
12	-9.85	0.40	0.731	-0.011	-0.011	0.002
15	-4.14	0.28	0.671	-0.006	-0.006	0.002
18	-6.86	0.29	0.761	-0.010	-0.010	0.002
21	-7.17	0.51	0.755	-0.012	-0.012	0.002
24	-3.72	0.22	0.702	-0.010	-0.010	0.002
27	-4.02	0.16	0.692	-0.008	-0.008	0.002
30	-5.11	0.16	0.808	-0.012	-0.012	0.002
33	-8.90	0.32	0.835	-0.014	-0.014	0.002
36	-5.76	0.14	0.841	-0.012	-0.012	0.002
sos						
0	1.59	0.93	10.492	-0.056	-0.056	0.009
3	-0.04	0.97	10.659	-0.060	-0.060	0.009
6	1.35	0.94	10.677	-0.055	-0.055	0.008
9	0.85	1.01	11.039	-0.071	-0.071	0.009
12	1.46	0.94	10.593	-0.062	-0.062	0.010
15	1.56	0.86	10.544	-0.054	-0.054	0.008
18	1.52	0.94	10.750	-0.059	-0.059	0.008
21	1.98	0.93	11.169	-0.073	-0.073	0.009
24	2.65	0.92	10.598	-0.059	-0.059	0.010
27	1.79	0.79	10.756	-0.056	-0.056	0.008
30	1.23	0.88	10.917	-0.058	-0.058	0.008
33	0.13	0.89	11.143	-0.066	-0.066	0.008
36	2.21	0.88	10.751	-0.064	-0.064	0.009
spr						
0	-5.39	0.88	0.657	-0.007	-0.007	0.002
3	-11.54	0.50	0.812	-0.014	-0.014	0.002
6	-15.74	0.44	0.841	-0.011	-0.011	0.002
9	-12.68	0.66	0.800	-0.012	-0.012	0.002
12	-12.72	0.79	0.758	-0.011	-0.011	0.002
15	-16.48	0.55	0.847	-0.013	-0.013	0.002
18	-16.76	0.41	0.820	-0.010	-0.010	0.002
21	-14.85	0.54	0.866	-0.013	-0.013	0.002
24	-14.12	0.76	0.800	-0.016	-0.016	0.002
27	-16.20	0.41	0.869	-0.012	-0.012	0.002
30	-21.73	0.43	0.968	-0.015	-0.015	0.002
33	-14.79	0.45	0.883	-0.013	-0.013	0.002
36	-11.80	0.54	0.804	-0.014	-0.014	0.002

tys						
0	-19.36	1.27	5.543	-0.013	-0.013	0.003
3	-13.55	0.93	5.687	-0.015	-0.015	0.002
6	-11.47	0.51	5.751	-0.013	-0.013	0.002
9	-9.39	0.66	5.947	-0.018	-0.018	0.002
12	-32.01	1.08	6.136	-0.019	-0.019	0.003
15	-13.69	0.67	5.873	-0.013	-0.013	0.002
18	-9.27	0.52	5.886	-0.015	-0.015	0.002
21	-11.26	0.77	5.891	-0.020	-0.020	0.003
24	-8.76	1.02	6.024	-0.023	-0.023	0.004
27	-2.31	0.57	5.928	-0.018	-0.018	0.002
30	-2.83	0.39	6.170	-0.019	-0.019	0.002
33	-6.58	0.60	6.319	-0.021	-0.021	0.003
36	-8.20	0.78	6.660	-0.023	-0.023	0.003
vin						
0	-0.07	1.04	17.474	-0.007	-0.007	0.006
3	-0.41	1.01	18.155	-0.007	-0.007	0.005
6	-0.20	1.11	18.775	-0.008	-0.008	0.005
9	-0.30	0.98	17.802	-0.007	-0.007	0.005
12	-0.23	1.07	17.403	-0.009	-0.009	0.006
15	-0.37	1.04	18.104	-0.007	-0.007	0.005
18	0.12	1.08	18.720	-0.008	-0.008	0.005
21	0.19	0.94	17.777	-0.007	-0.007	0.005
24	-0.11	1.02	17.411	-0.009	-0.009	0.007
27	-0.10	0.95	18.030	-0.007	-0.007	0.005
30	0.22	1.04	18.677	-0.008	-0.008	0.005
33	0.39	0.92	17.648	-0.007	-0.007	0.006
36	0.01	0.97	17.340	-0.010	-0.010	0.006

Table 9. Initial Kalman coefficients for the post-filtering of the entire population.

Θ_1	Θ_2	$\sum_1$	$\sum_2$	$\sum_3$	$\sum_4$	V	$E_{\max}$
0.0	1.0	10.0	0.0	0.0	0.1	500000	100000

Table 10. Resulting Kalman coefficients for the post-filtering of the entire population after one year of updating.

PL	Θ_1	Θ_2	$\sum_1$	$\sum_2$	$\sum_3$	$\sum_4$
0	-3.48	4.30	18.009	-0.002	-0.002	0.002
3	1.33	2.85	18.252	-0.003	-0.003	0.003
6	3.87	3.22	18.661	-0.002	-0.002	0.002
9	-0.26	4.34	17.875	-0.003	-0.003	0.003
12	-2.62	4.19	17.958	-0.002	-0.002	0.002
15	0.53	2.77	18.200	-0.003	-0.003	0.003
18	5.88	3.60	18.637	-0.003	-0.003	0.002
21	6.62	4.05	17.820	-0.003	-0.003	0.003
24	7.19	4.11	17.960	-0.002	-0.002	0.002
27	11.47	2.73	18.228	-0.003	-0.003	0.003
30	14.54	4.43	18.613	-0.003	-0.003	0.003
33	13.72	4.99	17.822	-0.004	-0.004	0.004
36	15.17	3.95	17.907	-0.003	-0.003	0.002

B The Risø Model

On the following pages each of the selected wind farms will be described.

Avedøre Holme

12 × Bonus 300 kW

55.6035° N 12.4612° E	UTM 32 E 718032 m N 6167525 m	0 m

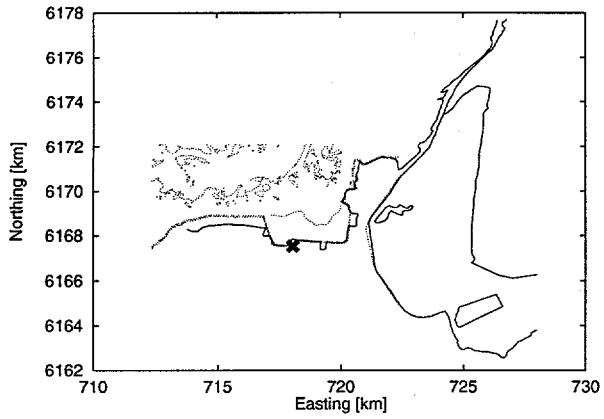

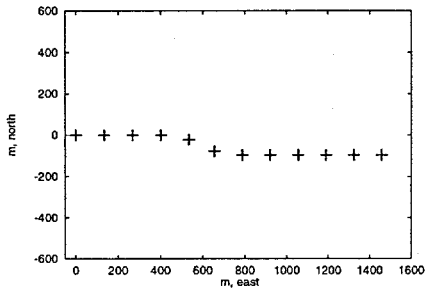

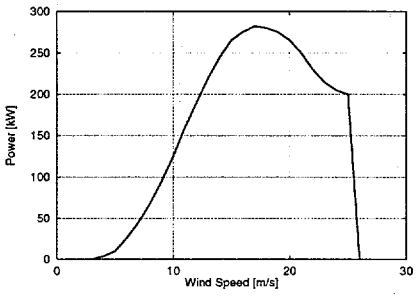

Sect	Obs	Rou	Oro		z_0
0	0.0	0.0	−0.3	0.0	0.5000
30	0.0	−2.4	−0.2	0.1	0.3615
60	0.0	−8.3	−0.0	0.1	0.1166
90	0.0	3.2	−0.0	−0.1	0.0873
120	0.0	1.4	−0.1	−0.0	0.0007
150	0.0	0.0	−0.2	0.0	0.0002
180	0.0	0.0	−0.2	0.0	0.0002
210	0.0	0.0	−0.1	0.0	0.0002
240	0.0	0.0	−0.0	0.0	0.0002
270	0.0	1.2	−0.1	−0.1	0.0006
300	0.0	5.3	−0.2	−0.1	0.2994
330	0.0	0.0	−0.3	0.0	0.5000

Sect	WASP	PARK	Phys.	MOS 1	MOS 2		Tot	
	a	a	a	a	a	b	a	b
0	0.997	1.000	0.997	1.69	1.000	186.5	1.685	186.5
30	0.974	1.000	0.974	1.56	1.000	186.5	1.519	186.5
60	0.916	0.950	0.870	1.48	1.000	186.5	1.288	186.5
90	1.031	0.800	0.825	1.20	1.000	186.5	0.990	186.5
120	1.012	0.939	0.950	1.14	1.000	186.5	1.083	186.5
150	0.998	0.989	0.987	1.15	1.000	186.5	1.135	186.5
180	0.998	1.000	0.998	1.05	1.000	186.5	1.048	186.5
210	0.999	1.000	0.999	1.00	1.000	186.5	0.999	186.5
240	1.000	0.932	0.932	1.04	1.000	186.5	0.969	186.5
270	1.012	0.726	0.735	1.09	1.000	186.5	0.801	186.5
300	1.050	0.923	0.969	1.34	1.000	186.5	1.299	186.5
330	0.997	0.992	0.989	1.47	1.000	186.5	1.454	186.5

Avedøre 1000

1 × 1000 kW

55.6027° N 12.4921° E	UTM 32 E 720047 m N 6167540 m	0 m

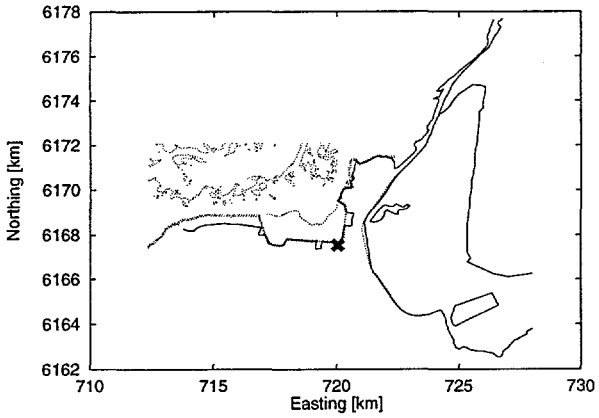

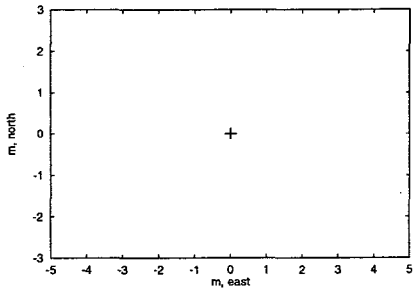

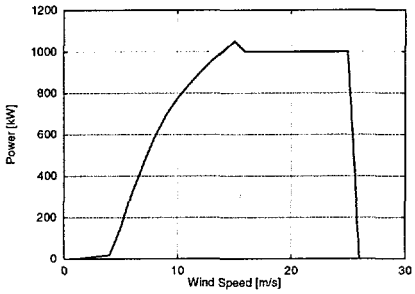

Sect	Obs	Rou	Oro		z_0
0	0.0	2.9	−0.2	0.0	0.3614
30	0.0	6.7	−0.1	0.1	0.0314
60	0.0	4.5	0.0	−0.0	0.0996
90	0.0	4.3	−0.1	−0.0	0.0883
120	0.0	−3.6	−0.1	−0.0	0.0041
150	0.0	0.0	−0.1	−0.0	0.0002
180	0.0	0.0	−0.1	0.0	0.0002
210	0.0	0.0	−0.0	0.0	0.0002
240	0.0	0.0	0.0	−0.0	0.0002
270	−1.0	−0.8	−0.1	−0.1	0.0040
300	−22.7	0.0	−0.2	−0.0	0.5000
330	0.0	0.0	−0.2	−0.0	0.5000

Sect	WASP	PARK	Phys.	MOS 1	MOS 2		Tot	
	a	a	a	a	a	b	a	b
0	1.027	1.000	1.027	0.65	1.000	20.9	0.668	20.9
30	1.067	1.000	1.067	0.87	1.000	20.9	0.928	20.9
60	1.045	1.000	1.045	0.87	1.000	20.9	0.909	20.9
90	1.042	1.000	1.042	0.82	1.000	20.9	0.854	20.9
120	0.963	1.000	0.963	0.79	1.000	20.9	0.761	20.9
150	0.999	1.000	0.999	0.79	1.000	20.9	0.789	20.9
180	0.999	1.000	0.999	0.73	1.000	20.9	0.729	20.9
210	1.000	1.000	1.000	0.70	1.000	20.9	0.700	20.9
240	1.000	1.000	1.000	0.70	1.000	20.9	0.700	20.9
270	0.980	1.000	0.980	0.65	1.000	20.9	0.637	20.9
300	0.772	1.000	0.772	1.09	1.000	20.9	0.841	20.9
330	0.998	1.000	0.998	0.81	1.000	20.9	0.808	20.9

Flakkebjerg

1 × Danwin 225 kW

55.3165° N 11.3873° E	UTM 32 E 651500 m N 6132740 m	35 m

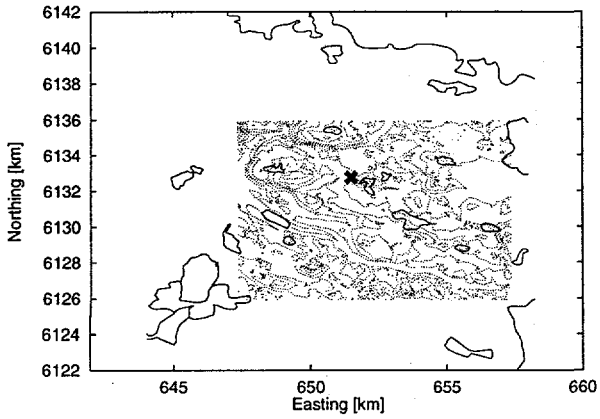

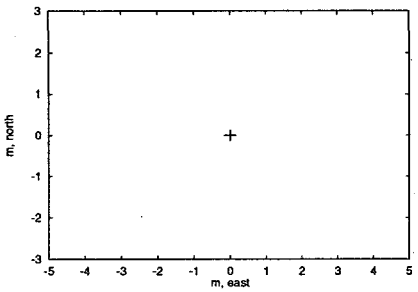

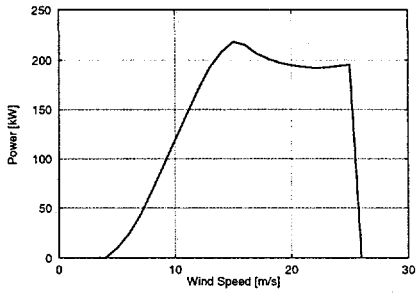

Sect	Obs	Rou	Oro		z_0
0	0.0	0.0	2.8	0.9	0.1000
30	0.0	0.0	3.6	−0.7	0.1000
60	0.0	0.0	2.0	−0.9	0.1000
90	0.0	0.0	0.8	−0.2	0.1000
120	0.0	0.0	0.9	−0.3	0.1000
150	0.0	0.0	1.2	0.6	0.1000
180	0.0	0.0	2.8	0.9	0.1000
210	0.0	0.0	3.6	−0.7	0.1000
240	0.0	0.0	2.0	−0.9	0.1000
270	0.0	0.0	0.8	−0.2	0.1000
300	0.0	0.0	0.9	−0.3	0.1000
330	0.0	0.0	1.2	0.6	0.1000

Sect	WASP	PARK	Phys.	MOS 1	MOS 2		Tot	
	a	a	a	a	a	b	a	b
0	1.028	1.000	1.028	0.31	1.000	6.1	0.319	6.1
30	1.036	1.000	1.036	0.70	1.000	6.1	0.725	6.1
60	1.020	1.000	1.020	0.96	1.000	6.1	0.979	6.1
90	1.008	1.000	1.008	0.96	1.000	6.1	0.968	6.1
120	1.009	1.000	1.009	0.39	1.000	6.1	0.394	6.1
150	1.012	1.000	1.012	0.97	1.000	6.1	0.982	6.1
180	1.028	1.000	1.028	1.00	1.000	6.1	1.028	6.1
210	1.036	1.000	1.036	1.04	1.000	6.1	1.077	6.1
240	1.020	1.000	1.020	0.98	1.000	6.1	1.000	6.1
270	1.008	1.000	1.008	1.10	1.000	6.1	1.109	6.1
300	1.009	1.000	1.009	1.03	1.000	6.1	1.039	6.1
330	1.012	1.000	1.012	0.82	1.000	6.1	0.830	6.1

Kappel

24 × Windane 400 kW

54.7659° N 11.0041° E	UTM 32 E 628940 m N 6070720 m	0 m

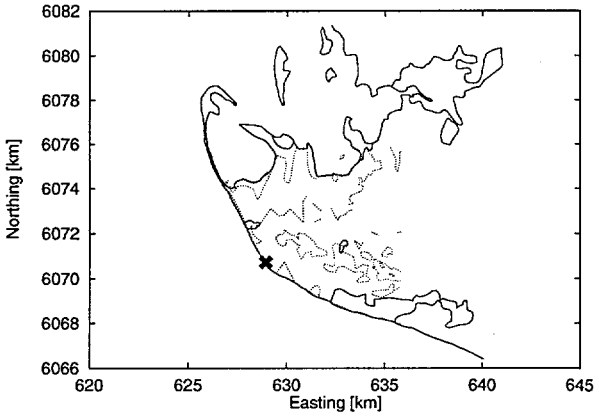

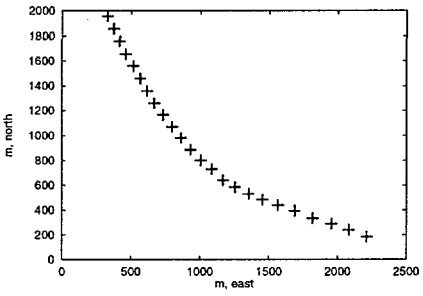

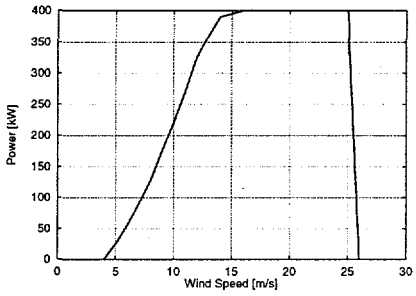

Sect	Obs	Rou	Oro		z_0
0	0.0	−18.4	−0.0	−0.3	0.0030
30	0.0	−9.0	−0.6	−0.3	0.0580
60	0.0	0.0	−0.8	0.1	0.2928
90	0.0	0.0	−0.4	0.3	0.3020
120	0.0	−8.7	0.2	0.2	0.0028
150	0.0	0.0	0.3	−0.1	0.0002
180	0.0	0.0	0.0	−0.2	0.0002
210	0.0	0.0	−0.4	−0.2	0.0002
240	0.0	0.0	−0.5	0.1	0.0002
270	0.0	0.0	−0.2	0.2	0.0002
300	0.0	0.0	0.2	0.2	0.0002
330	0.0	−8.1	0.3	−0.1	0.0010

Sect	WASP	PARK	Phys.	MOS 1	MOS 2		Tot	
	a	a	a	a	a	b	a	b
0	0.815	0.974	0.794	1.06	1.000	828.8	0.841	828.8
30	0.904	0.993	0.898	0.50	1.000	828.8	0.449	828.8
60	0.992	0.993	0.985	0.13	1.000	828.8	0.128	828.8
90	0.996	0.972	0.968	0.29	1.000	828.8	0.281	828.8
120	0.915	0.873	0.799	0.73	1.000	828.8	0.583	828.8
150	1.003	0.875	0.878	0.72	1.000	828.8	0.632	828.8
180	1.000	0.980	0.980	0.70	1.000	828.8	0.686	828.8
210	0.996	0.996	0.992	0.93	1.000	828.8	0.923	828.8
240	0.995	0.993	0.988	0.80	1.000	828.8	0.790	828.8
270	0.998	0.969	0.967	0.92	1.000	828.8	0.890	828.8
300	1.002	0.840	0.842	0.87	1.000	828.8	0.732	828.8
330	0.922	0.841	0.775	0.44	1.000	828.8	0.341	828.8

Kollerød

1 × Vestas 500 kW

55.8692° N 12.2888° E	UTM 32 E 705773 m N 6196547 m	43 m

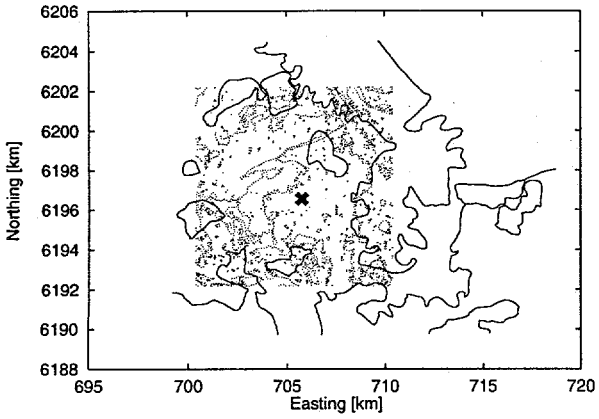

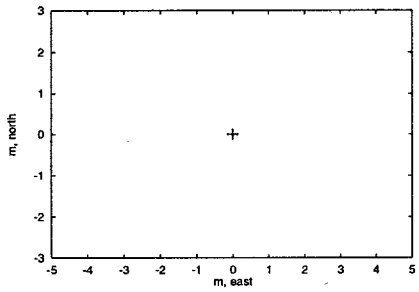

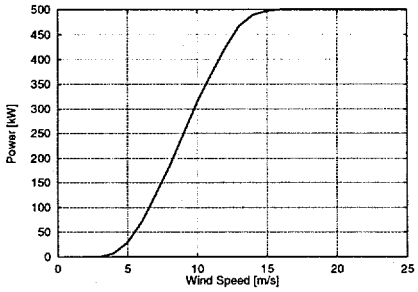

Sect	Obs	Rou	Oro		z_0
0	0.0	3.4	1.0	0.1	0.1997
30	0.0	1.9	1.0	0.0	0.1764
60	0.0	0.4	1.4	0.4	0.1346
90	0.0	2.1	2.2	0.4	0.1709
120	0.0	−2.2	2.0	−0.4	0.0787
150	0.0	4.6	1.3	−0.3	0.2178
180	0.0	0.0	1.0	0.1	0.1394
210	0.0	3.9	1.0	0.0	0.2269
240	0.0	0.0	1.4	0.4	0.1282
270	0.0	0.0	2.2	0.3	0.1081
300	0.0	0.0	2.0	−0.4	0.1014
330	0.0	0.0	1.3	−0.3	0.1056

Sect	WASP	PARK	Phys.	MOS 1	MOS 2		Tot	
	a	a	a	a	a	b	a	b
0	1.044	1.000	1.044	0.73	1.000	14.4	0.762	14.4
30	1.029	1.000	1.029	0.96	1.000	14.4	0.988	14.4
60	1.018	1.000	1.018	1.01	1.000	14.4	1.028	14.4
90	1.043	1.000	1.043	1.00	1.000	14.4	1.043	14.4
120	0.997	1.000	0.997	0.92	1.000	14.4	0.917	14.4
150	1.059	1.000	1.059	0.95	1.000	14.4	1.006	14.4
180	1.010	1.000	1.010	0.89	1.000	14.4	0.899	14.4
210	1.049	1.000	1.049	0.98	1.000	14.4	1.028	14.4
240	1.014	1.000	1.014	1.05	1.000	14.4	1.065	14.4
270	1.022	1.000	1.022	1.02	1.000	14.4	1.042	14.4
300	1.020	1.000	1.020	1.07	1.000	14.4	1.091	14.4
330	1.013	1.000	1.013	0.91	1.000	14.4	0.922	14.4

Kyndby

21 × Danwin 180 kW

55.8071° N 11.9055° E	UTM 32 E 682091 m N 6188571 m	18 m

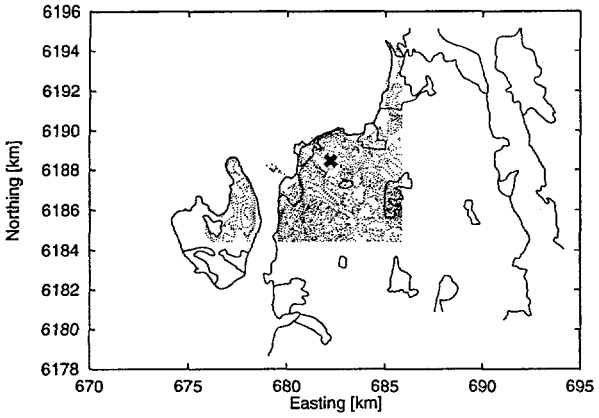

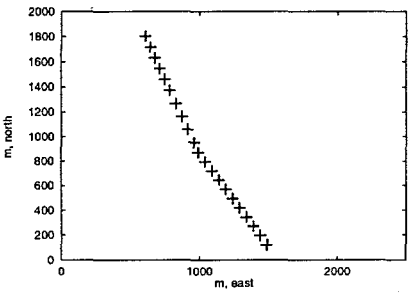

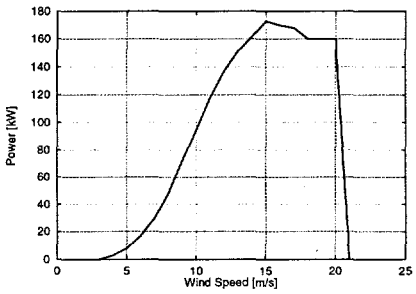

Sect	Obs	Rou	Oro		z_0
0	0.0	−8.0	−0.4	−0.5	0.0004
30	0.0	−3.9	−1.1	−0.2	0.0053
60	0.0	−3.8	−0.5	0.3	0.0473
90	0.0	−0.1	0.2	0.3	0.0952
120	0.0	−7.4	0.5	0.0	0.0289
150	0.0	0.0	0.2	−0.3	0.1070
180	0.0	0.0	−0.4	−0.3	0.1012
210	0.0	−12.7	−0.8	−0.1	0.0040
240	0.0	−10.3	−0.8	0.3	0.0036
270	0.0	−11.6	−0.5	0.4	0.0015
300	0.0	−9.3	0.2	0.3	0.0005
330	0.0	−9.0	0.4	−0.2	0.0004

Sect	WASP	PARK	Phys.	MOS 1	MOS 2		Tot	
	a	a	a	a	a	b	a	b
0	0.917	0.928	0.851	0.83	1.000	40.7	0.706	40.7
30	0.950	0.982	0.933	0.71	1.000	40.7	0.662	40.7
60	0.957	1.000	0.957	0.90	1.000	40.7	0.861	40.7
90	1.001	1.000	1.001	1.08	1.000	40.7	1.081	40.7
120	0.931	0.868	0.808	1.10	1.000	40.7	0.889	40.7
150	1.002	0.853	0.855	0.86	1.000	40.7	0.735	40.7
180	0.996	0.938	0.934	0.98	1.000	40.7	0.916	40.7
210	0.866	0.985	0.853	0.94	1.000	40.7	0.802	40.7
240	0.890	1.000	0.890	0.93	1.000	40.7	0.828	40.7
270	0.880	1.000	0.880	1.00	1.000	40.7	0.880	40.7
300	0.908	0.871	0.791	0.93	1.000	40.7	0.736	40.7
330	0.913	0.853	0.779	0.90	1.000	40.7	0.701	40.7

MAV82

1 × 750 kW

54.9972° N 11.8797° E	UTM 32 E 684205 m N 6098405 m	0 m

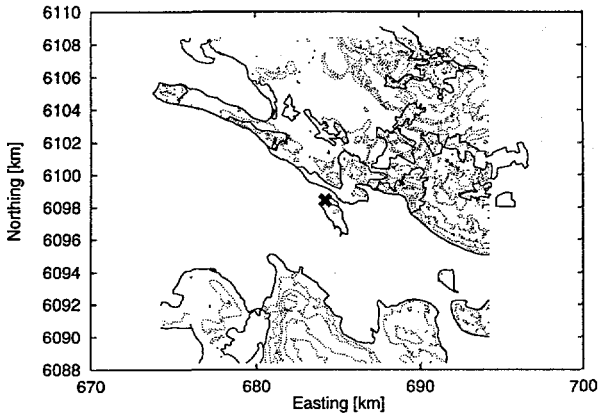

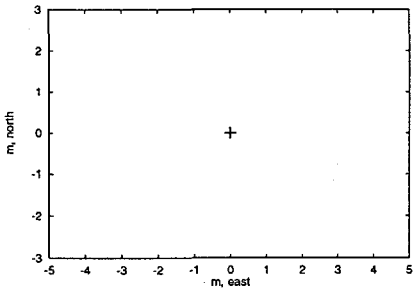

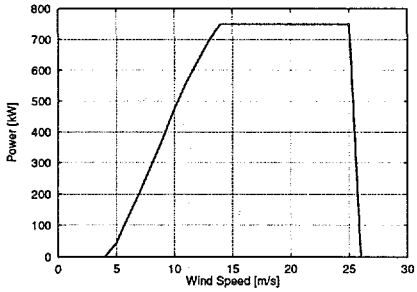

Sect	Obs	Rou	Oro		z_0
0	0.0	0.0	−1.4	0.2	0.0702
30	0.0	−1.6	−0.7	0.4	0.0954
60	0.0	−2.8	−0.1	0.2	0.1014
90	0.0	4.0	0.0	−0.3	0.0352
120	0.0	0.8	−0.8	−0.5	0.0007
150	0.0	0.1	−1.5	−0.2	0.0047
180	0.0	6.3	−1.3	0.3	0.0083
210	0.0	6.2	−0.6	0.4	0.0069
240	0.0	1.6	0.1	0.2	0.0006
270	0.0	0.0	0.1	−0.3	0.0002
300	0.0	0.8	−0.7	−0.4	0.0004
330	0.0	−1.5	−1.3	−0.2	0.0208

Sect	WASP	PARK	Phys.	MOS 1	MOS 2		Tot	
	a	a	a	a	a	b	a	b
0	0.986	1.000	0.986	0.43	1.000	40.5	0.424	40.5
30	0.977	1.000	0.977	0.24	1.000	40.5	0.234	40.5
60	0.972	1.000	0.972	0.33	1.000	40.5	0.321	40.5
90	1.040	1.000	1.040	0.24	1.000	40.5	0.250	40.5
120	1.000	1.000	1.000	0.34	1.000	40.5	0.340	40.5
150	0.986	1.000	0.986	0.46	1.000	40.5	0.454	40.5
180	1.049	1.000	1.049	0.34	1.000	40.5	0.357	40.5
210	1.056	1.000	1.056	0.29	1.000	40.5	0.306	40.5
240	1.017	1.000	1.017	0.36	1.000	40.5	0.366	40.5
270	1.001	1.000	1.001	0.75	1.000	40.5	0.751	40.5
300	1.001	1.000	1.001	0.65	1.000	40.5	0.651	40.5
330	0.972	1.000	0.972	0.38	1.000	40.5	0.369	40.5

Nybølle Hede

2 × Vestas 500 kW

54.9579° N 11.2317° E	UTM 32 E 642900 m N 6092520 m	0 m

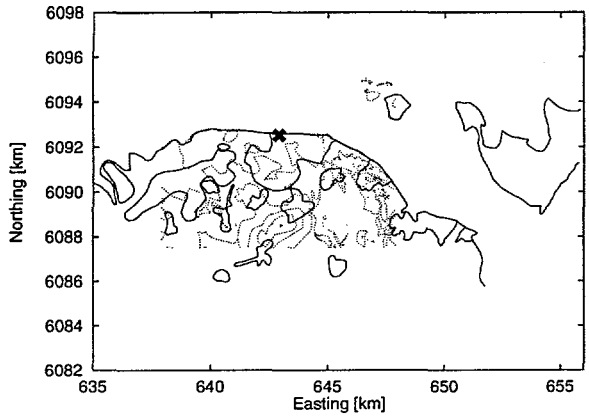

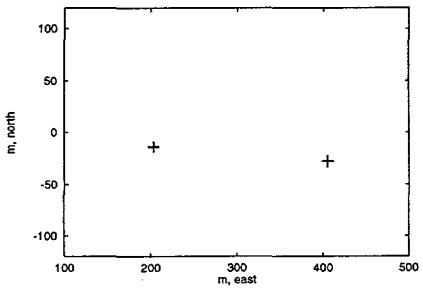

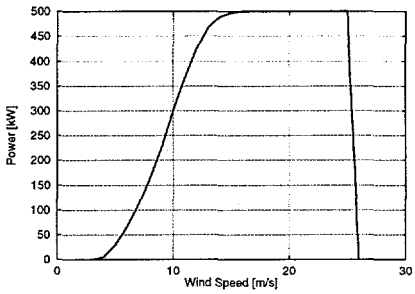

Sect	Obs	Rou	Oro		z_0
0	0.0	0.0	−0.5	0.0	0.0002
30	0.0	0.0	−0.3	0.1	0.0002
60	0.0	0.0	−0.1	0.1	0.0002
90	0.0	−0.2	−0.3	−0.1	0.0018
120	0.0	−8.4	−0.6	−0.1	0.0194
150	0.0	3.3	−0.7	0.0	0.2543
180	0.0	4.1	−0.7	−0.0	0.2406
210	0.0	3.5	−0.6	0.2	0.2495
240	0.0	1.5	−0.2	0.2	0.2238
270	0.0	−9.3	−0.2	−0.1	0.0017
300	0.0	0.0	−0.4	−0.1	0.0002
330	0.0	0.0	−0.5	0.0	0.0002

Sect	WASP	PARK	Phys.	MOS 1	MOS 2		Tot	
	a	a	a	a	a	b	a	b
0	0.995	1.000	0.995	0.92	1.000	24.3	0.915	24.3
30	0.997	1.000	0.997	0.89	1.000	24.3	0.887	24.3
60	0.999	0.991	0.990	0.84	1.000	24.3	0.832	24.3
90	0.995	0.962	0.957	0.91	1.000	24.3	0.871	24.3
120	0.910	0.991	0.902	1.06	1.000	24.3	0.956	24.3
150	1.025	1.000	1.025	1.17	1.000	24.3	1.199	24.3
180	1.033	1.000	1.033	1.10	1.000	24.3	1.136	24.3
210	1.029	1.000	1.029	1.17	1.000	24.3	1.204	24.3
240	1.012	0.992	1.004	1.08	1.000	24.3	1.084	24.3
270	0.905	0.966	0.874	1.01	1.000	24.3	0.883	24.3
300	0.996	0.992	0.988	1.01	1.000	24.3	0.998	24.3
330	0.995	1.000	0.995	1.00	1.000	24.3	0.995	24.3

Nøjsomhedsodde

23 × Danwin 225 kW

54.9428° N 11.0878° E	UTM 32 E 6337400 m N 6090550 m	0 m

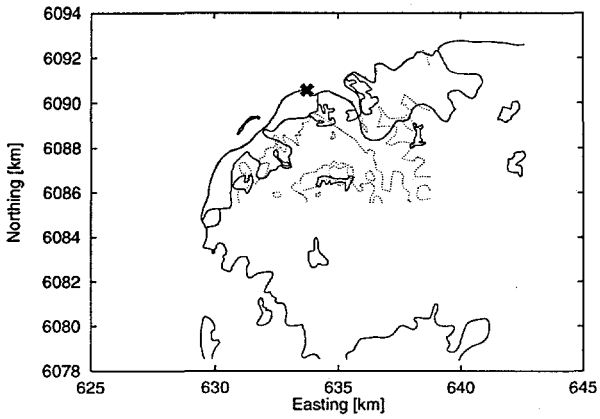

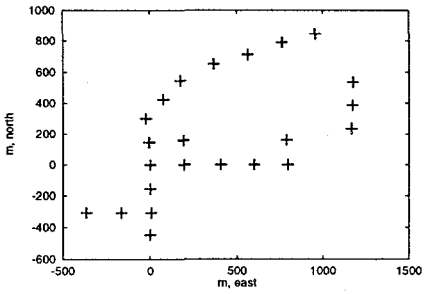

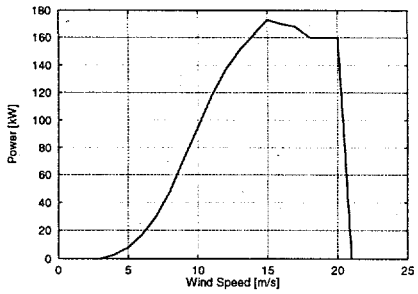

Sect	Obs	Rou	Oro		z_0
0	0.0	0.0	−0.6	−0.1	0.0002
30	0.0	0.0	−0.5	0.1	0.0002
60	0.0	−0.4	−0.1	0.2	0.0003
90	0.0	10.4	0.1	−0.2	0.0794
120	0.0	0.4	−0.4	−0.3	0.1997
150	0.0	2.2	−0.9	−0.1	0.2765
180	0.0	−6.5	−0.9	−0.1	0.0653
210	0.0	−12.6	−0.7	0.2	0.0065
240	0.0	−4.2	−0.2	0.3	0.0005
270	0.0	0.0	0.1	−0.2	0.0002
300	0.0	0.0	−0.3	−0.2	0.0002
330	0.0	0.0	−0.6	−0.1	0.0002

Sect	WASP	PARK	Phys.	MOS 1	MOS 2		Tot	
	a	a	a	a	a	b	a	b
0	0.994	0.940	0.934	0.91	1.000	107.6	0.850	107.6
30	0.995	0.946	0.941	1.02	1.000	107.6	0.960	107.6
60	0.995	0.954	0.949	1.35	1.000	107.6	1.281	107.6
90	1.105	0.971	1.073	0.81	1.000	107.6	0.869	107.6
120	1.000	0.985	0.985	0.74	1.000	107.6	0.729	107.6
150	1.013	0.983	0.996	1.18	1.000	107.6	1.175	107.6
180	0.927	0.966	0.895	0.90	1.000	107.6	0.806	107.6
210	0.868	0.964	0.837	1.03	1.000	107.6	0.862	107.6
240	0.956	0.965	0.923	0.87	1.000	107.6	0.803	107.6
270	1.001	0.967	0.968	0.88	1.000	107.6	0.852	107.6
300	0.997	0.978	0.975	0.86	1.000	107.6	0.839	107.6
330	0.994	0.971	0.965	1.01	1.000	107.6	0.975	107.6

Prejehøj

1 × Wind World 500 kW

54.7220° N 11.9494° E	UTM 32 E 689950 m N 6067980 m	19 m

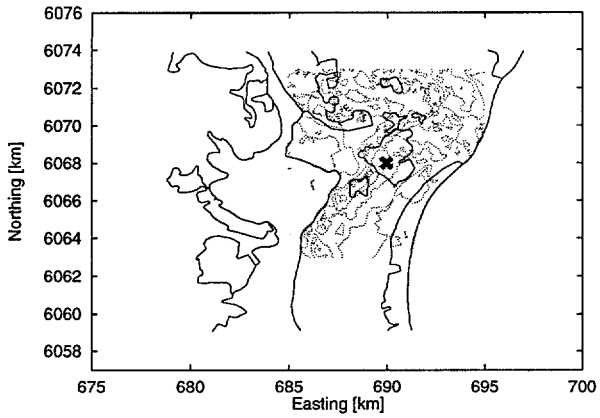

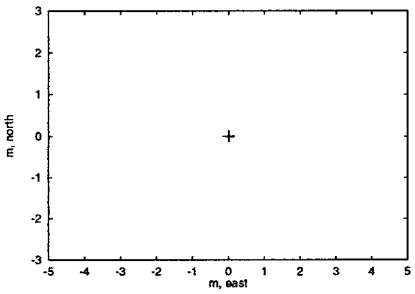

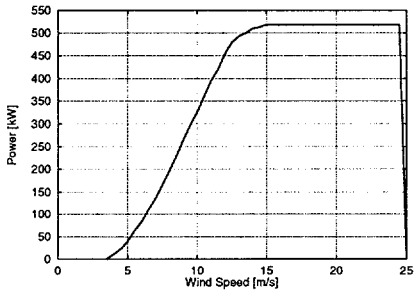

Sect	Obs	Rou	Oro		z_0
0	0.0	2.7	4.0	−0.3	0.2619
30	0.0	3.5	3.7	−0.1	0.2535
60	0.0	−11.5	3.7	−0.1	0.0101
90	0.0	−13.6	3.8	0.2	0.0020
120	0.0	−13.6	4.1	0.3	0.0011
150	0.0	−13.4	4.6	−0.2	0.0016
180	0.0	−3.5	4.2	−0.3	0.1452
210	0.0	−11.4	3.8	−0.1	0.0327
240	0.0	−5.1	3.8	−0.1	0.0465
270	0.0	−3.2	3.8	0.2	0.0550
300	0.0	−2.6	4.3	0.3	0.1103
330	0.0	1.6	4.6	−0.2	0.2989

Sect	WASP	PARK	Phys.	MOS 1	MOS 2		Tot	
	a	a	a	a	a	b	a	b
0	1.068	1.000	1.068	0.76	1.000	11.6	0.812	11.6
30	1.074	1.000	1.074	1.15	1.000	11.6	1.235	11.6
60	0.918	1.000	0.918	1.24	1.000	11.6	1.138	11.6
90	0.896	1.000	0.896	1.17	1.000	11.6	1.048	11.6
120	0.900	1.000	0.900	0.86	1.000	11.6	0.774	11.6
150	0.906	1.000	0.906	0.71	1.000	11.6	0.643	11.6
180	1.006	1.000	1.006	0.90	1.000	11.6	0.905	11.6
210	0.919	1.000	0.919	0.95	1.000	11.6	0.873	11.6
240	0.984	1.000	0.984	0.98	1.000	11.6	0.964	11.6
270	1.005	1.000	1.005	0.88	1.000	11.6	0.884	11.6
300	1.016	1.000	1.016	0.92	1.000	11.6	0.935	11.6
330	1.062	1.000	1.062	0.98	1.000	11.6	1.041	11.6

Rosendale

3 × Vestas 225 kW

55.2071° N 14.7715° E	UTM 33 E 485460 m N 6118000 m	95 m

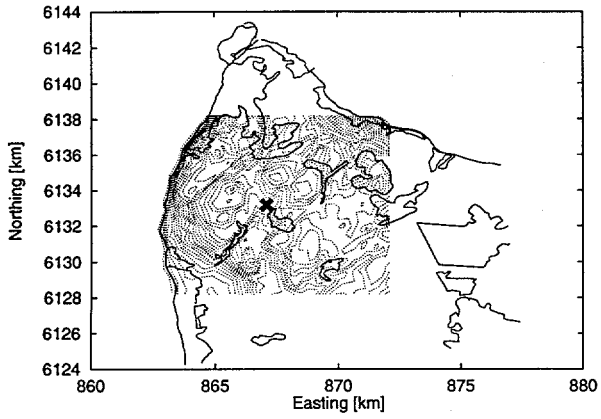

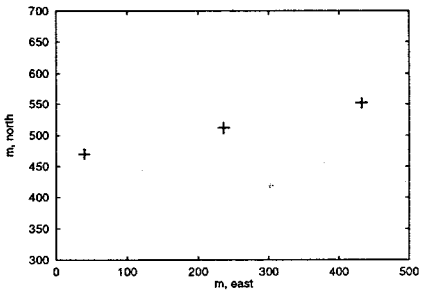

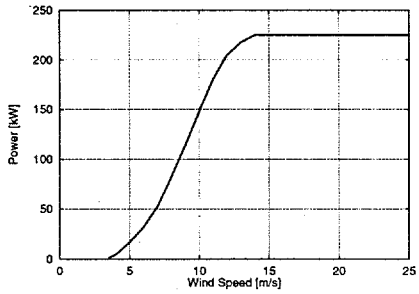

Sect	Obs	Rou	Oro		z_0
0	0.0	−12.8	1.3	0.6	0.0092
30	0.0	−13.0	1.5	−0.1	0.0040
60	0.0	−12.8	0.9	−0.7	0.0058
90	0.0	0.0	0.2	−0.7	0.1193
120	0.0	0.0	−0.5	−0.0	0.1319
150	0.0	0.0	0.2	0.6	0.1118
180	0.0	0.0	1.5	0.6	0.1023
210	0.0	−10.9	1.7	−0.1	0.0090
240	0.0	−13.0	0.6	−0.7	0.0022
270	0.0	−13.4	−0.6	−0.5	0.0016
300	0.0	−13.1	−1.0	0.1	0.0017
330	0.0	−13.0	−0.2	0.7	0.0028

Sect	WASP	PARK	Phys.	MOS 1	MOS 2		Tot	
	a	a	a	a	a	b	a	b
0	0.880	1.000	0.880	1.07	1.000	4.9	0.942	4.9
30	0.889	1.000	0.889	1.24	1.000	4.9	1.102	4.9
60	0.882	0.992	0.875	1.09	1.000	4.9	0.954	4.9
90	0.905	0.967	0.875	1.20	1.000	4.9	1.050	4.9
120	0.981	0.992	0.973	1.01	1.000	4.9	0.983	4.9
150	0.949	1.000	0.949	1.01	1.000	4.9	0.958	4.9
180	0.938	1.000	0.938	0.99	1.000	4.9	0.929	4.9
210	0.908	1.000	0.908	1.02	1.000	4.9	0.926	4.9
240	0.876	0.994	0.871	1.06	1.000	4.9	0.923	4.9
270	0.864	0.976	0.843	1.08	1.000	4.9	0.911	4.9
300	0.863	0.994	0.858	1.04	1.000	4.9	0.892	4.9
330	0.865	1.000	0.865	1.01	1.000	4.9	0.874	4.9

Skovlænge

2 × Wind World 150 kW

54.2513° N 11.2513° E	UTM 32 E 644650 m N 6077285 m	5 m

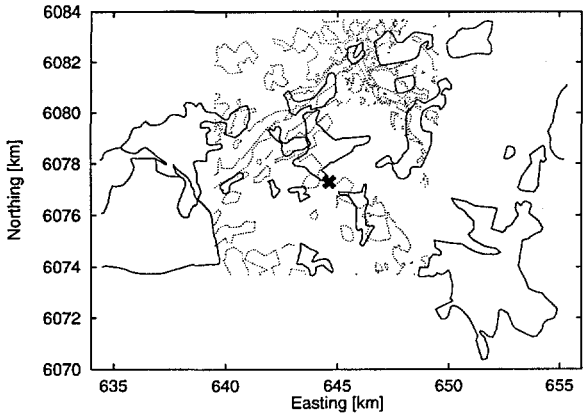

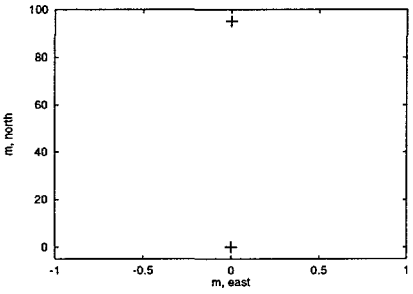

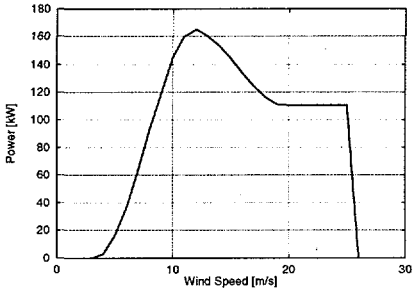

Sect	Obs	Rou	Oro		z_0
0	0.0	7.7	−0.1	−0.0	0.2064
30	0.0	4.3	−0.1	0.1	0.2379
60	0.0	0.0	0.1	0.1	0.3108
90	0.0	0.0	0.2	−0.1	0.3171
120	0.0	0.0	0.0	−0.1	0.3205
150	0.0	0.0	−0.1	−0.0	0.3020
180	0.0	0.0	−0.1	−0.0	0.3015
210	0.0	0.0	−0.1	0.1	0.3017
240	0.0	0.0	0.1	0.1	0.2590
270	0.0	−9.4	0.2	−0.1	0.0770
300	0.0	8.6	0.0	−0.1	0.2159
330	0.0	9.2	−0.1	−0.0	0.1757

Sect	WASP	PARK	Phys.	MOS 1	MOS 2		Tot	
	a	a	a	a	a	b	a	b
0	1.076	0.940	1.011	0.88	1.000	8.2	0.890	8.2
30	1.043	0.985	1.027	0.99	1.000	8.2	1.017	8.2
60	1.001	1.000	1.001	1.08	1.000	8.2	1.081	8.2
90	1.002	1.000	1.002	1.08	1.000	8.2	1.082	8.2
120	1.000	1.000	1.000	1.06	1.000	8.2	1.060	8.2
150	0.999	0.989	0.988	1.05	1.000	8.2	1.037	8.2
180	0.999	0.957	0.956	1.05	1.000	8.2	1.004	8.2
210	0.999	0.989	0.988	1.16	1.000	8.2	1.146	8.2
240	1.001	1.000	1.001	1.07	1.000	8.2	1.071	8.2
270	0.908	1.000	0.908	1.11	1.000	8.2	1.008	8.2
300	1.086	1.000	1.086	1.01	1.000	8.2	1.097	8.2
330	1.091	0.985	1.075	0.92	1.000	8.2	0.989	8.2

Sose

2 × Danwin 225 kW

55.0358° N 14.8979° E	UTM 33 E 493475 m N 6098910 m	26 m

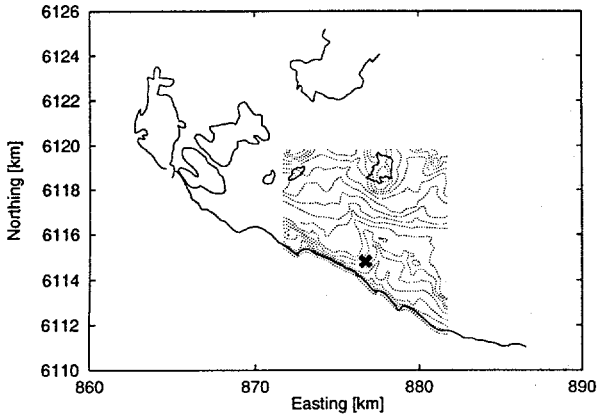

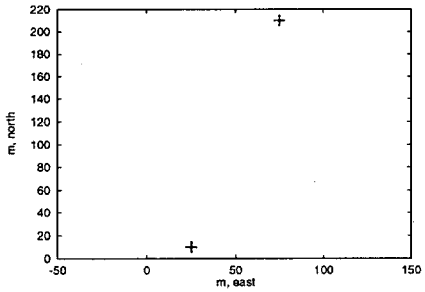

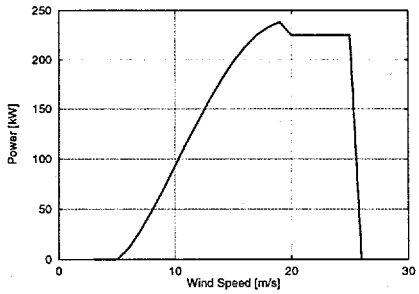

Sect	Obs	Rou	Oro		z_0
0	0.0	2.4	0.5	1.4	0.1503
30	0.0	0.0	2.7	0.8	0.1014
60	0.0	0.0	3.0	−0.5	0.1000
90	0.0	−4.7	1.1	−1.3	0.0458
120	0.0	−11.2	−1.0	−0.8	0.0041
150	0.0	−7.7	−1.2	0.5	0.0005
180	0.0	−1.5	0.3	1.1	0.0003
210	0.0	−1.6	2.0	0.7	0.0003
240	0.0	−1.0	2.4	−0.4	0.0003
270	0.0	−8.5	1.1	−1.2	0.0009
300	0.0	−3.8	−1.1	−0.8	0.0640
330	0.0	0.0	−1.4	0.5	0.1033

Sect	WASP	PARK	Phys.	MOS 1	MOS 2		Tot	
	a	a	a	a	a	b	a	b
0	0.953	0.949	0.904	1.21	1.000	-11.3	1.094	-11.3
30	0.952	0.987	0.940	1.35	1.000	-11.3	1.268	-11.3
60	0.971	1.000	0.971	1.27	1.000	-11.3	1.233	-11.3
90	0.926	1.000	0.926	1.28	1.000	-11.3	1.185	-11.3
120	0.881	1.000	0.881	1.11	1.000	-11.3	0.978	-11.3
150	0.906	0.989	0.896	1.08	1.000	-11.3	0.968	-11.3
180	0.971	0.955	0.927	1.01	1.000	-11.3	0.937	-11.3
210	0.992	0.989	0.981	1.09	1.000	-11.3	1.069	-11.3
240	0.999	1.000	0.999	1.01	1.000	-11.3	1.009	-11.3
270	0.933	1.000	0.933	0.99	1.000	-11.3	0.924	-11.3
300	0.911	1.000	0.911	1.14	1.000	-11.3	1.039	-11.3
330	0.947	0.987	0.935	1.10	1.000	-11.3	1.028	-11.3

Sprove

2 × Nordtank 150 kW

54.9641° N 12.1467° E	UTM 32 E 701443 m N 6095456 m	2 m

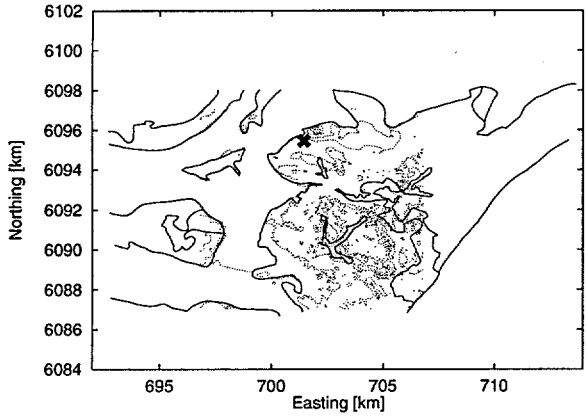

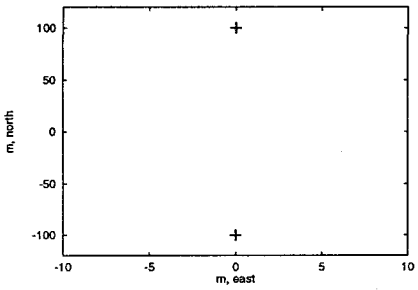

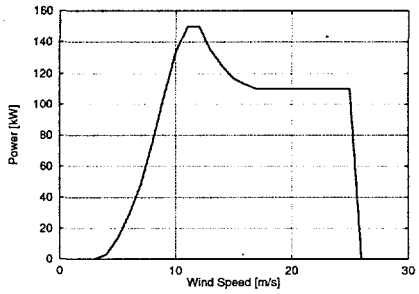

Sect	Obs	Rou	Oro		z_0
0	0.0	0.0	−1.2	0.2	0.0003
30	0.0	−3.4	−1.2	0.1	0.0004
60	0.0	−13.3	−0.7	0.6	0.0013
90	0.0	−10.7	0.4	0.6	0.0591
120	0.0	−17.2	−0.0	−0.7	0.0144
150	0.0	−10.3	−1.3	−0.6	0.0718
180	0.0	−6.4	−1.7	0.1	0.1048
210	0.0	−7.6	−1.7	0.1	0.0217
240	0.0	−8.4	−1.0	0.6	0.0038
270	0.0	3.2	0.3	0.5	0.0044
300	0.0	12.6	−0.1	−0.5	0.0572
330	0.0	6.5	−0.9	−0.4	0.0127

Sect	WASP	PARK	Phys.	MOS 1	MOS 2		Tot	
	a	a	a	a	a	b	a	b
0	0.988	0.976	0.964	0.82	1.000	5.4	0.791	5.4
30	0.955	0.994	0.949	1.04	1.000	5.4	0.987	5.4
60	0.861	1.000	0.861	1.06	1.000	5.4	0.913	5.4
90	0.897	1.000	0.897	1.31	1.000	5.4	1.175	5.4
120	0.828	1.000	0.828	1.08	1.000	5.4	0.894	5.4
150	0.886	0.996	0.882	0.93	1.000	5.4	0.821	5.4
180	0.920	0.985	0.906	0.91	1.000	5.4	0.825	5.4
210	0.908	0.996	0.904	1.01	1.000	5.4	0.913	5.4
240	0.907	1.000	0.907	1.10	1.000	5.4	0.998	5.4
270	1.035	1.000	1.035	0.96	1.000	5.4	0.994	5.4
300	1.125	1.000	1.125	0.90	1.000	5.4	1.013	5.4
330	1.055	0.994	1.049	0.85	1.000	5.4	0.891	5.4

Tystofte

3 × Bonus 450 kW

55.2484° N 11.3428° E	UTM 32 E 648930 m N 6125070 m	15 m

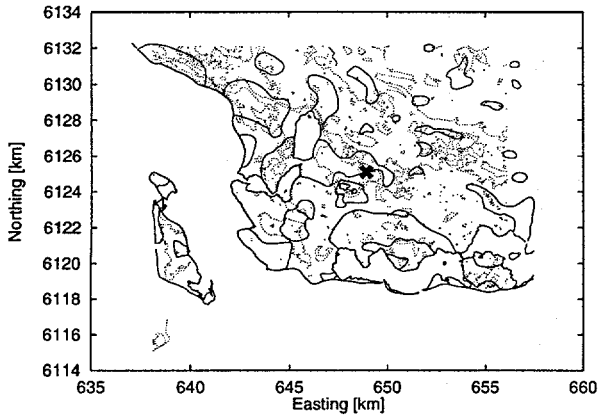

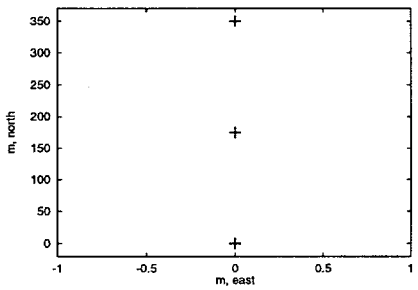

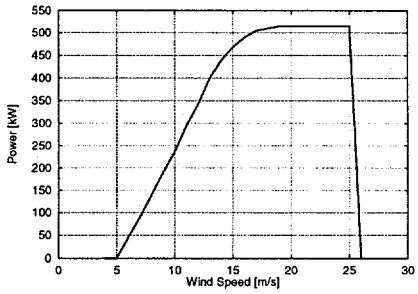

Sect	Obs	Rou	Oro		z_0
0	0.0	−3.6	0.1	0.2	0.1218
30	0.0	−2.0	0.8	0.4	0.1148
60	0.0	−1.2	1.1	−0.2	0.1149
90	0.0	0.0	0.5	−0.3	0.1109
120	0.0	−9.2	−0.0	−0.1	0.0163
150	0.0	−10.0	0.0	−0.1	0.0069
180	0.0	−11.2	0.1	0.2	0.0018
210	0.0	−10.4	0.6	0.4	0.0033
240	0.0	−11.7	1.1	−0.3	0.0051
270	0.0	−17.3	0.5	−0.4	0.0042
300	0.0	−10.0	0.0	−0.1	0.0441
330	0.0	−4.0	0.0	−0.1	0.1198

Sect	WASP	PARK	Phys.	MOS 1	MOS 2		Tot	
	a	a	a	a	a	b	a	b
0	0.965	0.928	0.896	0.50	1.000	38.5	0.448	38.5
30	0.988	0.982	0.970	0.75	1.000	38.5	0.728	38.5
60	0.999	1.000	0.999	1.02	1.000	38.5	1.019	38.5
90	1.005	1.000	1.005	1.07	1.000	38.5	1.075	38.5
120	0.908	1.000	0.908	1.09	1.000	38.5	0.990	38.5
150	0.900	0.983	0.885	1.06	1.000	38.5	0.938	38.5
180	0.888	0.930	0.826	1.06	1.000	38.5	0.875	38.5
210	0.901	0.983	0.886	1.00	1.000	38.5	0.886	38.5
240	0.892	1.000	0.892	0.96	1.000	38.5	0.856	38.5
270	0.831	1.000	0.831	1.00	1.000	38.5	0.831	38.5
300	0.900	1.000	0.900	1.08	1.000	38.5	0.972	38.5
330	0.961	0.982	0.944	0.94	1.000	38.5	0.887	38.5

Vindeby

11 × Bonus 450 kW

54.9655° N 11.1358° E	UTM 32 E 636740 m N 6093175 m	0 m

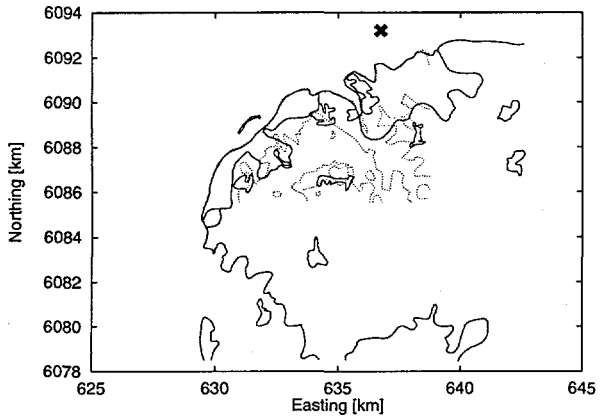

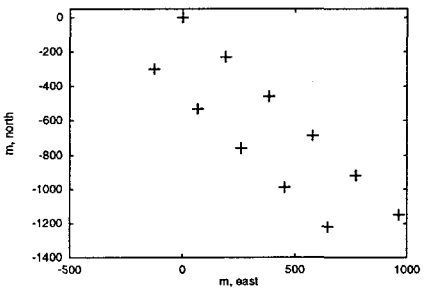

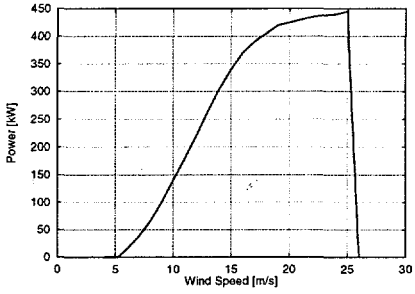

Sect	Obs	Rou	Oro		z_0
0	0.0	0.0	−0.1	0.0	0.0002
30	0.0	0.0	−0.1	0.0	0.0002
60	0.0	0.0	−0.0	0.0	0.0002
90	0.0	2.0	−0.1	−0.0	0.0012
120	0.0	10.1	−0.1	−0.0	0.0673
150	0.0	10.4	−0.1	0.0	0.0761
180	0.0	6.9	−0.1	0.0	0.0606
210	0.0	1.6	−0.1	0.0	0.0043
240	0.0	0.1	−0.0	0.0	0.0003
270	0.0	0.0	−0.0	−0.0	0.0002
300	0.0	0.0	−0.1	−0.0	0.0002
330	0.0	0.0	−0.1	0.0	0.0002

Sect	WASP	PARK	Phys.	MOS 1	MOS 2		Tot	
	a	a	a	a	a	b	a	b
0	0.999	0.971	0.970	0.88	1.000	115.1	0.854	115.1
30	0.999	0.982	0.981	1.01	1.000	115.1	0.991	115.1
60	1.000	0.983	0.983	1.04	1.000	115.1	1.022	115.1
90	1.019	0.977	0.996	0.84	1.000	115.1	0.836	115.1
120	1.099	0.955	1.050	0.76	1.000	115.1	0.798	115.1
150	1.102	0.957	1.055	1.04	1.000	115.1	1.097	115.1
180	1.068	0.985	1.052	0.95	1.000	115.1	0.999	115.1
210	1.015	0.988	1.003	1.01	1.000	115.1	1.013	115.1
240	1.001	0.985	0.986	0.98	1.000	115.1	0.966	115.1
270	1.000	0.974	0.974	1.01	1.000	115.1	0.984	115.1
300	0.999	0.941	0.940	1.02	1.000	115.1	0.959	115.1
330	0.999	0.940	0.939	1.01	1.000	115.1	0.948	115.1

Østermarie

7 × Danwin 225 kW

55.1415° N 15.0860° E	UTM 33 E 505480 m N 6110670 m	60 m

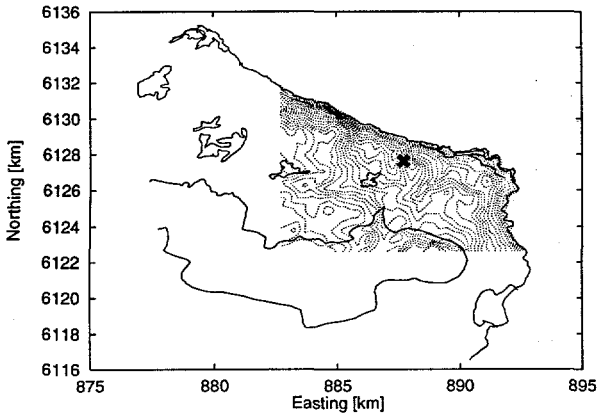

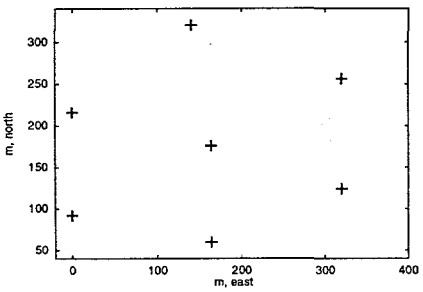

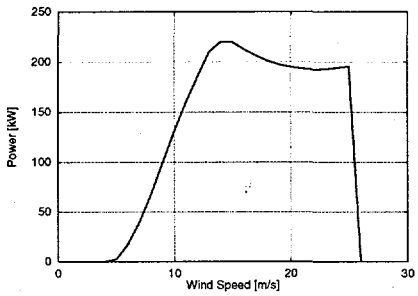

Sect	Obs	Rou	Oro		z_0
0	0.0	−6.0	6.9	1.1	0.0004
30	0.0	−6.9	7.8	−0.3	0.0004
60	0.0	−9.0	6.3	−1.4	0.0005
90	0.0	−12.8	3.8	−1.3	0.0015
120	0.0	−13.1	2.7	0.4	0.0024
150	0.0	−11.8	5.1	1.8	0.0083
180	0.0	1.0	8.3	1.2	0.1300
210	0.0	0.7	9.2	−0.5	0.1429
240	0.0	1.5	6.8	−1.7	0.1387
270	0.0	0.0	3.6	−1.3	0.1267
300	0.0	−4.8	2.7	0.5	0.0414
330	0.0	−10.1	4.6	1.5	0.0007

Sect	WASP	PARK	Phys.	MOS 1	MOS 2		Tot	
	a	a	a	a	a	b	a	b
0	0.990	0.858	0.849	1.09	1.000	43.0	0.926	43.0
30	1.004	0.887	0.891	0.96	1.000	43.0	0.855	43.0
60	0.964	0.895	0.863	1.05	1.000	43.0	0.906	43.0
90	0.905	0.893	0.808	1.04	1.000	43.0	0.840	43.0
120	0.899	0.943	0.848	0.92	1.000	43.0	0.780	43.0
150	0.916	0.944	0.865	0.79	1.000	43.0	0.683	43.0
180	0.987	0.895	0.883	0.93	1.000	43.0	0.822	43.0
210	1.017	0.922	0.938	0.88	1.000	43.0	0.825	43.0
240	1.007	0.929	0.936	0.89	1.000	43.0	0.833	43.0
270	0.993	0.922	0.916	0.94	1.000	43.0	0.861	43.0
300	0.987	0.950	0.938	0.89	1.000	43.0	0.835	43.0
330	0.926	0.934	0.865	0.89	1.000	43.0	0.770	43.0

B.1 The ASCII forecast file

On the following pages an example of the complete forecast file for one of the daily predictions is shown.

```
-------------------------------------------------------
                    EFP prognose
-------------------------------------------------------

  Prognose ID: HIRLAM/Risoe

  TOTAL PRODUCTION:

    Time    Prod   Error  Runtime
  --------------------------------
  95042600  11084       0 95042600
  95042603   8406       0 95042600
  95042606   8095       0 95042600
  95042609   6542       0 95042600
  95042612   7077       0 95042600
  95042615   5579       0 95042600
  95042618   6645       0 95042600
  95042621   5820       0 95042600
  95042700   4219       0 95042600
  95042703   2843       0 95042600
  95042706   2647       0 95042600
  95042709   2056       0 95042600
  95042712   1781       0 95042600


 Individual forecasts for 95042600:
  95042600                Avedoere_1000_kW   1    393       0 95042600   6.4   47.5
  95042600                           Kyndby  21    199       0 95042600   4.9   47.3
  95042600                         Kolleroed   1    140       0 95042600   7.0   48.6
  95042600                       Oestermarie   7   1054       0 95042600  11.0   33.7
  95042600                     Sose_Vindfarm   2    271       0 95042600  12.1   27.9
  95042600                         Rosendale   3    620       0 95042600  12.0   35.6
  95042600                             MAV82   1     40       0 95042600   2.1   48.9
  95042600                           Vindeby  11   3392       0 95042600  13.9   54.8
  95042600                   Kappel_Vindfarm  24    829       0 95042600   0.9   45.2
  95042600                         Flakkebjerg   1     28       0 95042600   5.8   41.3
  95042600          Noejsomhedsodde_Vindfarm  23   1258       0 95042600   6.4   54.9
  95042600                         Tystofte   3    195       0 95042600   6.2   41.8
  95042600                           Sprove   2    149       0 95042600   7.9   49.5
  95042600                       Skovlaenge   2    193       0 95042600   8.0   39.3
  95042600                         Prejehoej   1    197       0 95042600   7.8   53.8
  95042600                      Nyboelle_Hede   2    632       0 95042600  10.1   52.1
  95042600                     Avedoere_Holme  12   1495       0 95042600   9.5   45.8

 Individual forecasts for 95042603:
  95042603                Avedoere_1000_kW   1    264       0 95042600   5.5   45.2
  95042603                           Kyndby  21    223       0 95042600   5.1   42.8
  95042603                         Kolleroed   1     73       0 95042600   5.7   40.2
  95042603                       Oestermarie   7    852       0 95042600   9.9   32.3
  95042603                     Sose_Vindfarm   2    228       0 95042600  11.1   27.2
```

95042603	Rosendale	3	564	0	95042600	11.2	34.3
95042603	MAV82	1	40	0	95042600	1.3	39.8
95042603	Vindeby	11	2422	0	95042600	11.8	46.6
95042603	Kappel_Vindfarm	24	829	0	95042600	3.8	38.4
95042603	Flakkebjerg	1	22	0	95042600	5.4	36.6
95042603	Noejsomhedsodde_Vindfarm	23	863	0	95042600	5.5	46.0
95042603	Tystofte	3	139	0	95042600	5.7	37.6
95042603	Sprove	2	94	0	95042600	6.8	42.0
95042603	Skovlaenge	2	171	0	95042600	7.6	37.1
95042603	Prejehoej	1	99	0	95042600	6.1	32.7
95042603	Nyboelle_Hede	2	514	0	95042600	9.3	47.7
95042603	Avedoere_Holme	12	1010	0	95042600	8.0	39.4

Individual forecasts for 95042606:

95042606	Avedoere_1000_kW	1	239	0	95042600	5.4	45.9
95042606	Kyndby	21	155	0	95042600	4.5	59.2
95042606	Kolleroed	1	59	0	95042600	5.4	37.3
95042606	Oestermarie	7	989	0	95042600	10.7	31.5
95042606	Sose_Vindfarm	2	250	0	95042600	11.6	25.6
95042606	Rosendale	3	568	0	95042600	11.3	35.6
95042606	MAV82	1	40	0	95042600	1.6	46.5
95042606	Vindeby	11	2468	0	95042600	11.9	49.3
95042606	Kappel_Vindfarm	24	829	0	95042600	3.8	40.4
95042606	Flakkebjerg	1	15	0	95042600	4.9	41.5
95042606	Noejsomhedsodde_Vindfarm	23	898	0	95042600	5.6	50.5
95042606	Tystofte	3	56	0	95042600	5.1	40.2
95042606	Sprove	2	59	0	95042600	5.9	57.8
95042606	Skovlaenge	2	132	0	95042600	7.0	38.6
95042606	Prejehoej	1	71	0	95042600	5.4	32.8
95042606	Nyboelle_Hede	2	418	0	95042600	8.5	49.7
95042606	Avedoere_Holme	12	849	0	95042600	7.4	39.9

Individual forecasts for 95042609:

95042609	Avedoere_1000_kW	1	186	0	95042600	5.1	34.9
95042609	Kyndby	21	64	0	95042600	3.4	37.8
95042609	Kolleroed	1	47	0	95042600	5.1	31.6
95042609	Oestermarie	7	970	0	95042600	10.6	34.4
95042609	Sose_Vindfarm	2	241	0	95042600	11.4	27.1
95042609	Rosendale	3	544	0	95042600	11.0	33.7
95042609	MAV82	1	40	0	95042600	1.0	24.1
95042609	Vindeby	11	1865	0	95042600	10.5	52.8
95042609	Kappel_Vindfarm	24	829	0	95042600	0.7	45.4
95042609	Flakkebjerg	1	10	0	95042600	4.3	38.3
95042609	Noejsomhedsodde_Vindfarm	23	603	0	95042600	4.8	52.6
95042609	Tystofte	3	38	0	95042600	4.7	39.9
95042609	Sprove	2	54	0	95042600	5.7	44.0
95042609	Skovlaenge	2	92	0	95042600	6.2	39.1
95042609	Prejehoej	1	62	0	95042600	5.2	17.2
95042609	Nyboelle_Hede	2	325	0	95042600	7.7	51.2
95042609	Avedoere_Holme	12	572	0	95042600	6.3	28.6

Individual forecasts for 95042612:

95042612	Avedoere_1000_kW	1	37	0	95042600	3.7	51.0
95042612	Kyndby	21	46	0	95042600	3.1	57.5

95042612	Kolleroed	1	20	0	95042600	3.9	47.9
95042612	Oestermarie	7	894	0	95042600	10.2	27.2
95042612	Sose_Vindfarm	2	206	0	95042600	10.9	20.0
95042612	Rosendale	3	471	0	95042600	10.2	27.3
95042612	MAV82	1	40	0	95042600	1.0	50.6
95042612	Vindeby	11	1881	0	95042600	10.6	39.0
95042612	Kappel_Vindfarm	24	829	0	95042600	3.5	30.6
95042612	Flakkebjerg	1	11	0	95042600	4.5	29.3
95042612	Noejsomhedsodde_Vindfarm	23	1746	0	95042600	7.4	39.7
95042612	Tystofte	3	38	0	95042600	4.8	29.9
95042612	Sprove	2	23	0	95042600	4.6	60.6
95042612	Skovlaenge	2	84	0	95042600	6.1	27.2
95042612	Prejehoej	1	26	0	95042600	4.2	46.3
95042612	Nyboelle_Hede	2	387	0	95042600	8.3	38.8
95042612	Avedoere_Holme	12	337	0	95042600	5.2	47.1

Individual forecasts for 95042615:

95042615	Avedoere_1000_kW	1	85	0	95042600	4.4	29.7
95042615	Kyndby	21	41	0	95042600	2.7	36.3
95042615	Kolleroed	1	14	0	95042600	3.0	12.5
95042615	Oestermarie	7	939	0	95042600	10.4	29.9
95042615	Sose_Vindfarm	2	226	0	95042600	11.1	23.0
95042615	Rosendale	3	477	0	95042600	10.3	30.1
95042615	MAV82	1	40	0	95042600	1.0	21.1
95042615	Vindeby	11	1625	0	95042600	10.0	45.3
95042615	Kappel_Vindfarm	24	829	0	95042600	3.2	36.8
95042615	Flakkebjerg	1	7	0	95042600	4.0	36.5
95042615	Noejsomhedsodde_Vindfarm	23	533	0	95042600	4.6	45.9
95042615	Tystofte	3	38	0	95042600	4.3	38.3
95042615	Sprove	2	36	0	95042600	5.1	41.5
95042615	Skovlaenge	2	57	0	95042600	5.4	33.5
95042615	Prejehoej	1	12	0	95042600	3.2	8.5
95042615	Nyboelle_Hede	2	242	0	95042600	7.0	45.6
95042615	Avedoere_Holme	12	377	0	95042600	5.4	20.1

Individual forecasts for 95042618:

95042618	Avedoere_1000_kW	1	194	0	95042600	5.1	39.9
95042618	Kyndby	21	41	0	95042600	2.8	45.9
95042618	Kolleroed	1	27	0	95042600	4.2	15.6
95042618	Oestermarie	7	1067	0	95042600	11.1	25.0
95042618	Sose_Vindfarm	2	246	0	95042600	11.9	18.5
95042618	Rosendale	3	567	0	95042600	11.3	26.5
95042618	MAV82	1	40	0	95042600	1.6	10.1
95042618	Vindeby	11	2032	0	95042600	10.9	45.2
95042618	Kappel_Vindfarm	24	829	0	95042600	3.4	34.5
95042618	Flakkebjerg	1	10	0	95042600	4.4	39.9
95042618	Noejsomhedsodde_Vindfarm	23	636	0	95042600	4.9	45.8
95042618	Tystofte	3	38	0	95042600	4.8	40.5
95042618	Sprove	2	47	0	95042600	5.5	50.4
95042618	Skovlaenge	2	64	0	95042600	5.6	36.2
95042618	Prejehoej	1	12	0	95042600	3.2	6.7
95042618	Nyboelle_Hede	2	291	0	95042600	7.4	47.1
95042618	Avedoere_Holme	12	504	0	95042600	6.0	30.4

Individual forecasts for 95042621:

95042621	Avedoere_1000_kW	1	159	0	95042600	4.9	48.5
95042621	Kyndby	21	77	0	95042600	3.6	67.2
95042621	Kolleroed	1	42	0	95042600	4.9	61.3
95042621	Oestermarie	7	1072	0	95042600	11.5	21.5
95042621	Sose_Vindfarm	2	194	0	95042600	10.6	14.2
95042621	Rosendale	3	597	0	95042600	11.7	24.3
95042621	MAV82	1	40	0	95042600	1.0	69.3
95042621	Vindeby	11	1311	0	95042600	9.3	43.5
95042621	Kappel_Vindfarm	24	829	0	95042600	3.1	34.5
95042621	Flakkebjerg	1	6	0	95042600	4.0	38.8
95042621	Noejsomhedsodde_Vindfarm	23	466	0	95042600	4.3	45.5
95042621	Tystofte	3	38	0	95042600	4.3	38.4
95042621	Sprove	2	42	0	95042600	5.3	52.2
95042621	Skovlaenge	2	49	0	95042600	5.2	36.8
95042621	Prejehoej	1	31	0	95042600	4.4	46.1
95042621	Nyboelle_Hede	2	226	0	95042600	6.8	47.0
95042621	Avedoere_Holme	12	639	0	95042600	6.6	47.6

Individual forecasts for 95042700:

95042700	Avedoere_1000_kW	1	38	0	95042600	4.0	69.3
95042700	Kyndby	21	62	0	95042600	3.4	69.3
95042700	Kolleroed	1	25	0	95042600	4.2	80.9
95042700	Oestermarie	7	893	0	95042600	10.2	24.7
95042700	Sose_Vindfarm	2	210	0	95042600	11.0	18.4
95042700	Rosendale	3	493	0	95042600	10.4	27.8
95042700	MAV82	1	40	0	95042600	0.9	100.1
95042700	Vindeby	11	752	0	95042600	7.8	44.4
95042700	Kappel_Vindfarm	24	829	0	95042600	2.6	35.4
95042700	Flakkebjerg	1	6	0	95042600	3.4	38.7
95042700	Noejsomhedsodde_Vindfarm	23	276	0	95042600	3.6	47.7
95042700	Tystofte	3	38	0	95042600	3.6	38.0
95042700	Sprove	2	14	0	95042600	4.1	58.7
95042700	Skovlaenge	2	30	0	95042600	4.6	39.2
95042700	Prejehoej	1	12	0	95042600	3.3	122.9
95042700	Nyboelle_Hede	2	141	0	95042600	5.8	48.3
95042700	Avedoere_Holme	12	357	0	95042600	5.5	73.8

Individual forecasts for 95042703:

95042703	Avedoere_1000_kW	1	29	0	95042600	2.4	77.6
95042703	Kyndby	21	41	0	95042600	1.9	64.2
95042703	Kolleroed	1	14	0	95042600	2.8	100.2
95042703	Oestermarie	7	684	0	95042600	9.1	22.7
95042703	Sose_Vindfarm	2	96	0	95042600	8.4	14.0
95042703	Rosendale	3	348	0	95042600	9.0	20.9
95042703	MAV82	1	40	0	95042600	1.0	117.7
95042703	Vindeby	11	325	0	95042600	6.2	43.6
95042703	Kappel_Vindfarm	24	829	0	95042600	2.1	33.1
95042703	Flakkebjerg	1	6	0	95042600	2.6	36.1
95042703	Noejsomhedsodde_Vindfarm	23	108	0	95042600	2.9	47.0
95042703	Tystofte	3	38	0	95042600	2.8	35.8
95042703	Sprove	2	5	0	95042600	2.7	46.6
95042703	Skovlaenge	2	11	0	95042600	3.5	37.5
95042703	Prejehoej	1	12	0	95042600	2.5	130.8

95042703	Nyboelle_Hede	2	58	0	95042600	4.5	47.3
95042703	Avedoere_Holme	12	198	0	95042600	3.3	88.0

Individual forecasts for 95042706:

95042706	Avedoere_1000_kW	1	31	0	95042600	2.7	109.1
95042706	Kyndby	21	41	0	95042600	2.0	85.1
95042706	Kolleroed	1	14	0	95042600	2.9	120.4
95042706	Oestermarie	7	586	0	95042600	8.7	15.6
95042706	Sose_Vindfarm	2	81	0	95042600	8.0	7.3
95042706	Rosendale	3	166	0	95042600	7.0	14.2
95042706	MAV82	1	40	0	95042600	1.2	126.8
95042706	Vindeby	11	193	0	95042600	5.6	38.9
95042706	Kappel_Vindfarm	24	829	0	95042600	1.9	28.5
95042706	Flakkebjerg	1	6	0	95042600	2.2	32.9
95042706	Noejsomhedsodde_Vindfarm	23	298	0	95042600	3.7	43.1
95042706	Tystofte	3	38	0	95042600	2.4	31.9
95042706	Sprove	2	5	0	95042600	2.3	65.9
95042706	Skovlaenge	2	8	0	95042600	3.0	32.7
95042706	Prejehoej	1	12	0	95042600	3.0	133.6
95042706	Nyboelle_Hede	2	40	0	95042600	4.1	43.0
95042706	Avedoere_Holme	12	258	0	95042600	4.4	121.2

Individual forecasts for 95042709:

95042709	Avedoere_1000_kW	1	33	0	95042600	3.1	139.6
95042709	Kyndby	21	41	0	95042600	2.6	133.5
95042709	Kolleroed	1	16	0	95042600	3.2	147.1
95042709	Oestermarie	7	330	0	95042600	7.2	23.2
95042709	Sose_Vindfarm	2	25	0	95042600	6.5	14.5
95042709	Rosendale	3	146	0	95042600	6.7	26.0
95042709	MAV82	1	40	0	95042600	1.8	156.7
95042709	Vindeby	11	115	0	95042600	4.4	71.2
95042709	Kappel_Vindfarm	24	829	0	95042600	0.3	54.3
95042709	Flakkebjerg	1	6	0	95042600	2.4	78.5
95042709	Noejsomhedsodde_Vindfarm	23	108	0	95042600	2.9	66.3
95042709	Tystofte	3	38	0	95042600	2.6	74.4
95042709	Sprove	2	5	0	95042600	1.9	113.5
95042709	Skovlaenge	2	8	0	95042600	2.3	74.2
95042709	Prejehoej	1	12	0	95042600	2.7	156.6
95042709	Nyboelle_Hede	2	25	0	95042600	3.0	79.0
95042709	Avedoere_Holme	12	279	0	95042600	4.6	147.0

Individual forecasts for 95042712:

95042712	Avedoere_1000_kW	1	36	0	95042600	3.5	171.1
95042712	Kyndby	21	41	0	95042600	2.5	161.4
95042712	Kolleroed	1	20	0	95042600	3.8	170.8
95042712	Oestermarie	7	121	0	95042600	5.6	25.0
95042712	Sose_Vindfarm	2	-11	0	95042600	5.0	14.9
95042712	Rosendale	3	54	0	95042600	5.0	27.3
95042712	MAV82	1	40	0	95042600	1.7	175.8
95042712	Vindeby	11	115	0	95042600	3.4	92.9
95042712	Kappel_Vindfarm	24	829	0	95042600	0.6	77.2
95042712	Flakkebjerg	1	6	0	95042600	0.9	108.5
95042712	Noejsomhedsodde_Vindfarm	23	108	0	95042600	1.9	91.2
95042712	Tystofte	3	38	0	95042600	2.6	108.9

95042712	Sprove	2	5	0	95042600	2.1	151.8
95042712	Skovlaenge	2	8	0	95042600	1.9	106.3
95042712	Prejehoej	1	13	0	95042600	3.6	167.1
95042712	Nyboelle_Hede	2	24	0	95042600	3.0	103.5
95042712	Avedoere_Holme	12	333	0	95042600	5.1	175.3

B.2 Full results

In this section the resluts of the analyysis of all the wind farms are displayed.

Skill scores

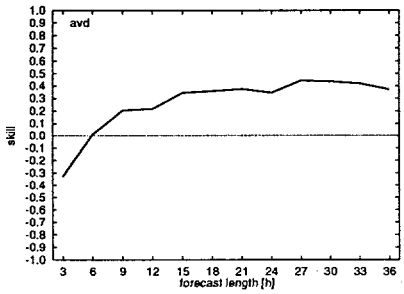

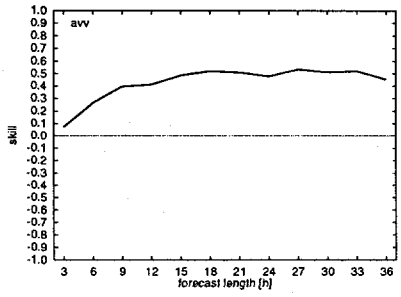

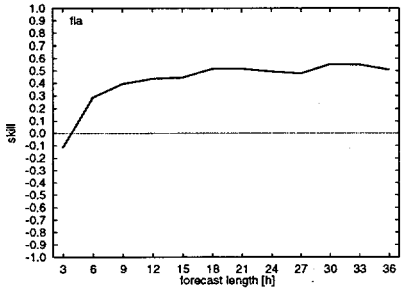

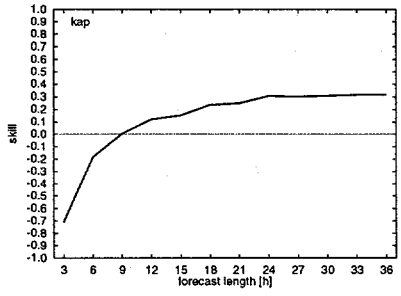

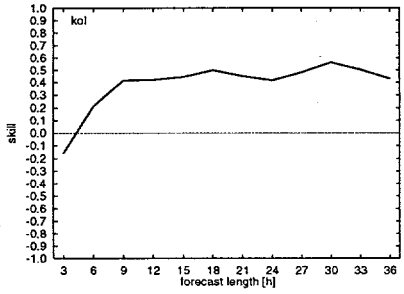

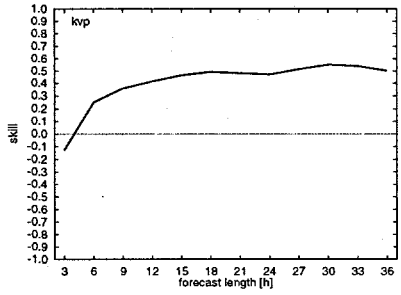

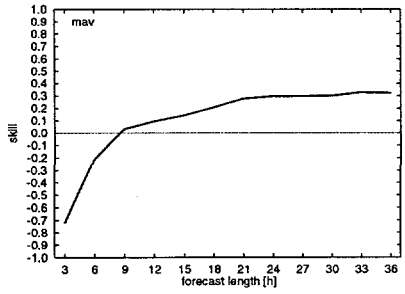

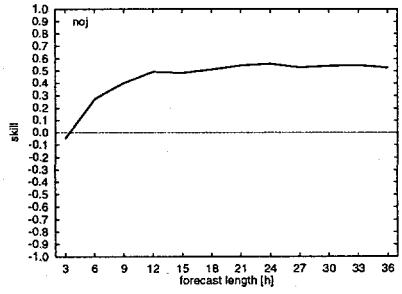

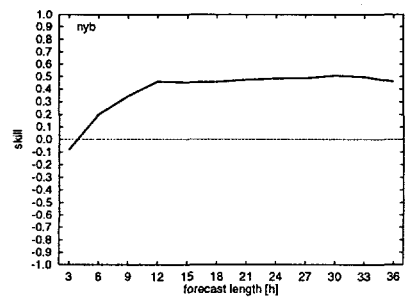
nyb
skill
forecast length [h]

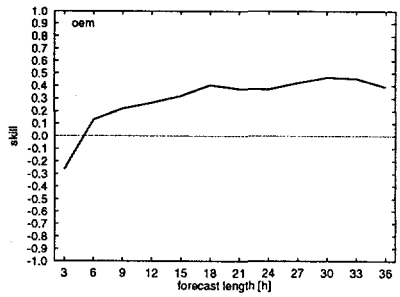
oem
skill
forecast length [h]

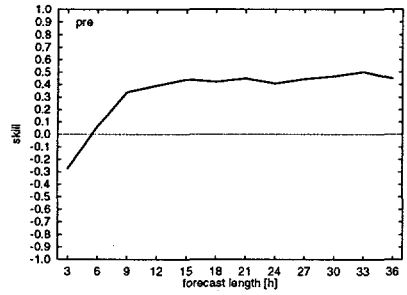
pre
skill
forecast length [h]

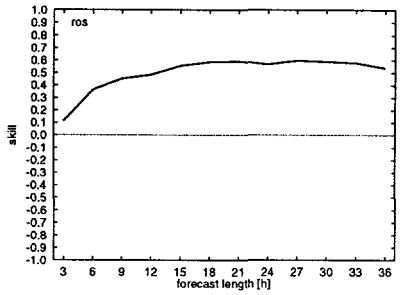
ros
skill
forecast length [h]

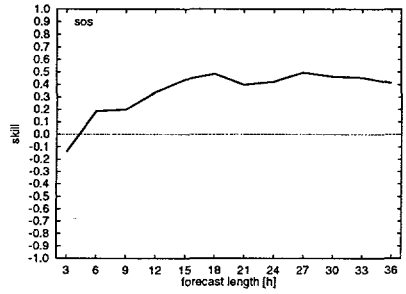
sos
skill
forecast length [h]

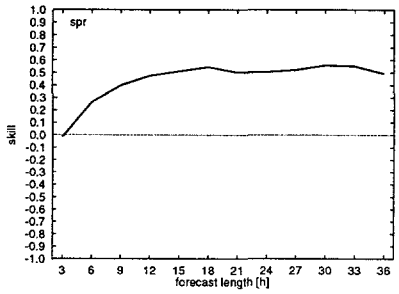
spr
skill
forecast length [h]

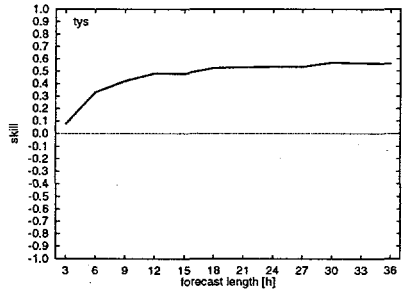
tys
skill
forecast length [h]

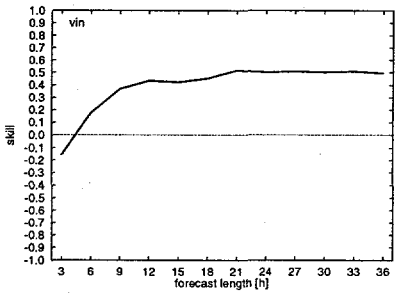
vin
skill
forecast length [h]

Result plots

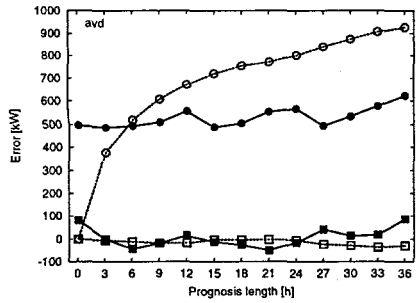

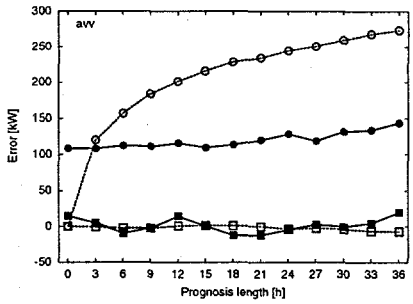

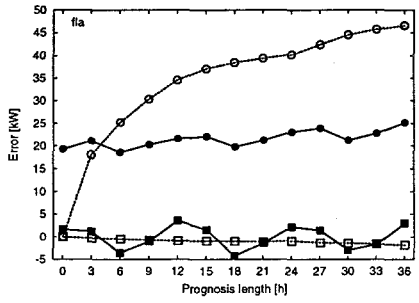

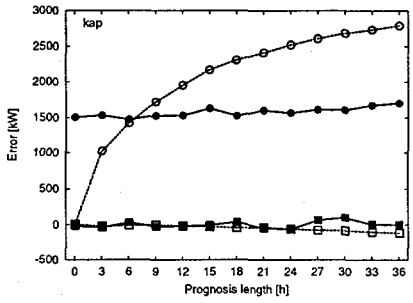

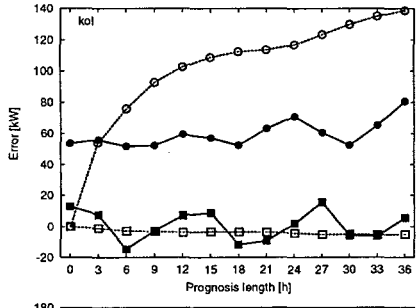

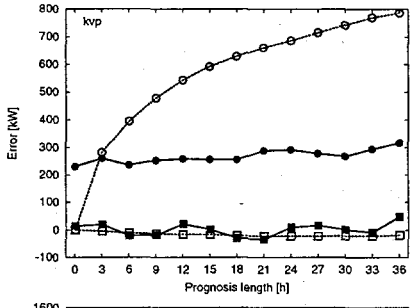

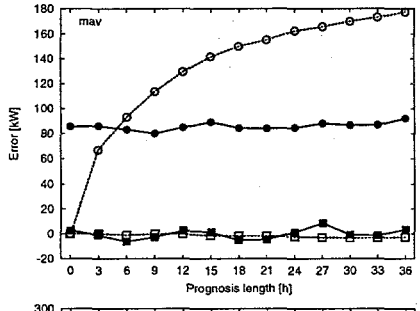

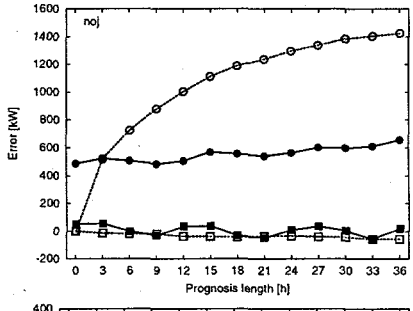

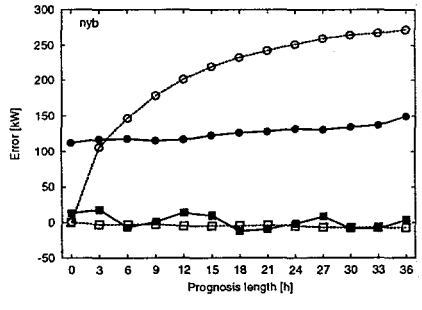

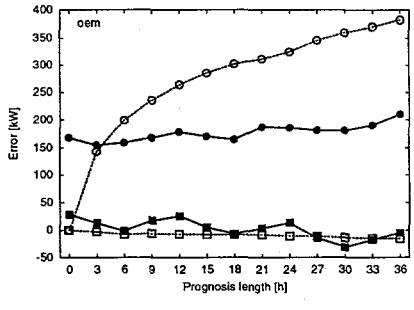

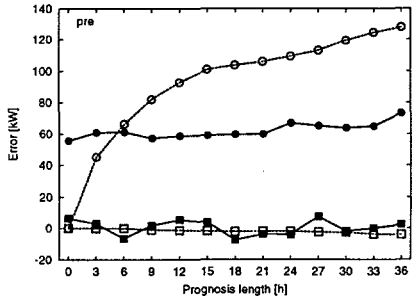
pre
Error [kW]
Prognosis length [h]

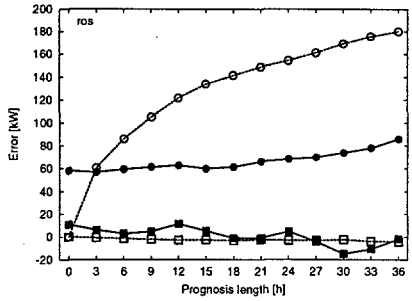
ros
Error [kW]
Prognosis length [h]

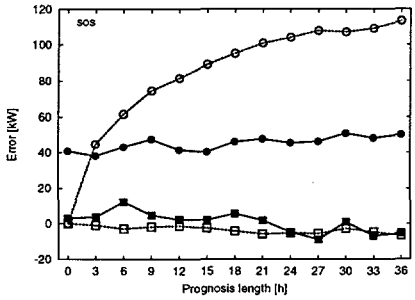
sos
Error [kW]
Prognosis length [h]

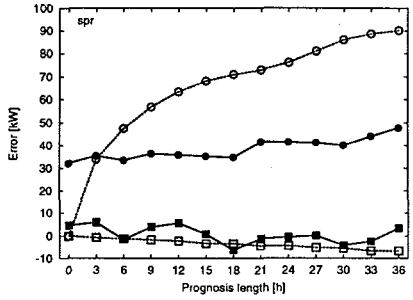
spr
Error [kW]
Prognosis length [h]

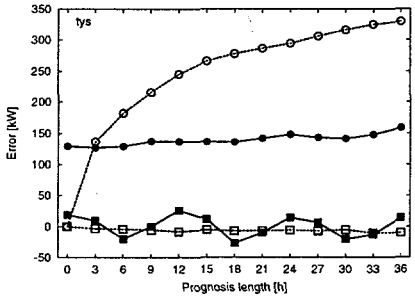
tys
Error [kW]
Prognosis length [h]

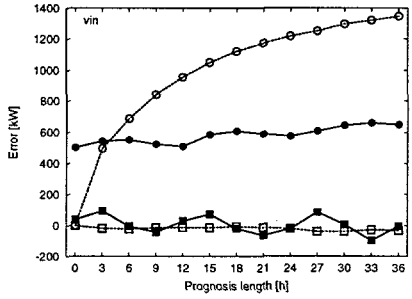
vin
Error [kW]
Prognosis length [h]

Relative plots

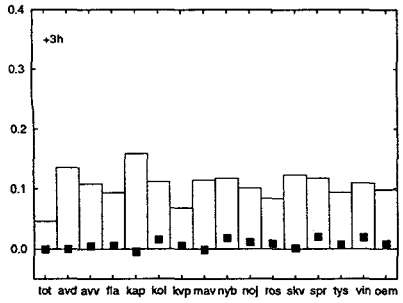

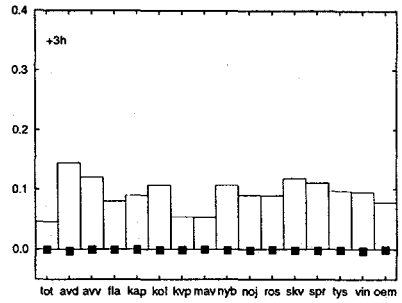

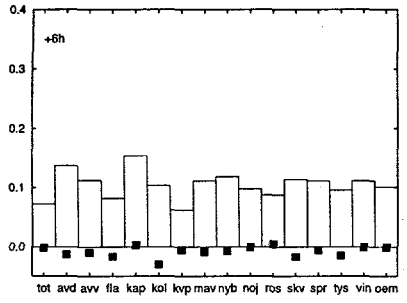

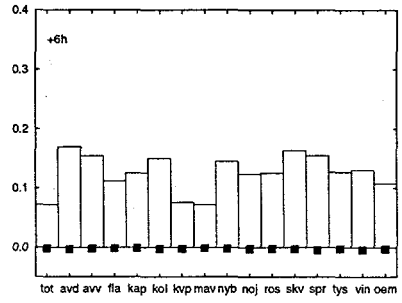

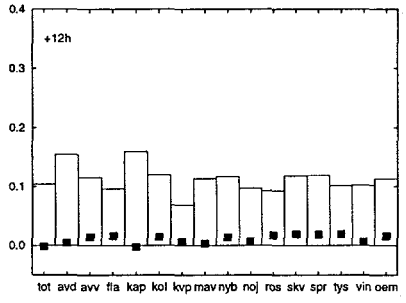

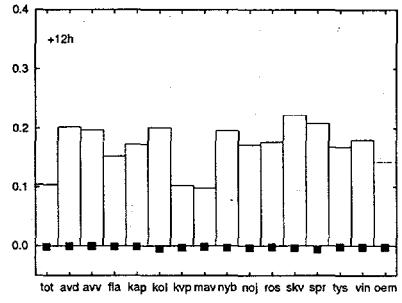

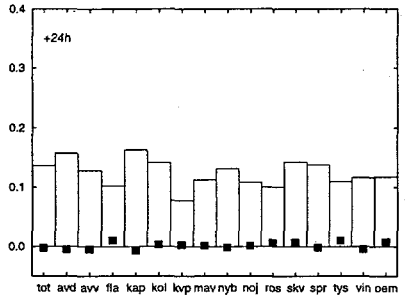

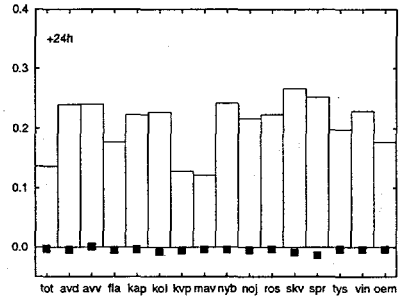

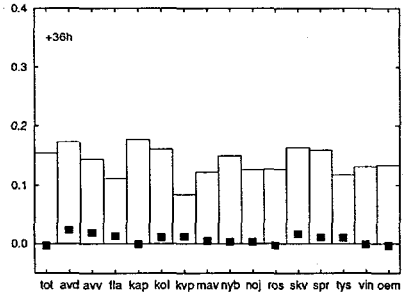

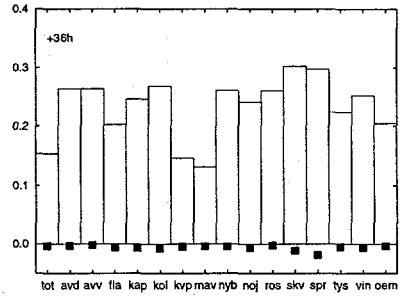

Scatter plots

In this section the scatter plots of the +12h forecast for all the wind farms are plotted (left hand side) and compared to the scatter plots of the persistence model (right hand side).

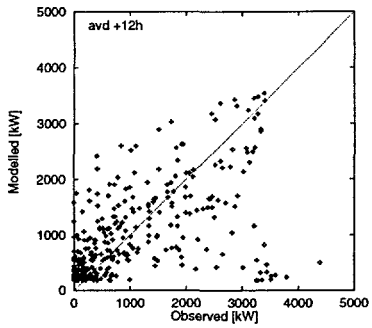

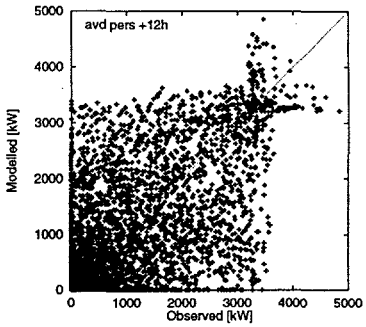

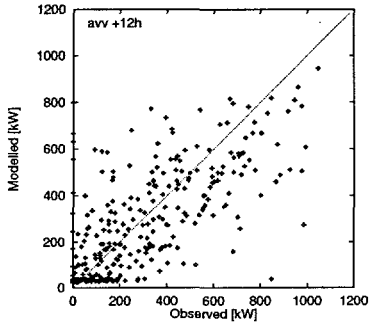

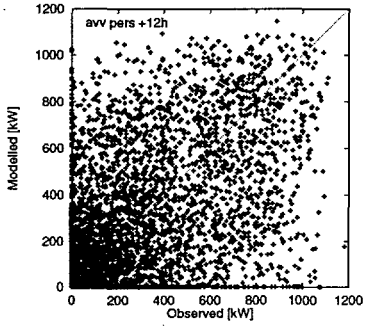

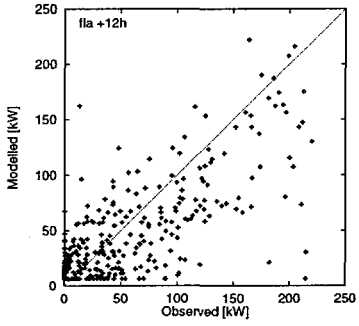

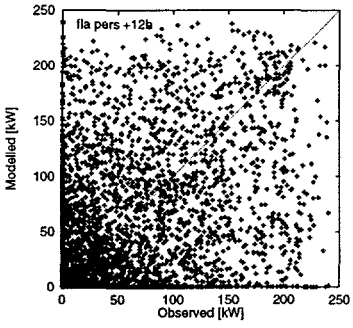

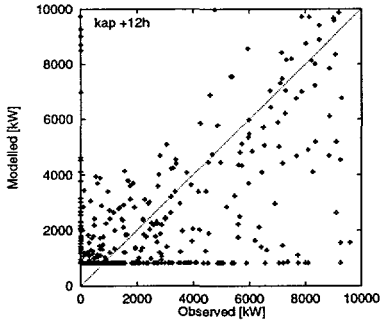

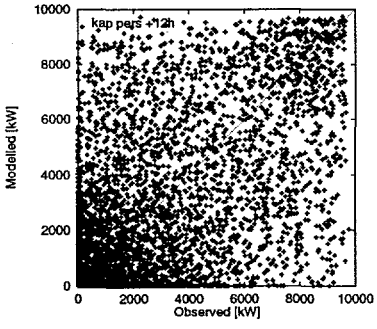

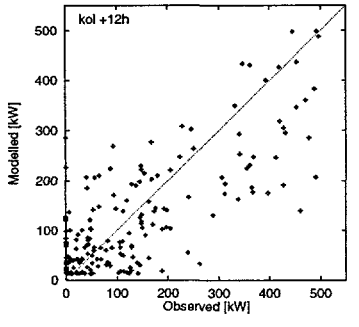

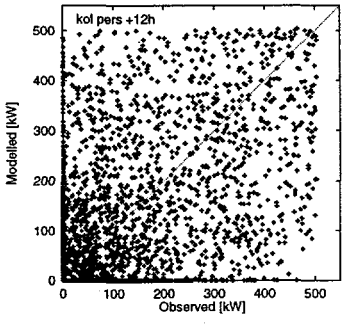

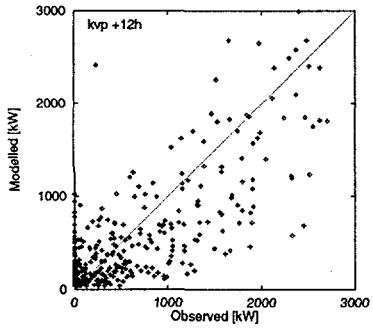
kvp +12h
Modelled [kW]
Observed [kW]
0
1000
2000
3000

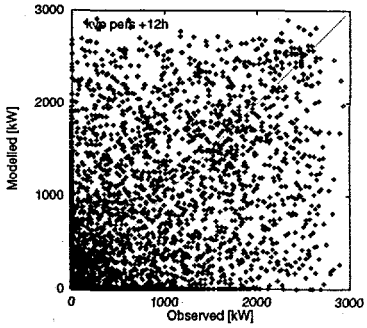
kvp pers +12h
Modelled [kW]
Observed [kW]
0
1000
2000
3000

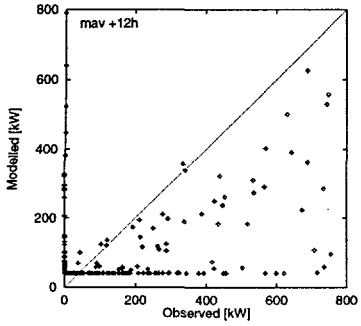
mav +12h
Modelled [kW]
Observed [kW]
0
200
400
600
800

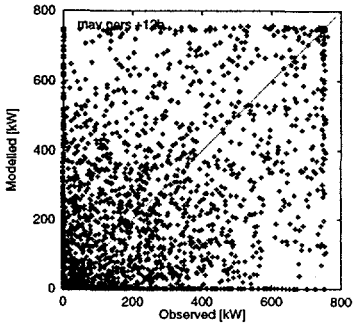
mav pers +12h
Modelled [kW]
Observed [kW]
0
200
400
600
800

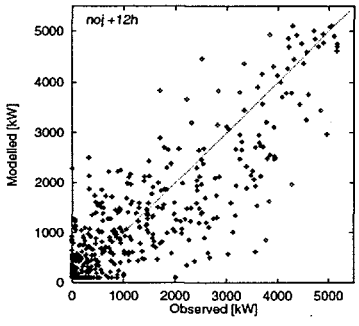
noj +12h
Modelled [kW]
Observed [kW]
0
1000
2000
3000
4000
5000

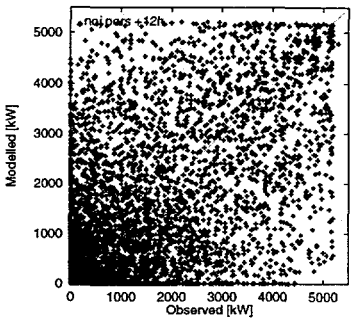
noj pers +12h
Modelled [kW]
Observed [kW]
0
1000
2000
3000
4000
5000

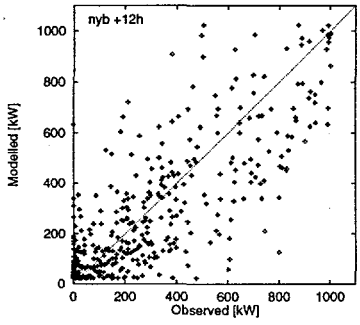
nyb +12h
Modelled [kW]
Observed [kW]
0
200
400
600
800
1000

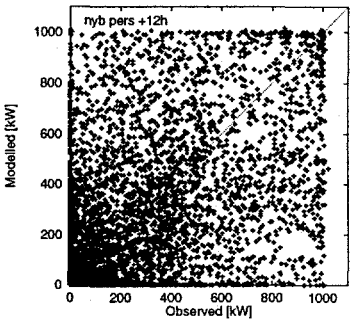
nyb pers +12h
Modelled [kW]
Observed [kW]
0
200
400
600
800
1000

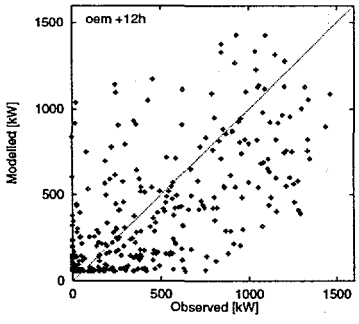
oem +12h
Modelled [kW]
Observed [kW]
0
500
1000
1500

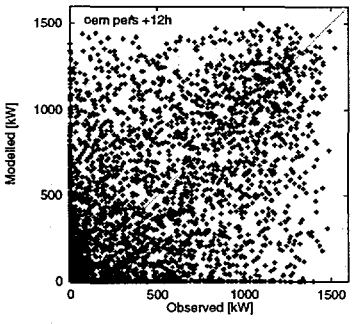
oem pers +12h
Modelled [kW]
Observed [kW]
0
500
1000
1500

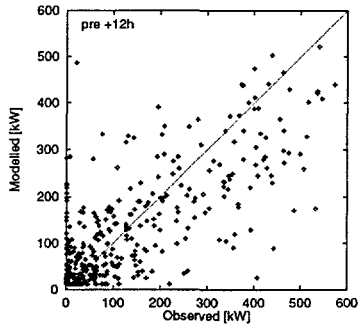
pre +12h
Modelled [kW]
Observed [kW]
0
100
200
300
400
500
600

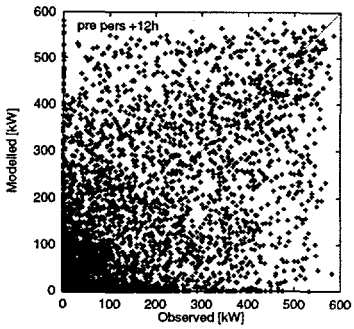
pre pers +12h
Modelled [kW]
Observed [kW]
0
100
200
300
400
500
600

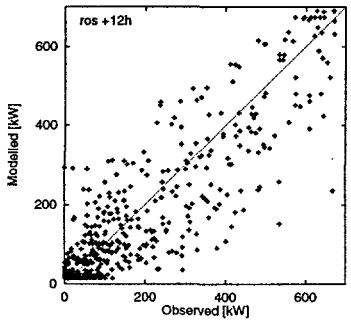
ros +12h
Modelled [kW]
Observed [kW]
0
200
400
600

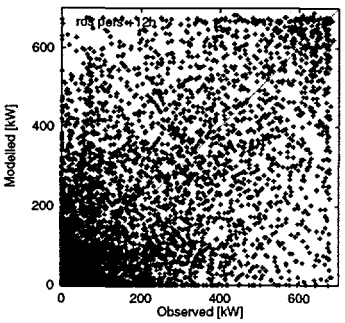
ros pers +12h
Modelled [kW]
Observed [kW]
0
200
400
600

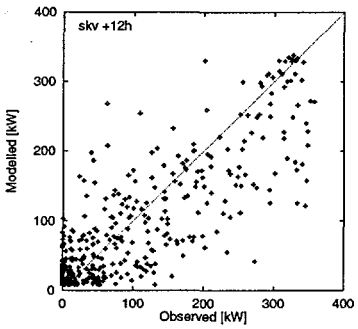
skv +12h
Modelled [kW]
Observed [kW]
0
100
200
300
400

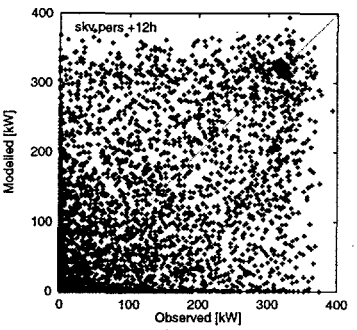
skv pers +12h
Modelled [kW]
Observed [kW]
0
100
200
300
400

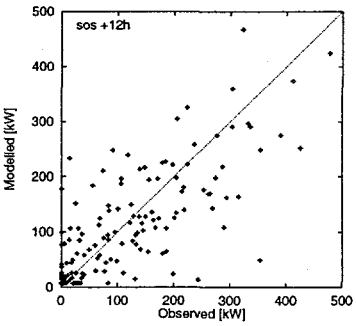
sos +12h
Modelled [kW]
Observed [kW]
0
100
200
300
400
500

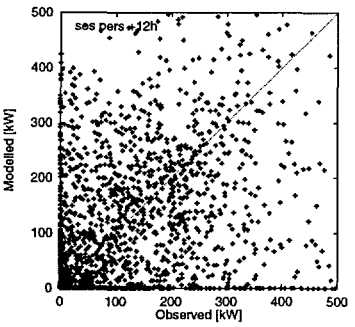
ses pers +12h
Modelled [kW]
Observed [kW]
0
100
200
300
400
500

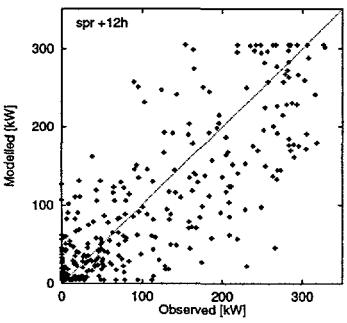
spr +12h
Modelled [kW]
Observed [kW]
0
100
200
300

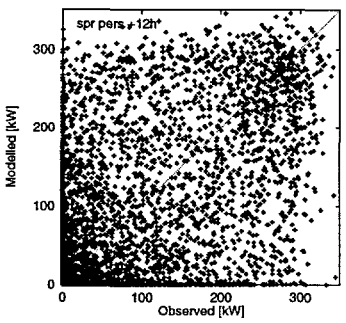
spr pers +12h
Modelled [kW]
Observed [kW]
0
100
200
300

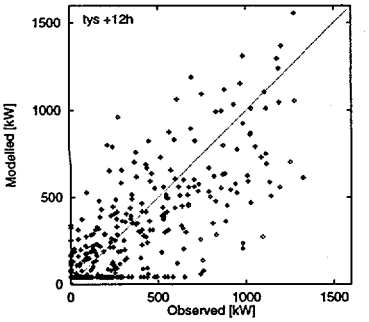
lys +12h
Modelled [kW]
Observed [kW]
0
500
1000
1500

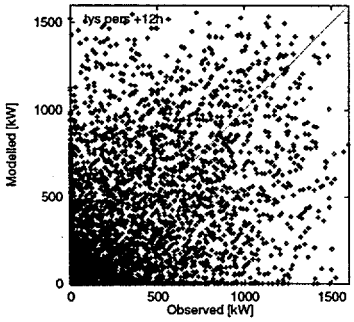
lys pers +12h
Modelled [kW]
Observed [kW]
0
500
1000
1500

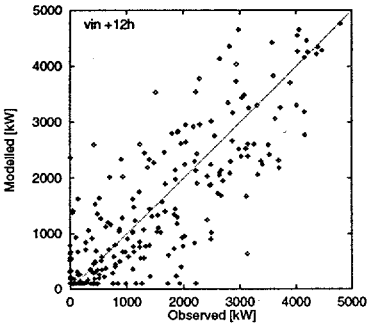
vin +12h
Modelled [kW]
Observed [kW]
0
1000
2000
3000
4000
5000

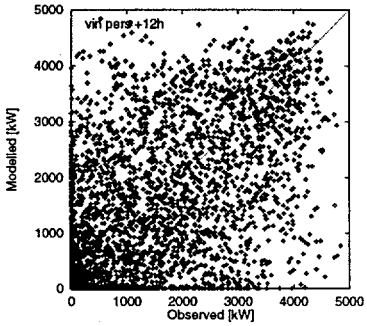
vin pers +12h
Modelled [kW]
Observed [kW]
0
1000
2000
3000
4000
5000

C Results

In this section the results of the two models will be given. The results are given as a single plot for each wind farm and for each model. For further detail refer to the previous appendices.

The figures on the left-hand side are the figures representing the results of the DMI model and the figures on the right-hand side represent the Risø model.

Looking through the wind farms it can be seen that the two models perform equally well, with respect to the mean error and the mean absolute error.

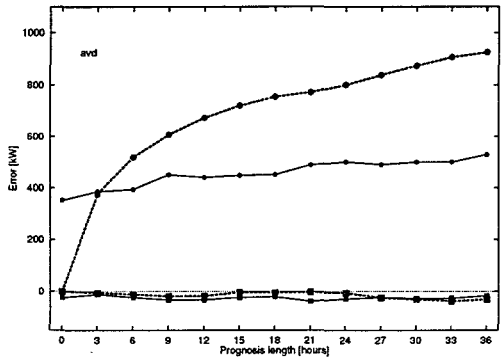

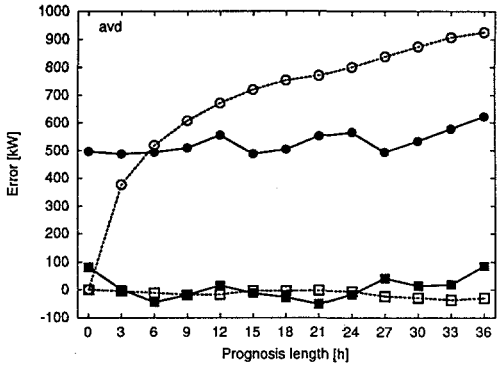

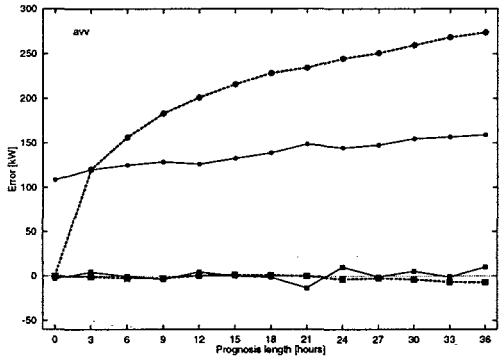

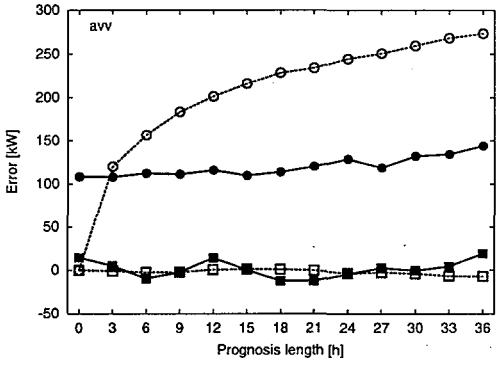

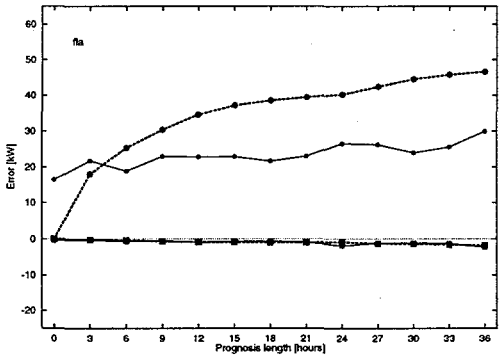

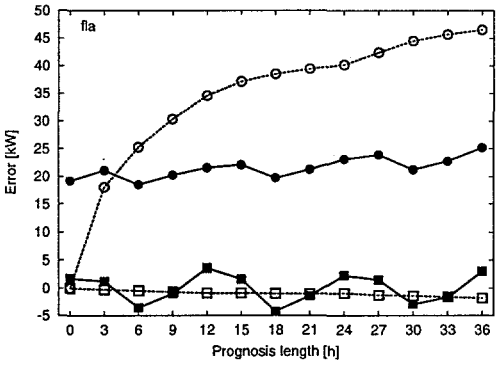

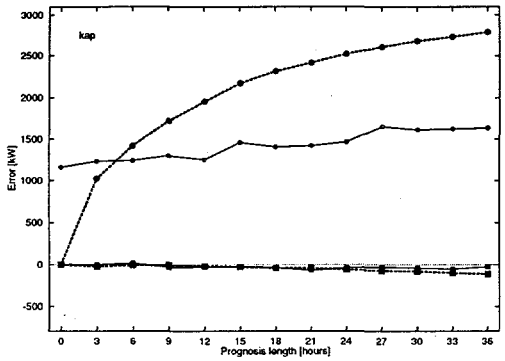
kap
Error [kW]
Prognosis length [hours]

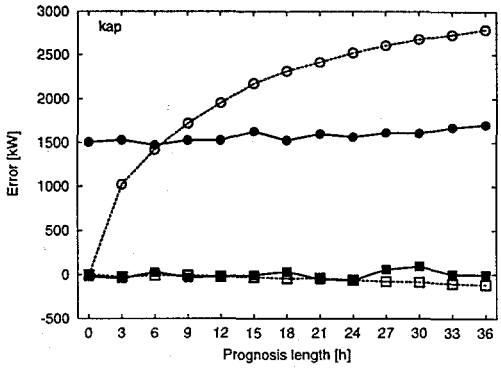
kap
Error [kW]
Prognosis length [h]

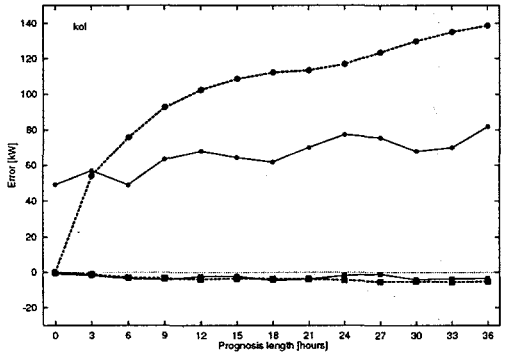
kol
Error [kW]
Prognosis length [hours]

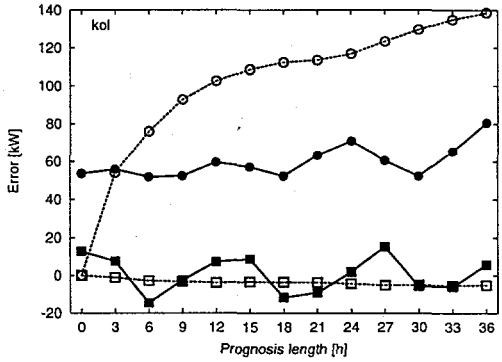
kol
Error [kW]
Prognosis length [h]

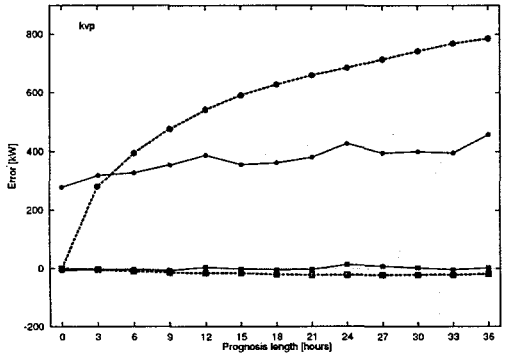
kvp
Error [kW]
Prognosis length [hours]

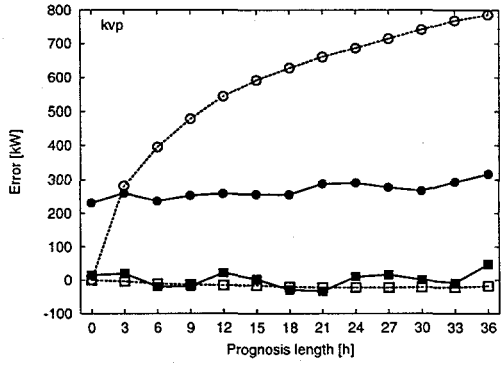
kvp
Error [kW]
Prognosis length [h]

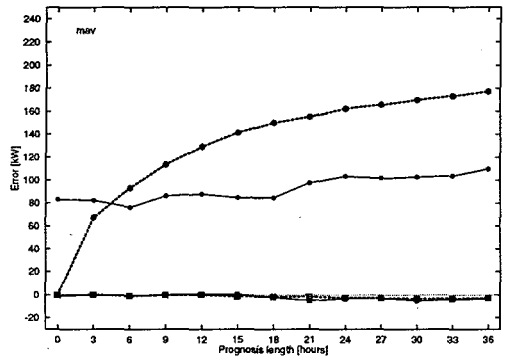
mav
Error [kW]
Prognosis length [hours]

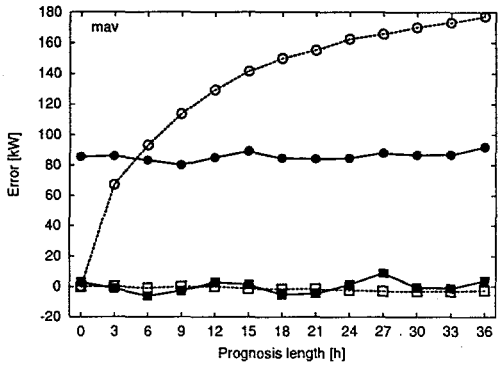
mav
Error [kW]
Prognosis length [h]

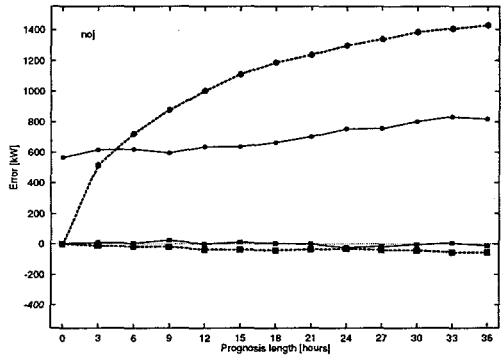
noj
Error [kW]
Prognosis length [hours]

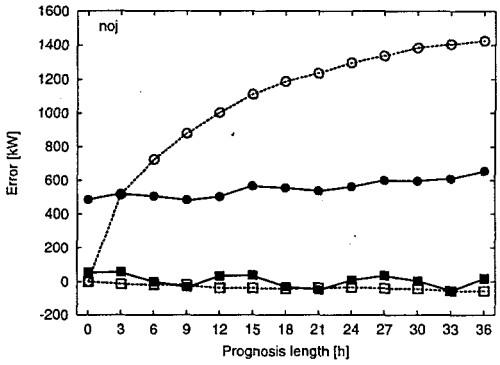
noj
Error [kW]
Prognosis length [h]

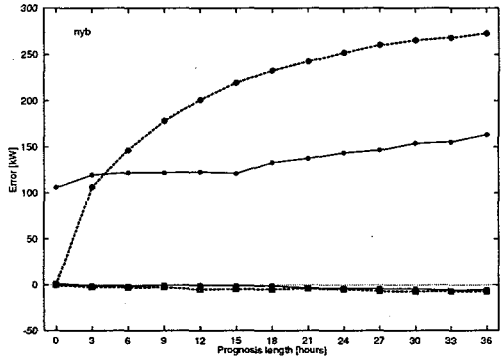
nyb
Error [kW]
Prognosis length [hours]

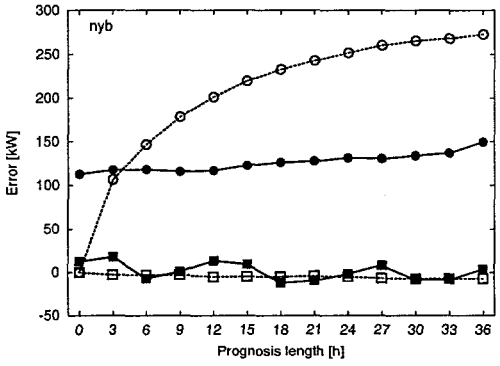
nyb
Error [kW]
Prognosis length [h]

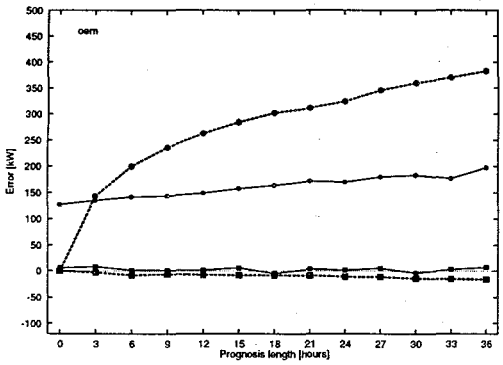
oem
Error [kW]
Prognosis length [hours]

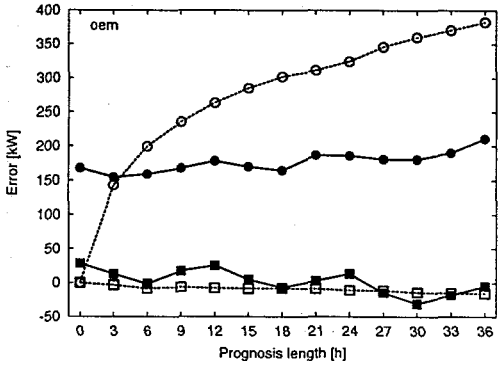
oem
Error [kW]
Prognosis length [h]

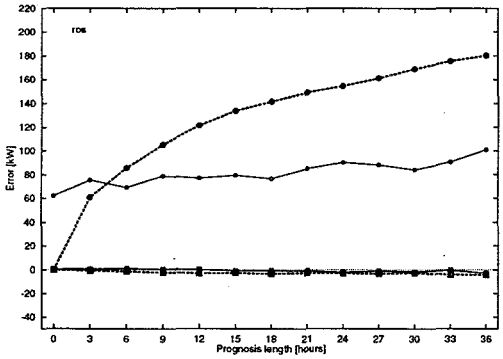
ros
Error [kW]
Prognosis length [hours]

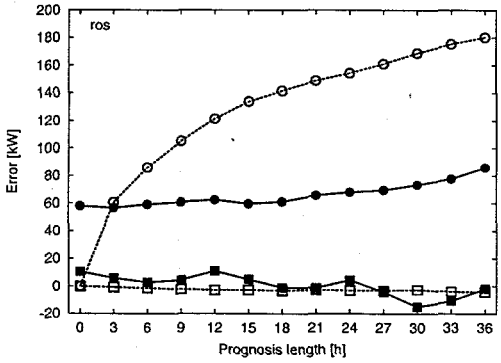
ros
Error [kW]
Prognosis length [h]

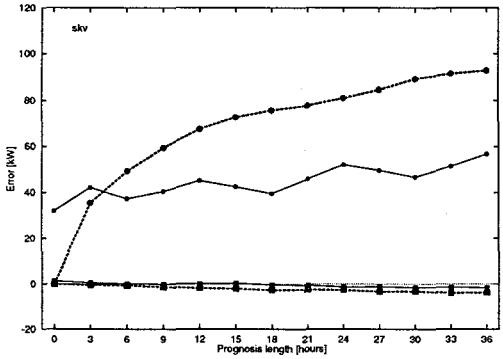
skv
Error [kW]
Prognosis length [hours]

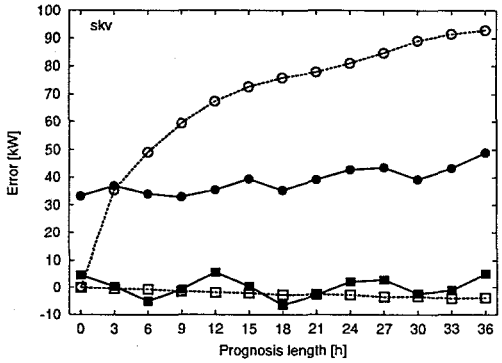
skv
Error [kW]
Prognosis length [h]

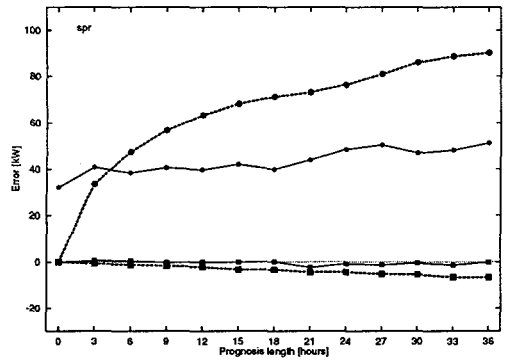
spr
Error [kW]
Prognosis length [hours]

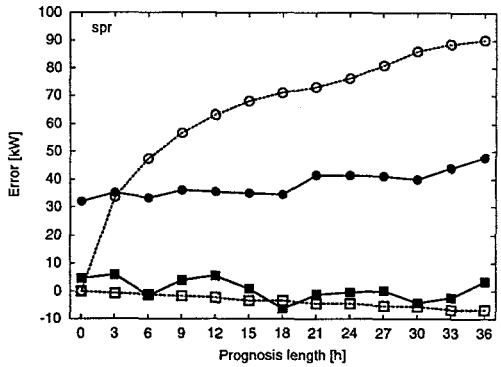
spr
Error [kW]
Prognosis length [h]

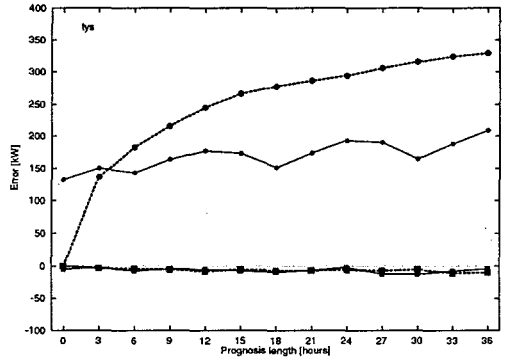
tys
Error [kW]
Prognosis length [hours]

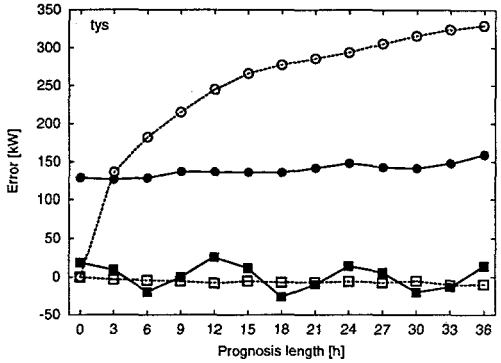
tys
Error [kW]
Prognosis length [h]

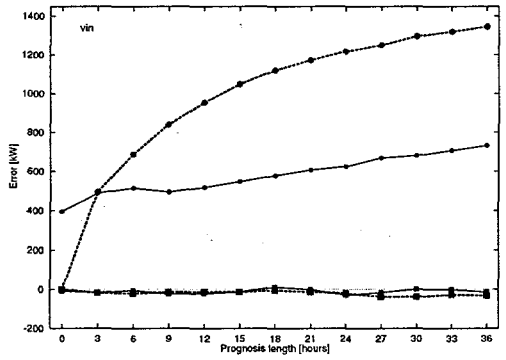
vin
Error [kW]
Prognosis length [hours]

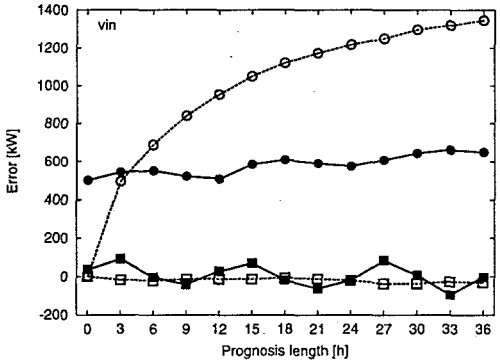
vin
Error [kW]
Prognosis length [h]

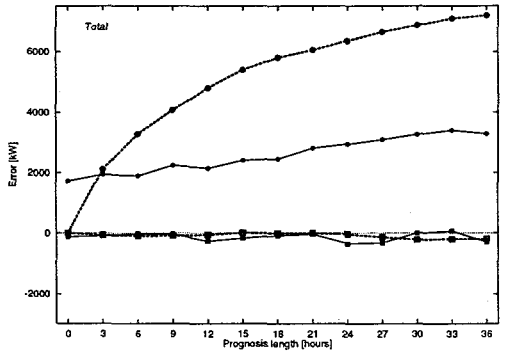
Total
Error [kW]
Prognosis length [hours]

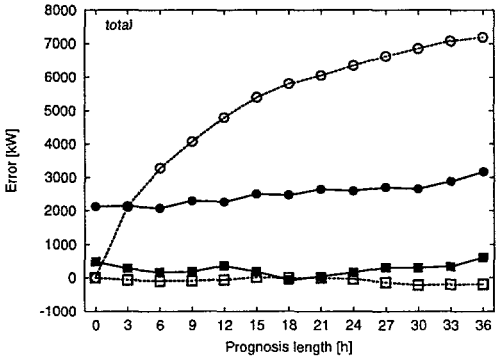
total
Error [kW]
Prognosis length [h]

Bibliographic Data Sheet **Risø-R-929(EN)**

Title and author(s)

Implementing wind forecasting at a utility

L. Landberg, M.A. Hansen, K. Vesterager, W. Bergstrøm

ISBN	ISSN
87–550–2229–4	0106–2840
Dept. or group	Date
VEA/VKM	March 1997
Groups own reg. number(s)	Project/contract No.
VIR-03893-01	ENS-1363/94-0005

Pages	Tables	Illustrations	References
123	10	65	14

Abstract (Max. 2000 char.)

This report describes a project – funded by the Danish Ministry of Energy and the Environment – that has as its aim to implement prediction of the power produced by wind farms in the daily planning at the Danish utility ELKRAFT. The predictions are generated from forecasts from HIRLAM (HIgh Resolution Limited Area Model) of the Danish Meteorological Institute. These predictions are then made valid at individual sites (wind farms) by applying either a matrix generated by the sub-models of WASP (Wind Atlas Application and Analysis Program) or by use of a Kalman filter. In the project 17 wind farms have been selected for study. The farms are located on the Zealand (13) and Bornholm (4) islands and all belonging to the Danish utility ELKRAFT.

Descriptors INIS/EDB

DENMARK, ELECTRIC UTILITIES, FORECASTING, MATHEMATICAL MODELS, METEOROLOGY, PLANNING, W CODES, WIND POWER, WIND TURBINE ARRAYS

Available on request from:
Information Service Department, Risø National Laboratory
(Afdelingen for Informationsservice, Forskningscenter Risø)
P.O. Box 49, DK–4000 Roskilde, Denmark
Phone (+45) 46 77 46 77, ext. 4004/4005 · Fax (+45) 46 75 56 27 · Telex 43 116